Nuclear Structure Studies with High-Resolution In-Beam γ-Spectroscopy

A.Gadea IFIC-CSIC Valencia
<andres.gadea@ific.uv.es>

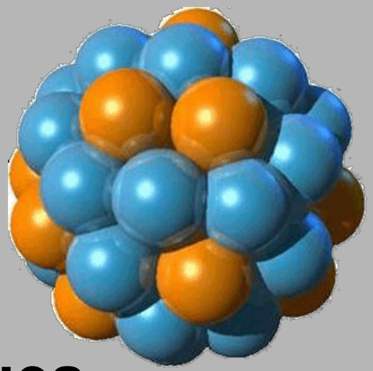

- **General Introduction**
- **Introduction to the HR in-beam techniques**
- **Instrumentation**
- **Spectroscopy Studies and Nuclear Reactions**

<u>**PHASE SPACE**</u>

Spin, Temperature, Isospin. Additionally strangeness.

<u>**Population:**</u>

Nuclear reactions. Low and high energy, stable and radioactive beams. De-excitation following decay

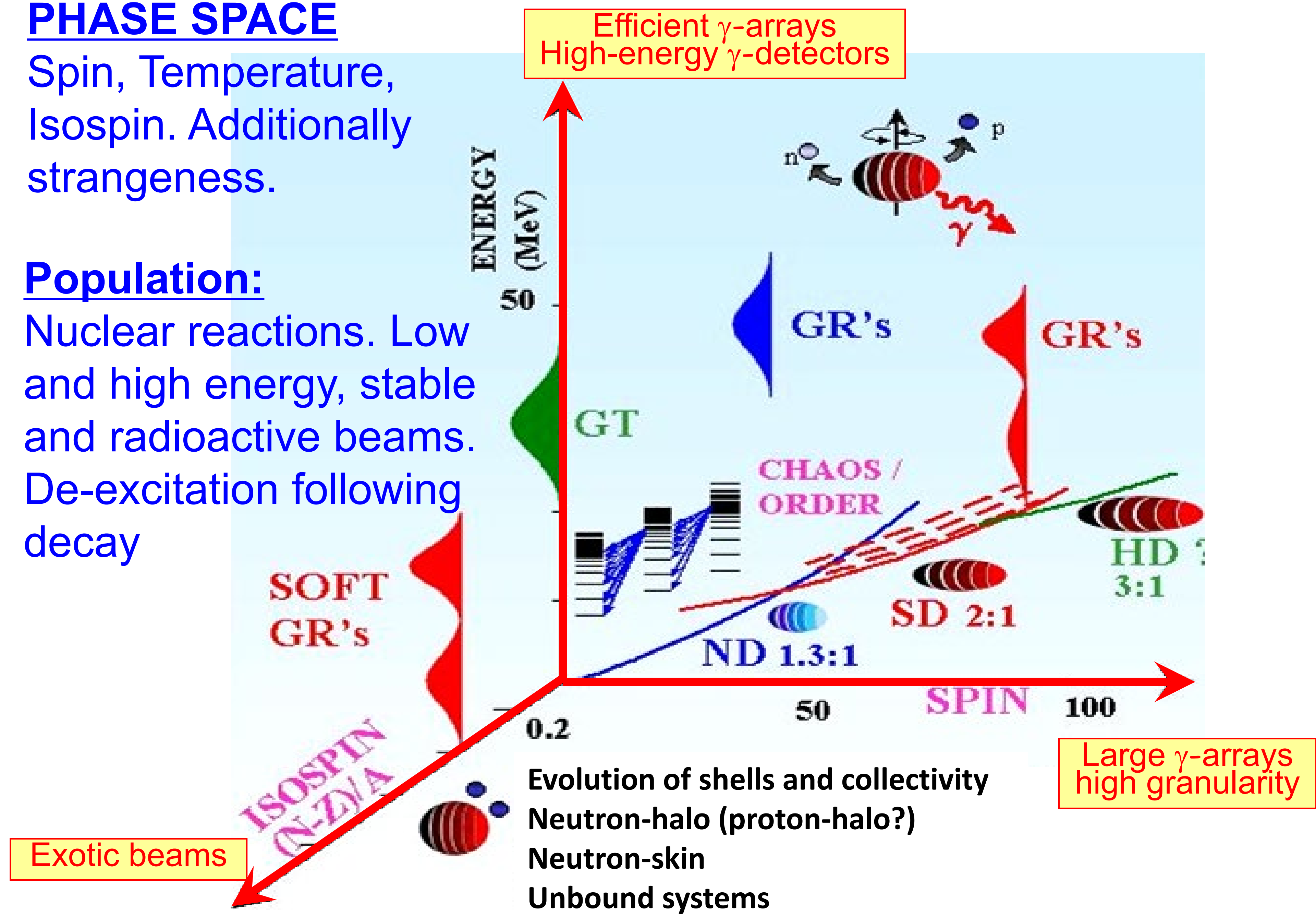

Evolution of shells and collectivity
Neutron-halo (proton-halo?)
Neutron-skin
Unbound systems
etc…

Nuclear Collectivity

Examples of Nuclear Shapes

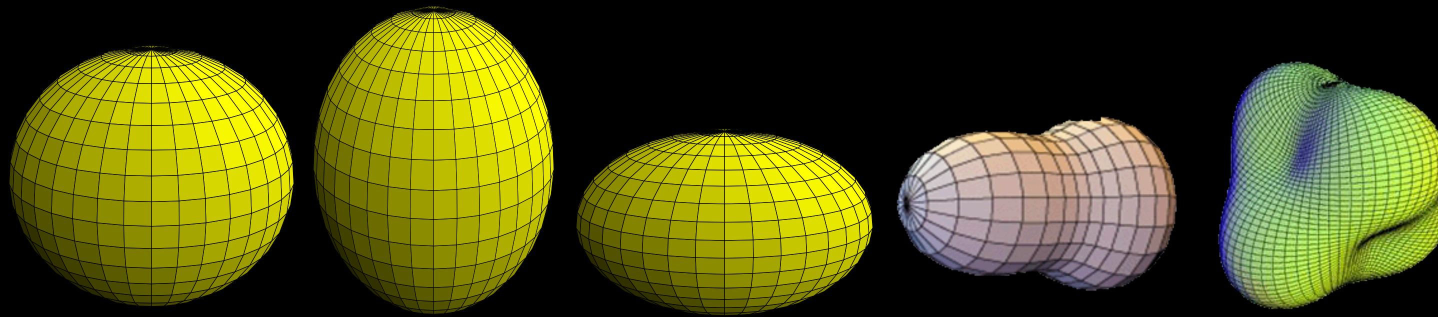

Examples of Nuclear Shape Vibrations

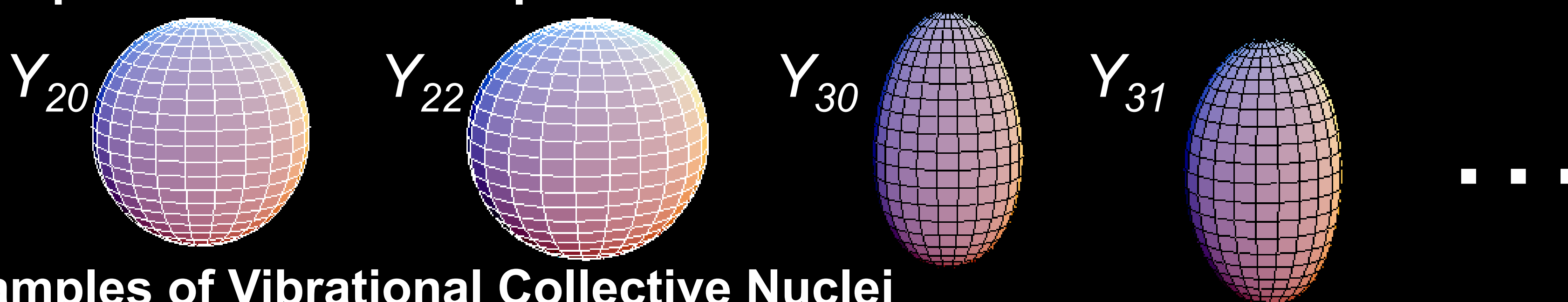

Examples of Vibrational Collective Nuclei

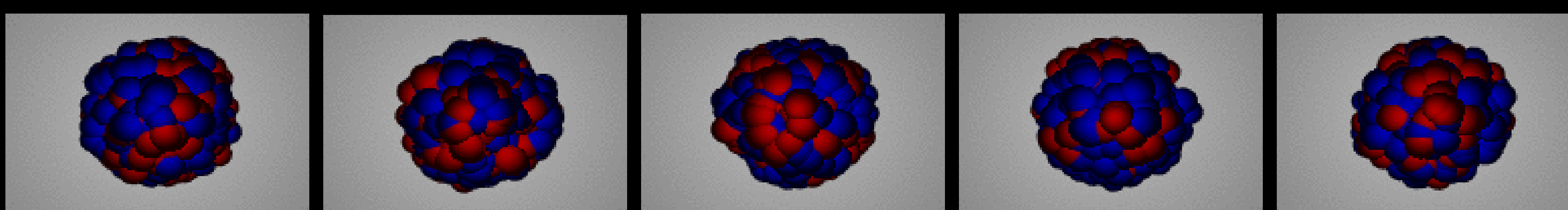

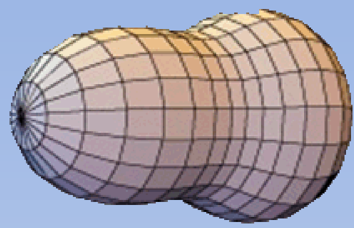

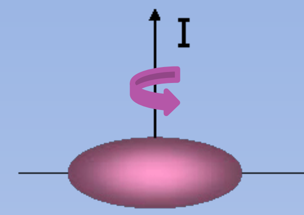

I=Jω

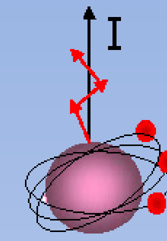

$I = \Sigma\, \mathbf{I}_j$

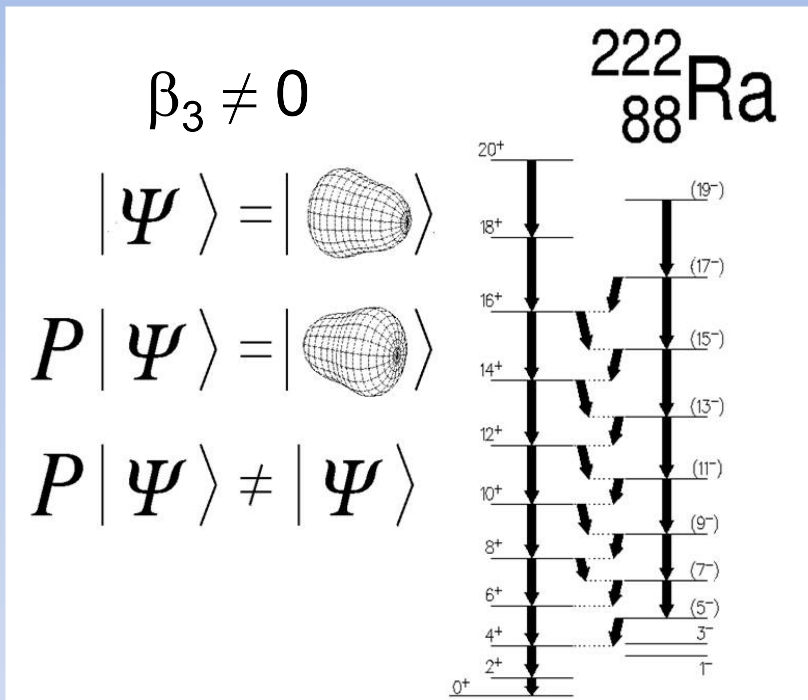

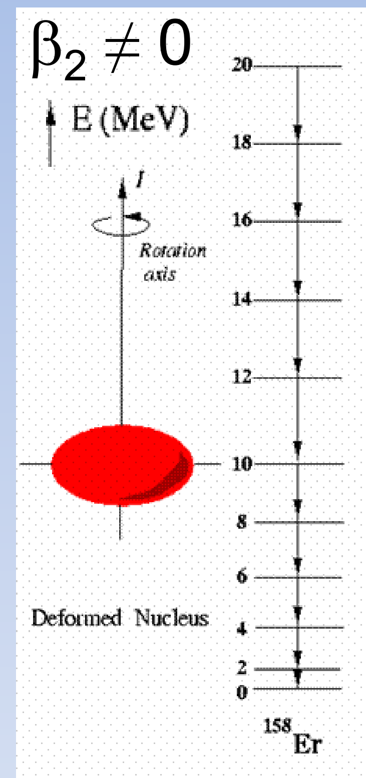

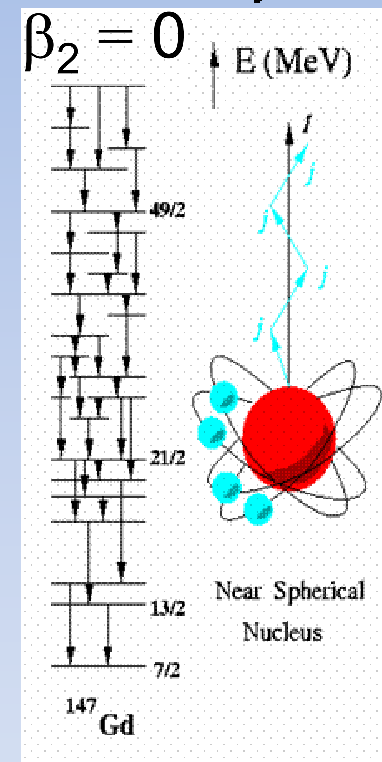

Rayleigh shape in terms of multipole expansion for an axial symmetric nucleus

$$R(\theta) = R_0 \sum_{\lambda=0}^{\lambda_{max}} \beta_\lambda P_\lambda(\cos\theta),$$

Some Scientific Topics

Organization of Nuclear Matter and Emerging Phenomena. In-media Fundamental Interactions, Origin and Evolution of Nuclear Matter

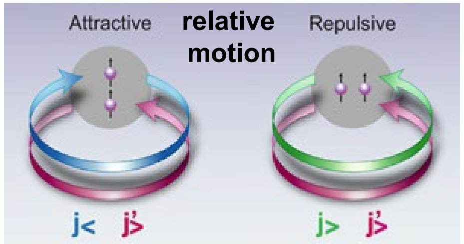

- **Shell Structure Far From Stability:** large nucleon asymmetry lead to shell modifications driven by the spin-isospin nucleon-nucleon interaction and close to the drip-line by the weakening of the spin-orbit interaction

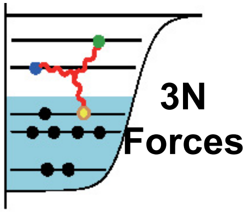

- **Three Body Forces:** testing the role of three nucleon (3N) forces in the microscopic description of the atomic nucleus. Indications of important role in the vicinity of proton as well as neutron drip-lines.

- **Nuclear Shapes:** coexistence of different nuclear shapes, Large deformation, high-rank symmetries, phase transition, dynamic and critical point symmetries.

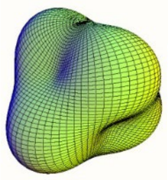

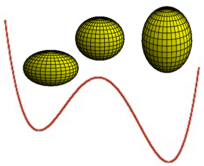

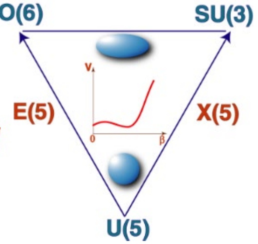

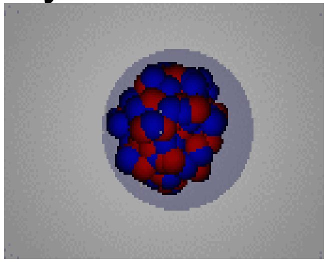

- **Spin-isospin Response Of Nuclei:** out-of-phase density oscillations of the neutron and proton fluids provided information on macroscopic nuclear properties associated with isovector fields.

- **Nuclear Matter Appearance and Evolution:** nuclear astrophysics, explosive scenarios and the rp-process, the origin of the elements heavier than Iron and the r-process

- **and Clustering in Nuclei, New forms of nuclear pairing, In-Media isospin breaking interactions, Study of Open Quantum Systems, etc …**

What Can We Measure?

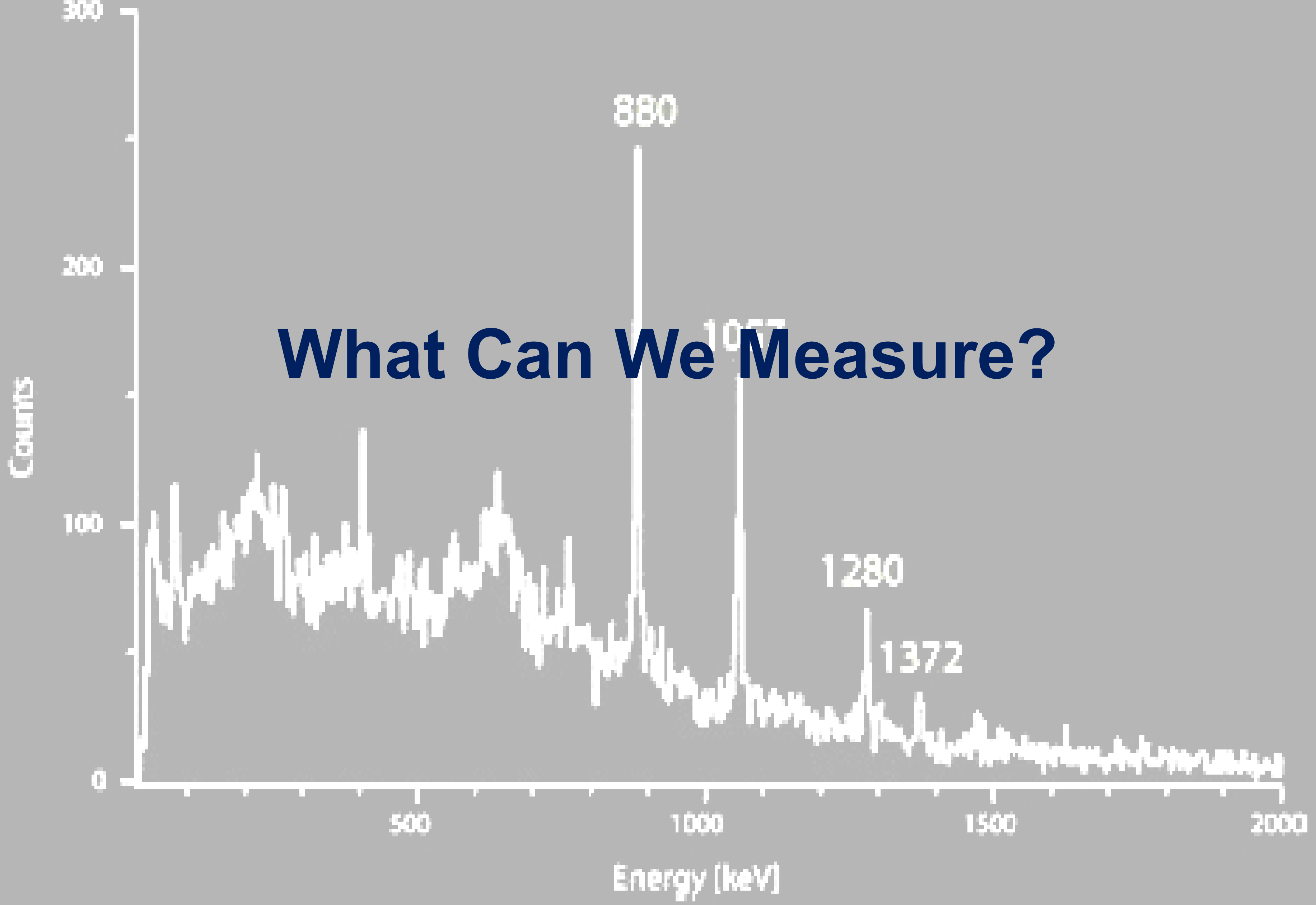

In-Beam Spectroscopy Key Aspects

- Direct detection of the "prompt" de-excitation γ-rays emitted by the nucleus of interest

- The nucleus to be studied "must" be in a excited state:
  - The nucleus can be created in a excited state or
  - The nucleus must be excited during the reaction process

- The detection system are installed around the reaction point
  - Key factors are Efficiency, Peak-to-Total, i.e. signal-to-noise and Selectivity.
  - Reaction rates could by limited by the detector counting rates limit.

- In addition to the γ-ray detector, frequently, complementary detectors and devices are necessary to improve selectivity or to perform a particular measurement.

In-beam Experiments in γ-ray Spectroscopy

An experiment consist of exciting, or produce excited, a nucleus, then measure the γ-ray emitted during transitions between nuclear states.

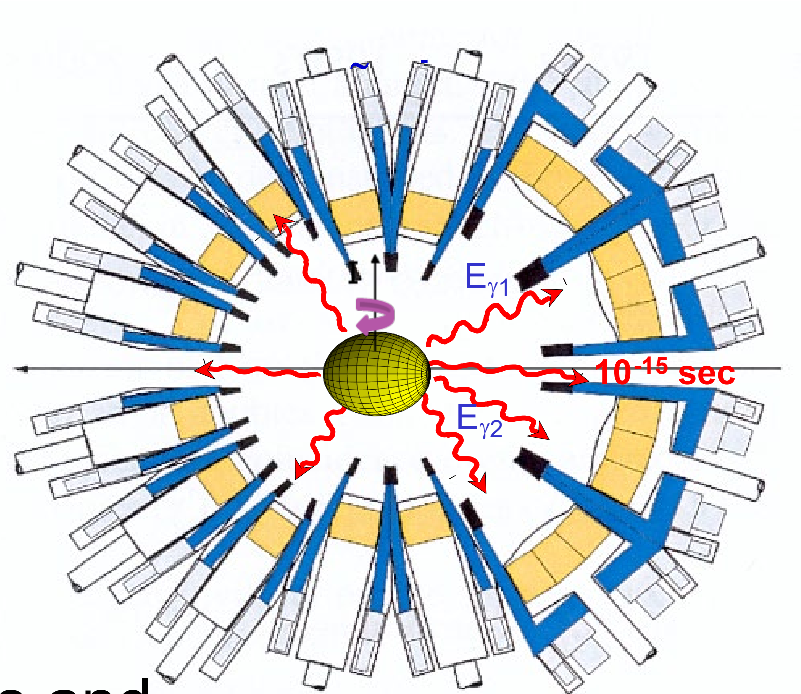

~4π coverage helps detection efficiency and provides angular distribution information

Energies, Intensities and peak shapes with geometrical or other conditions

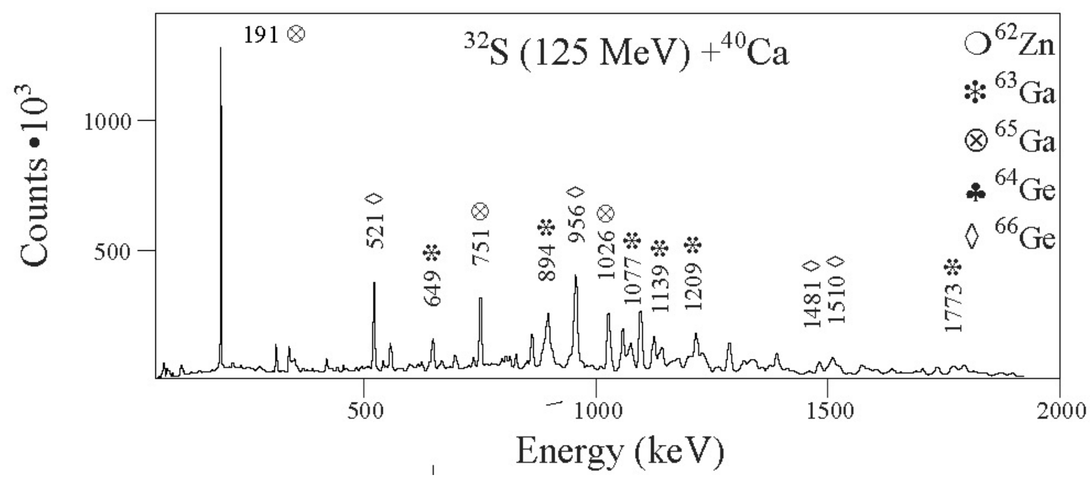

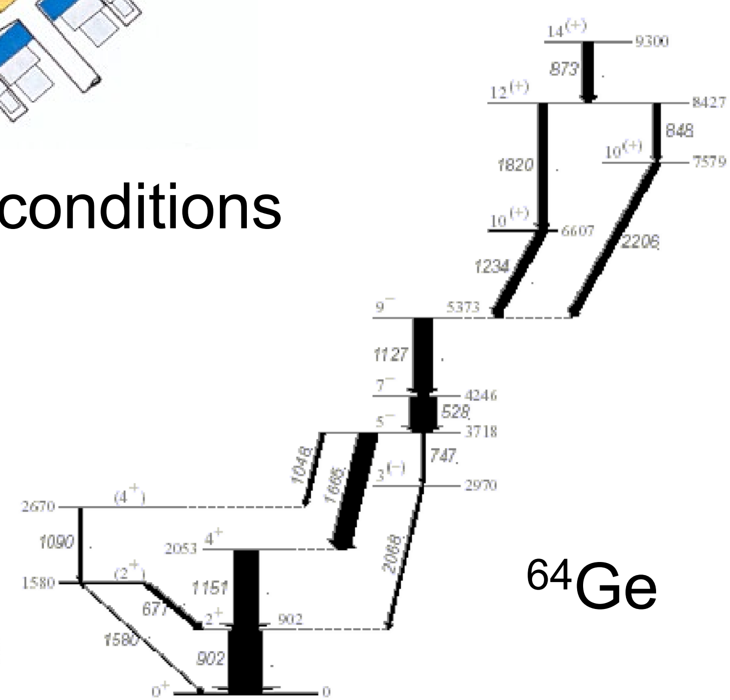

High Resolution γ-ray Spectroscopy

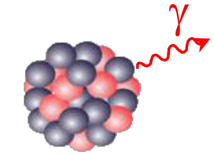

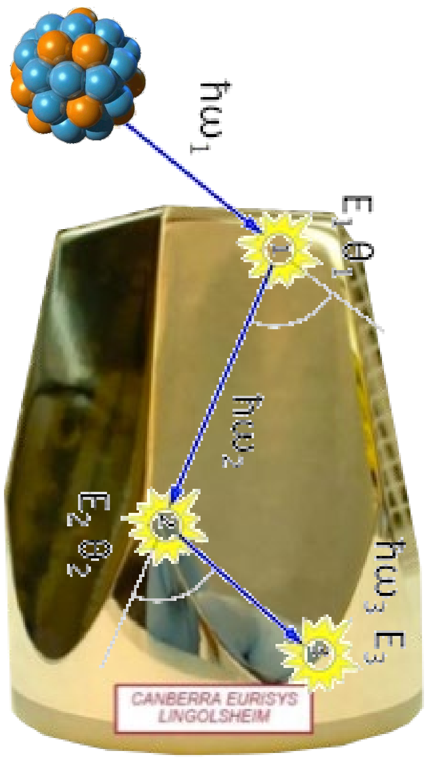

Sequence of Excited States: γ-ray Energy, intensity and coincidence analysis

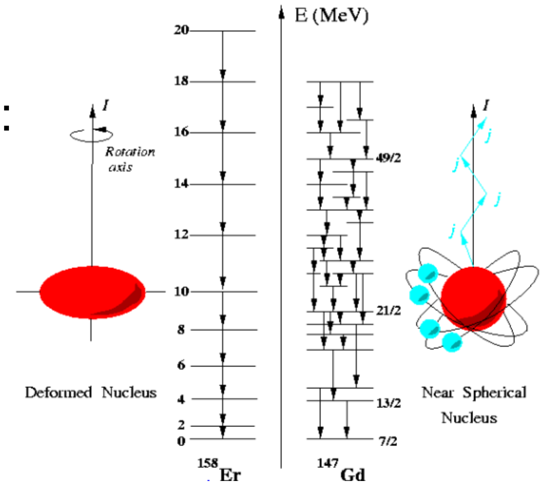

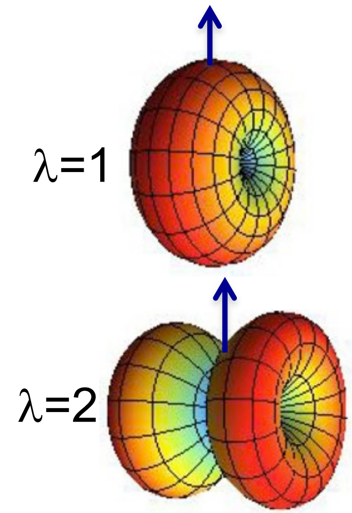

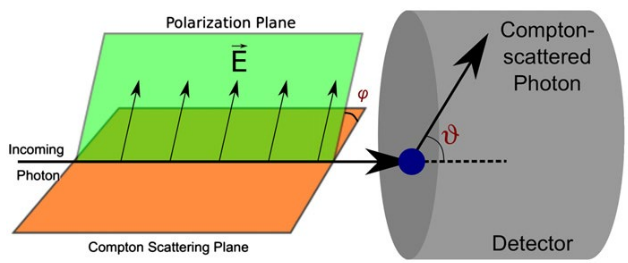

State Quantum numbers J^{π} γ-ray angular distribution, correlations and linear polarization

Transition probabilities by Doppler or indirect methods B(E/Mλ)

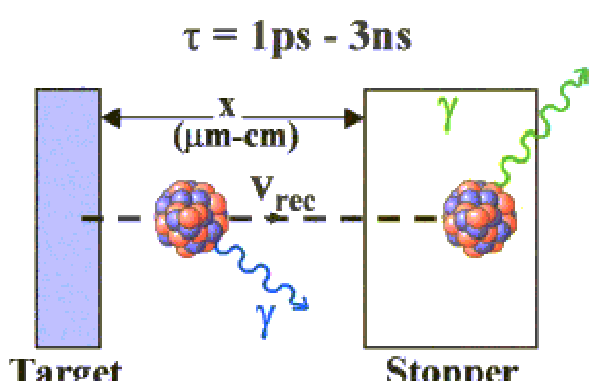

Nuclear Moments (e.g.: g-factors magnetic field)

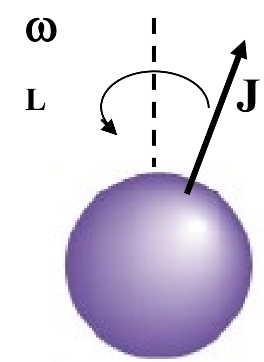

Electromagnetic decay

- There are three types of electromagnetic decay, γ-ray emission, internal conversion (IC) and pair production (E>1.02MeV).
- In electromagnetic decays ΔN=ΔZ=ΔA=0, with just a lowering of the excitation energy of the nucleus.
- In γ-ray emission, the emitted photons are mono-energetic and have an energy corresponding to almost all of the energy difference between the final and initial state of the system.

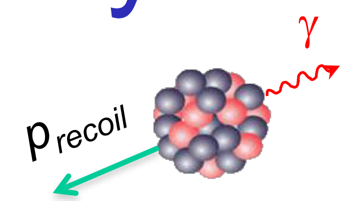

$$p_\gamma = p_{recoil}$$

$$T_{recoil} = \frac{p_{recoil}^2}{2m_{recoil}} = \frac{p_\gamma^2}{2m_{recoil}} = \frac{E_\gamma^2}{2m_{recoil}c^2}$$

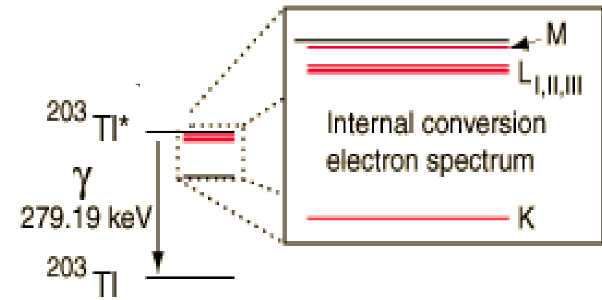

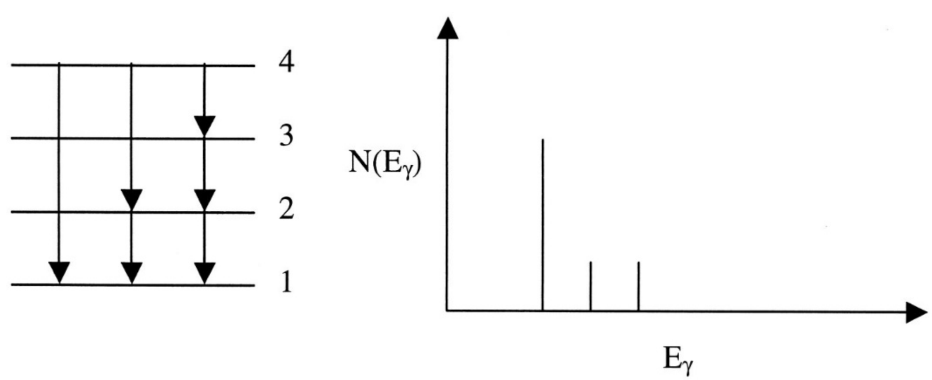

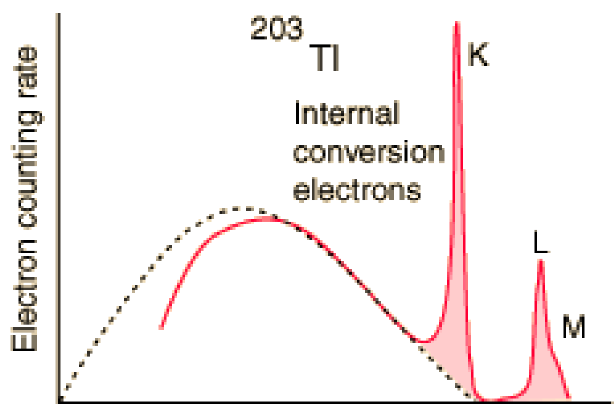

Electromagnetic Decay
Transition Character and Multipolarity

- The initial and final states have a definite I^{π}. The photon carries away a definite amount of angular momentum. I and π must be conserved.
- Multipolarity is a measure of the angular momentum carried away by the photon.
- Transitions could be stretched $\ell = (I_i - I_f)$ or non-stretched $\ell > (I_i - I_f)$.
- Transitions are classified as electric or magnetic based on whether the radiation is due to a shift in the charge distribution or a shift in the current distribution.
- Based on the type of operator involved, there are restrictions on the parity change in the transition.
- E0 transitions does not happen by γ-ray emission, only by Internal Conversion or Pair Production.

$$\left|\left(I_i - I_f\right)\right| \le \ell \le \left(I_i + I_f\right)\hbar$$

A photon with ℓ units of angular momentum is called a 2^{ℓ}-pole photon.

$\ell = 1 \Rightarrow$ *dipole*

$\ell = 2 \Rightarrow$ *quadrupole*

$\ell = 3 \Rightarrow$ *octupole*

TABLE 9.1 γ-Ray Selection Rules and Multipolarities

Radiation Type	Name	$l = \Delta I$	$\Delta\pi$
E1	Electric dipole	1	Yes
M1	Magnetic dipole	1	No
E2	Electric quadrupole	2	No
M2	Magnetic quadrupole	2	Yes
E3	Electric octupole	3	Yes
M3	Magnetic octupole	3	No
E4	Electric hexadecapole	4	No
M4	Magnetic hexadecapole	4	Yes

Electromagnetic Decay

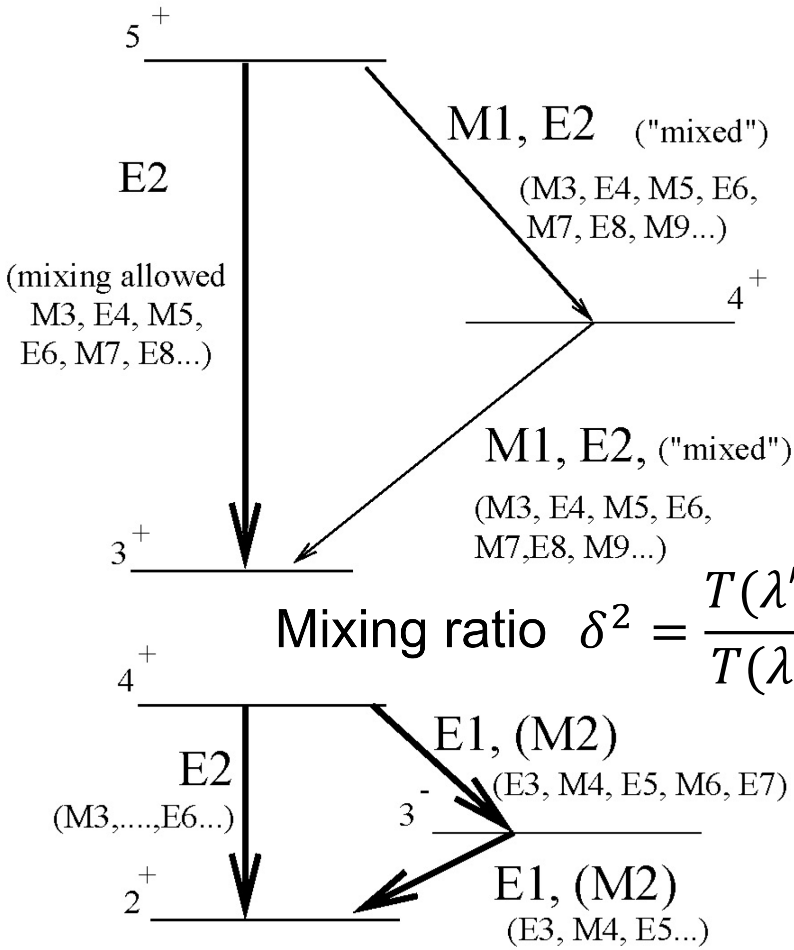

Mixing ratio $\delta^2 = \frac{T(\lambda')}{T(\lambda)}$

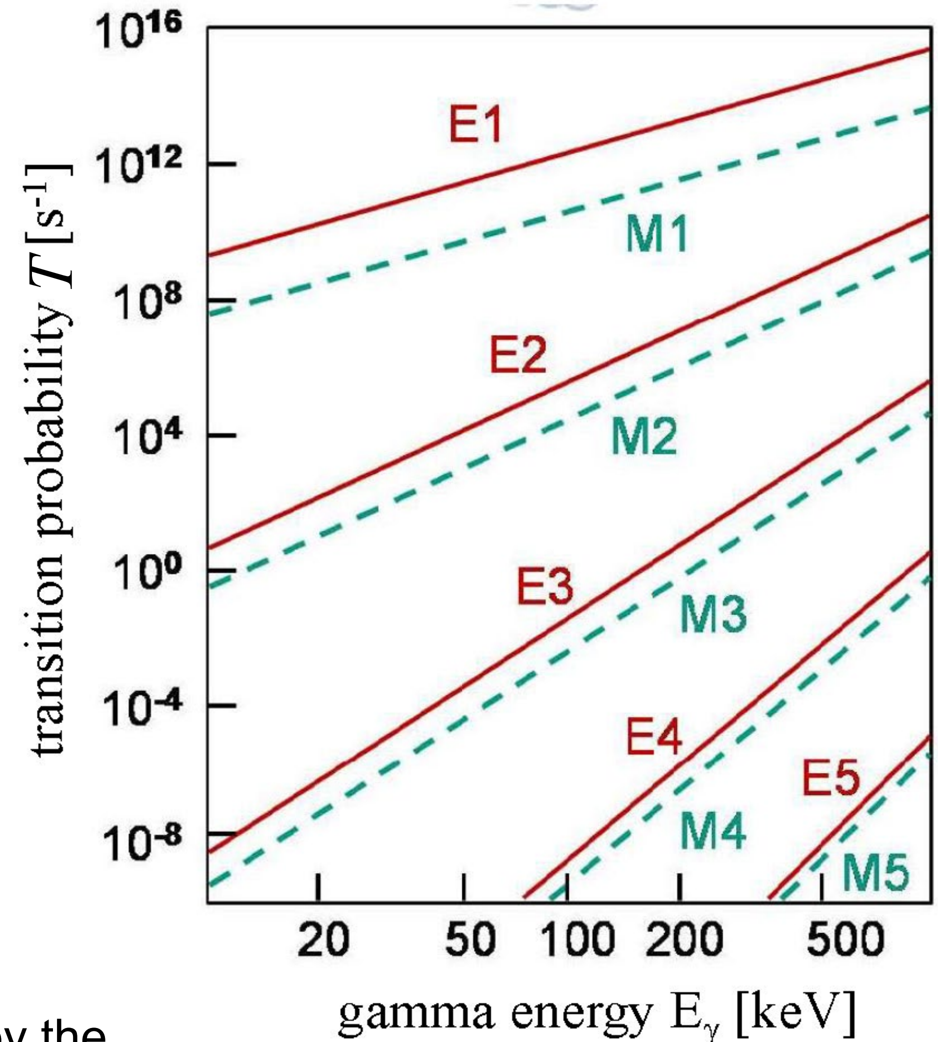

The transition probability is governed by the matrix element of the multipole operator

B(E/Mλ) $m_{fi}(\sigma L) = \int \Psi_f^* m(\sigma L) \Psi_i dv$

Single particle estimates (Weisskopf Estimates)

γ-ray Coincidence Analysis

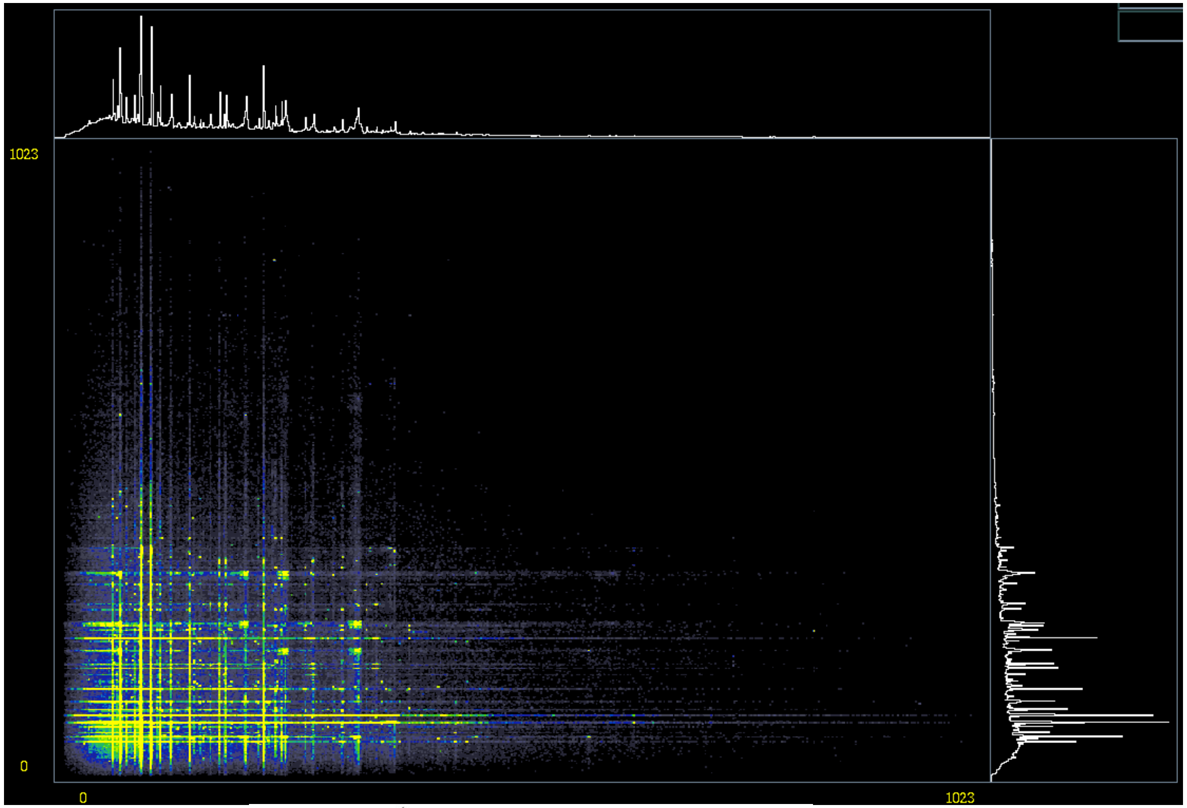

- With two or more detectors it is possible to create two (2D) or higher dimension histograms.
- The 1D projection with a condition in one of the axis provides the spectrum of γ-rays "in coincidence".
- The "coincidence" relationships allow to create the energy level scheme of the nucleus for a particular reaction.

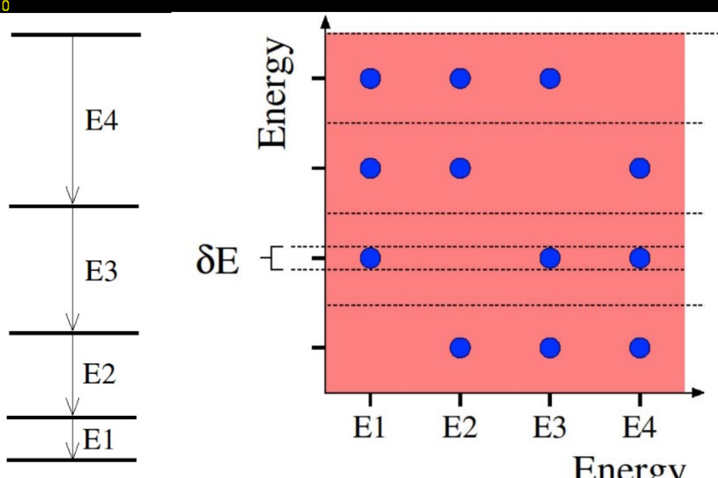

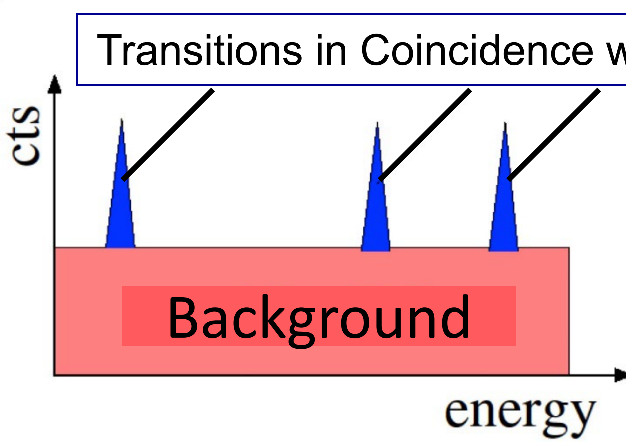

The Compton background is as well in coincidence with the transition

Example: Coincidence Analysis in Fusion-Evaporation Reactions

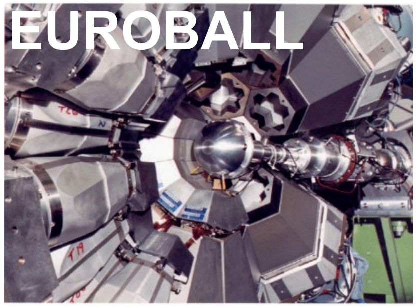

$^{40}Ca(^{40}Ca,4pn)^{75}Kr^{*}$

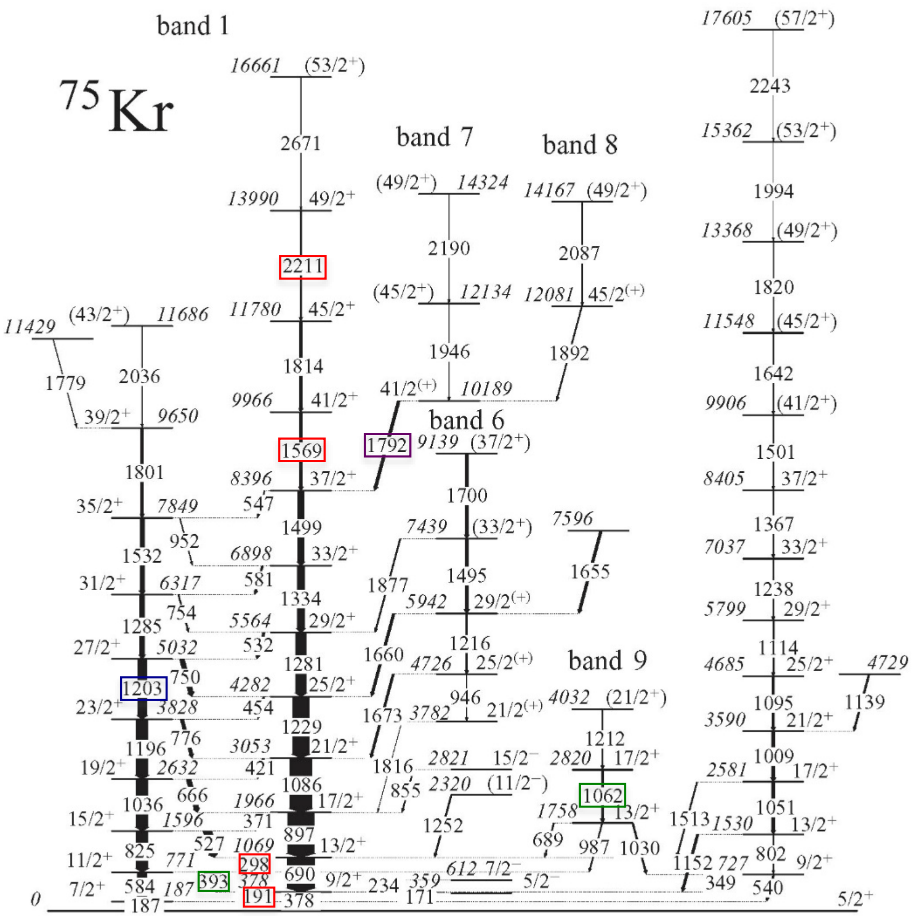

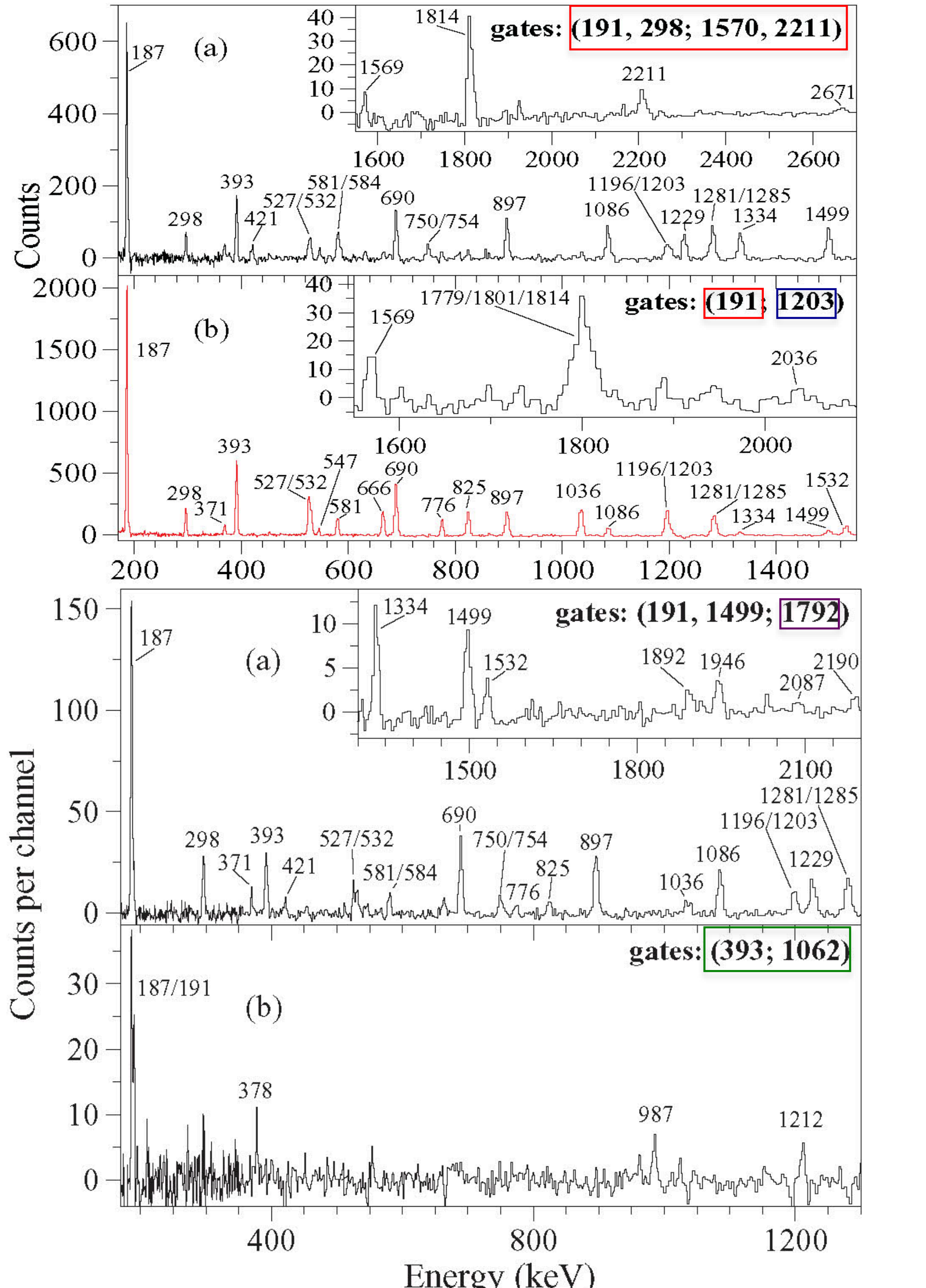

Th. Steinhardt, et al., Phys. Rev. C **86**, 064310 (2012)

Electromagnetic emission: Angular distributions $Z_{\ell \pm m}(\theta)$

Intensity of γ-ray follows a distribution described by the spherical harmonics

$$Z_{1\pm1}(\theta) = 1/4\pi \left\{1 + 1/2\, P_2(\cos\theta)\right\}$$

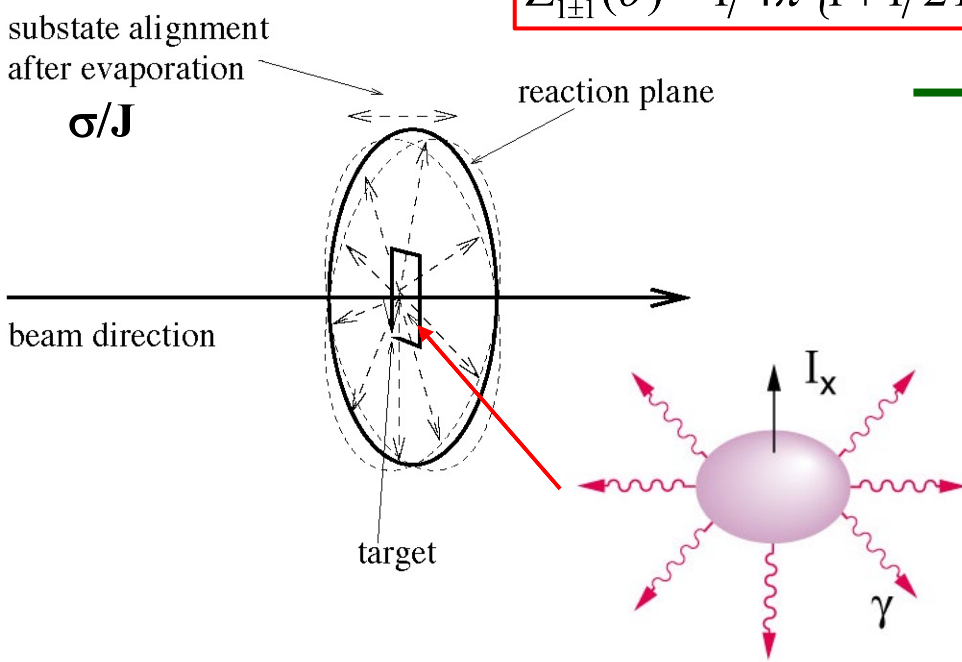

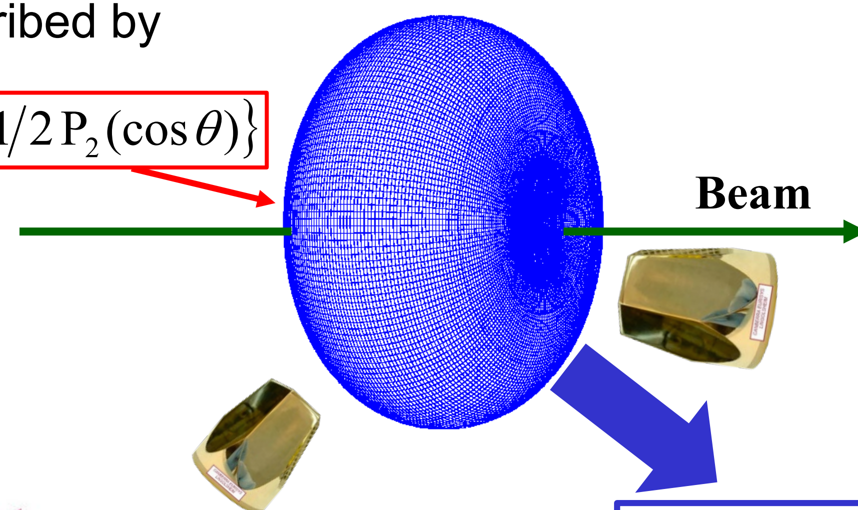

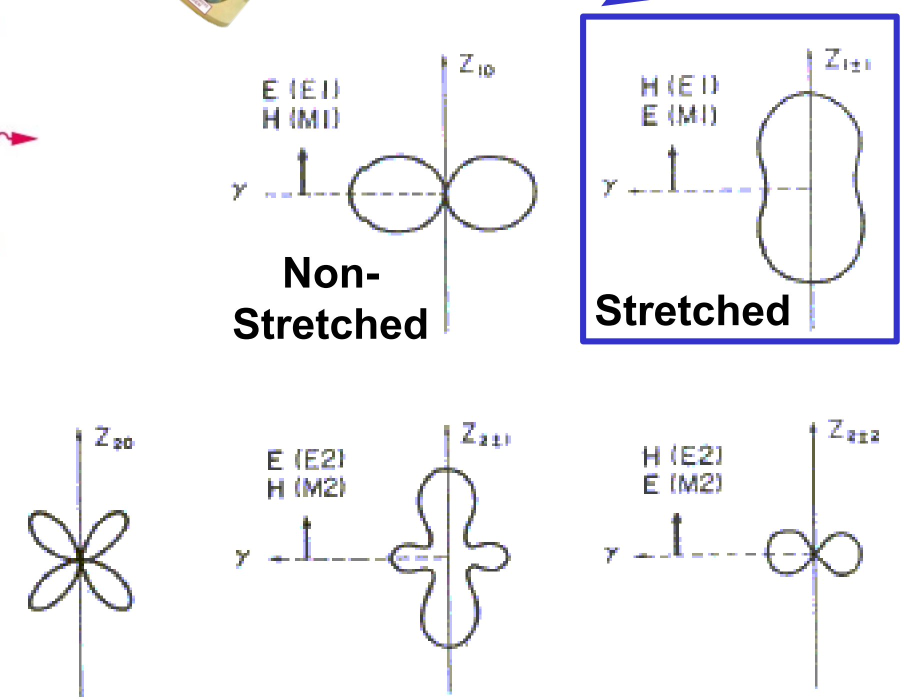

Angular Distributions: available for oriented nuclei.
Angular Correlations: available for non-oriented & oriented nuclei
Angular distributions and correlations are only sensitive to the multipolarity ℓ

Measurement of the linear polarization

• γ-rays emitted by oriented nuclei are partially polarized. The polarization vector is different for stretched E and M transitions (Sensitive to the Character)

•Compton scattering can be used to measure the degree of polarization through the dependency with the polarization vector

$$\frac{d\sigma_{KN}}{d\Omega} = \frac{r_0^2}{4}\left(\frac{E'}{E}\right)^2\left[\frac{E'}{E} + \frac{E}{E'} - 2\sin^2\theta\cos^2\varphi\right]$$

φ = angle between the scattering plane and the initial polarization plane

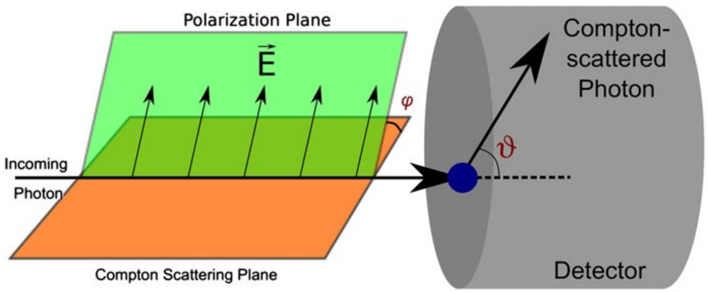

$$P_E(\theta) = \frac{1}{Q}\cdot\frac{N_\perp - N_{||}}{N_\perp + N_{||}}$$

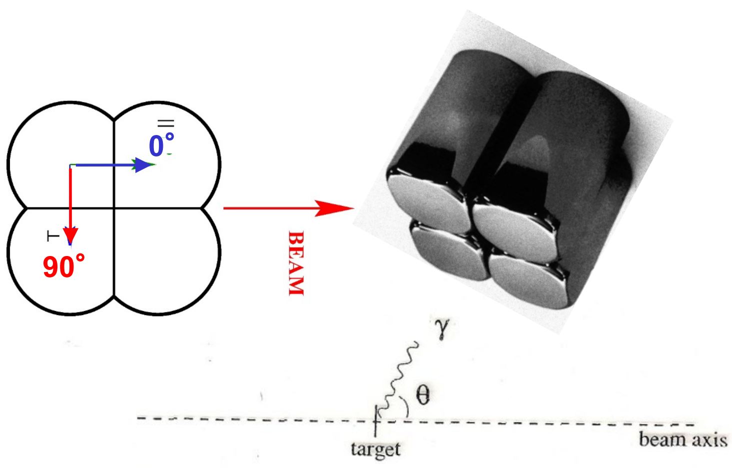

Experiments measure the asymmetry.
Q is the sensibility of the polarimeter

Stretched Eλ transitions will have positive asymmetry
Stretched Mλ transitions will have negative asymmetry

L.M. Garcia-Raffi et al., NIM A 391 (1997) 461

Techniques for lifetime measurements

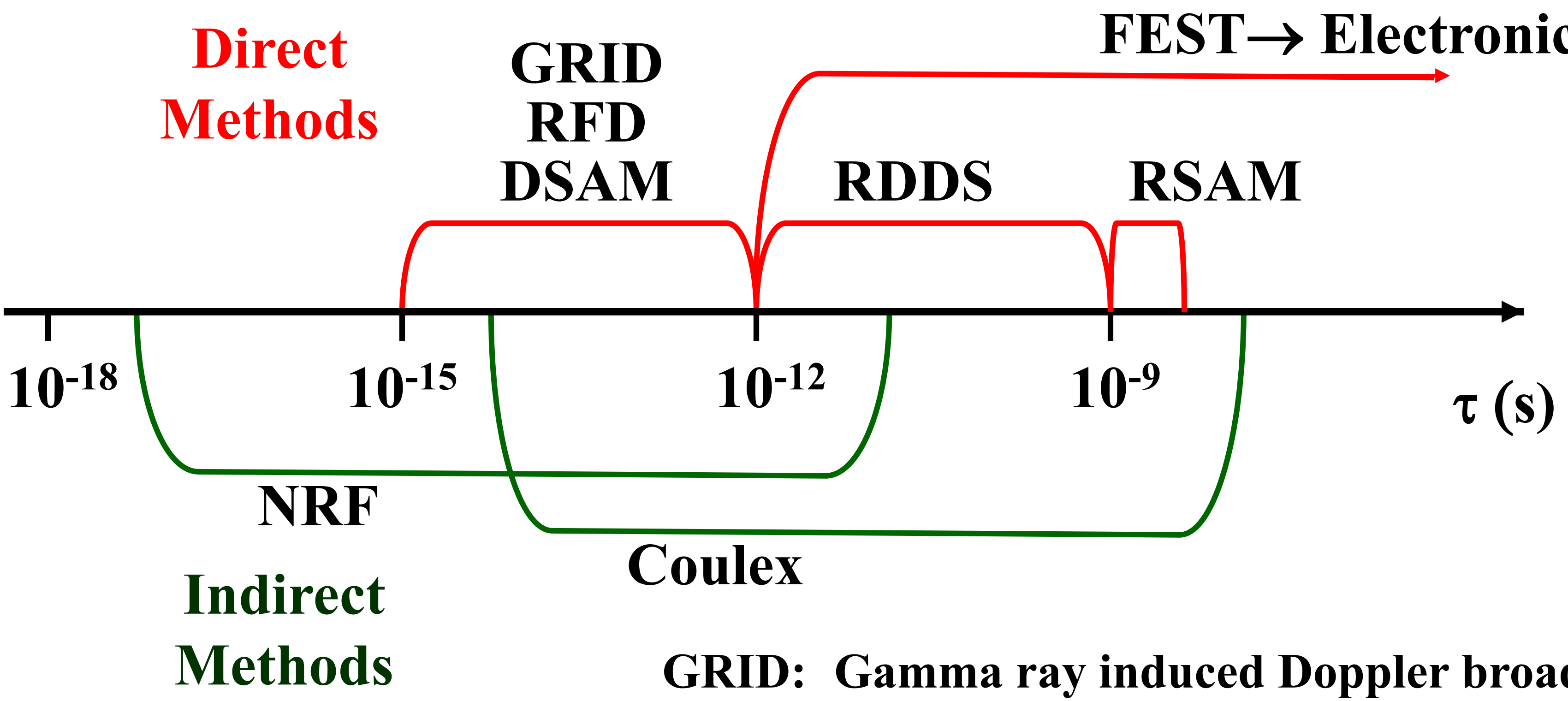

Doppler Techniques

$E^{cm}_{\gamma} = E_{\gamma}(1-\beta\cos\Theta)/(1-\beta^2)^{-1/2}$

GRID: Gamma ray induced Doppler broadening
RFD: Recoil straggling method
DSAM: Doppler shift attenuation method
RDDS: Recoil distance Doppler shift method
RSAM: Recoil shadow anisotropy method
FEST: Fast electronic scintillation method
NFR: Nuclear resonance fluorescence
Coulex: Coulomb excitation cross section

Doppler Shift Attenuation Method

$\tau = 0.1 - 1.5$ ps

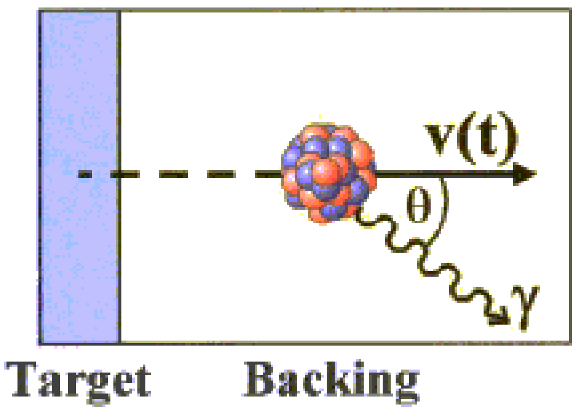

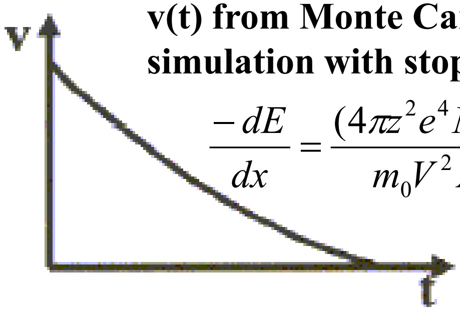

v(t) from Monte Carlo simulation with stopping power

$$\frac{-dE}{dx} = \frac{(4\pi z^2 e^4 NZ)}{m_0 V^2 A}\ln\left(\frac{2m_0 V^2}{I}\right)$$

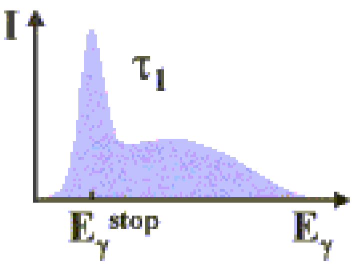

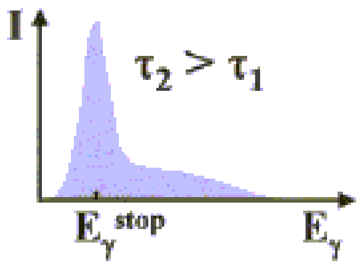

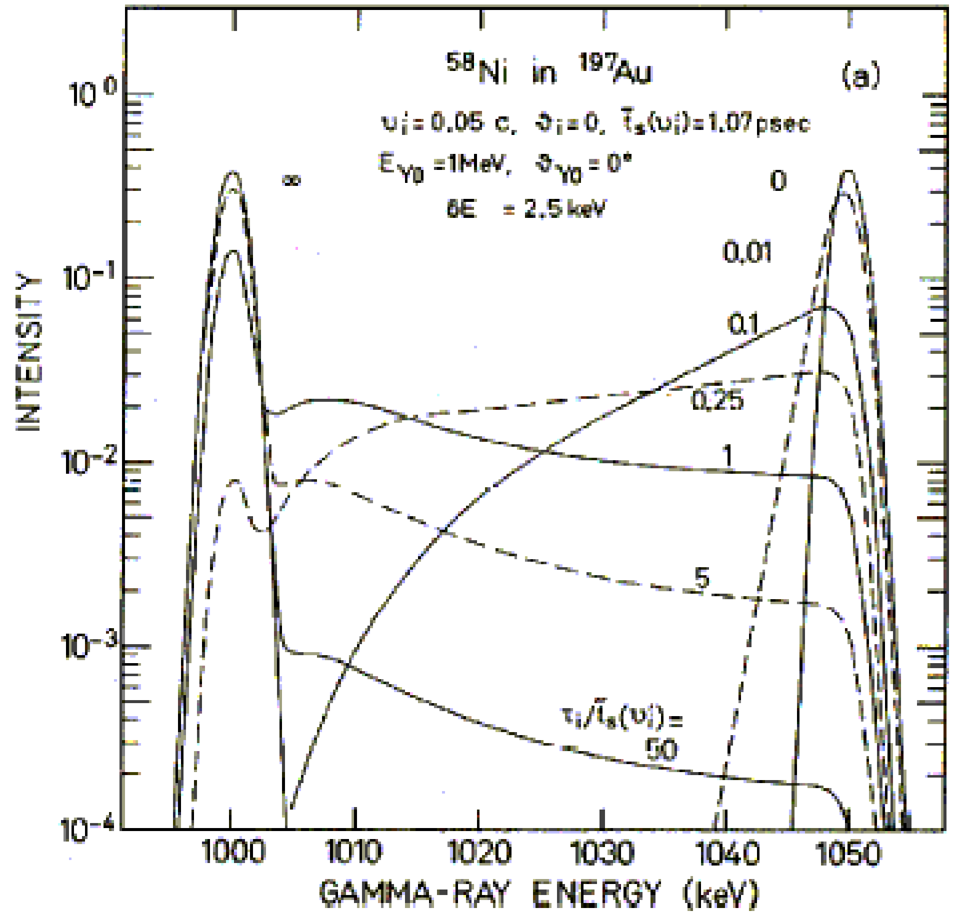

Line shapes for ^{58}Ni stopped in ^{197}Au with a beam velocity of v/c=0.05 and measured at θ=0°

R.G. Stokstad, et al, Nucl. Phys. A 156 (1970) 145.

Recoil Distance Doppler Shift Method

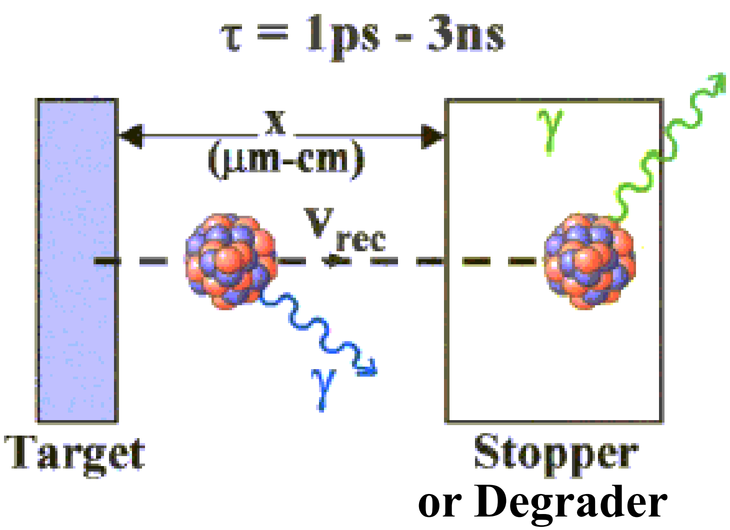

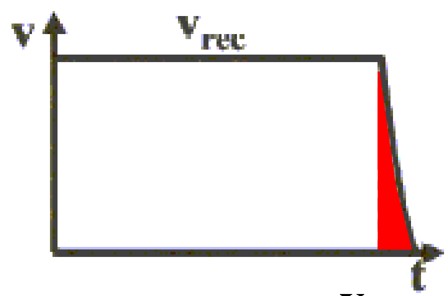

$$E\gamma(u) \approx E\gamma(s)\left(1+\frac{v_{rec}}{c}\cos\theta\right)$$

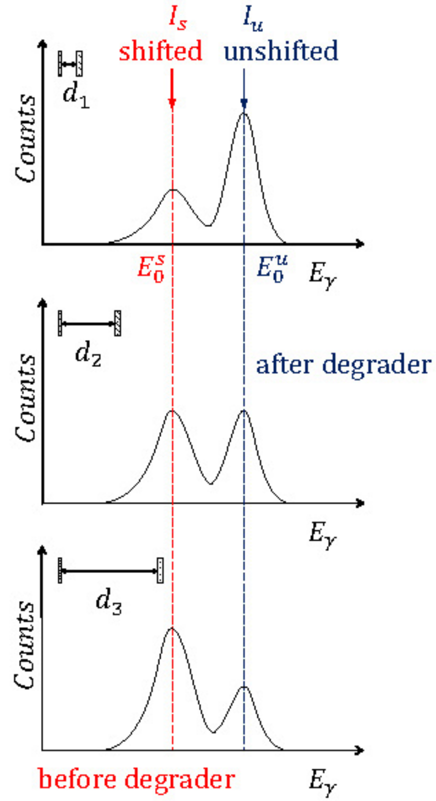

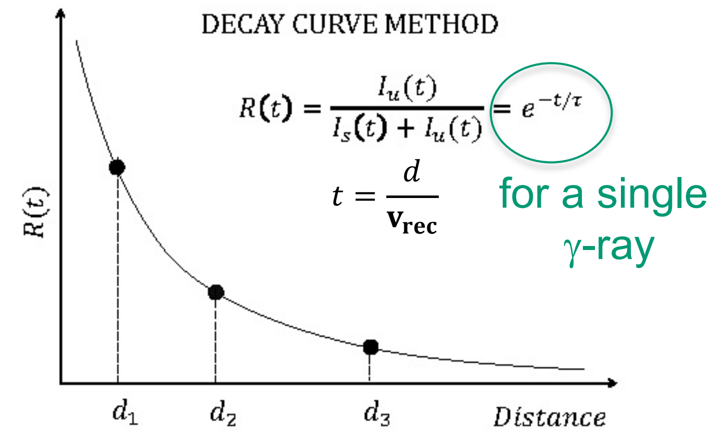

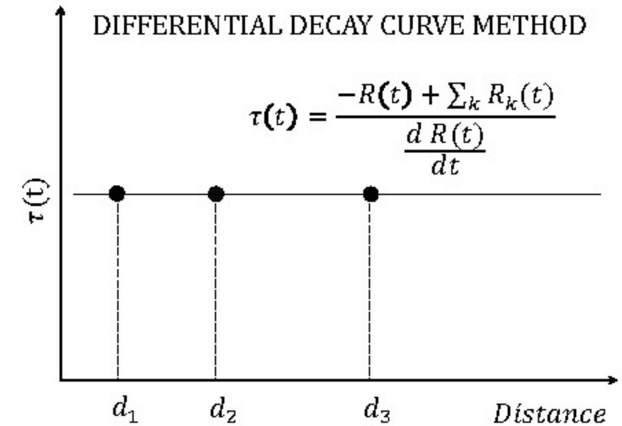

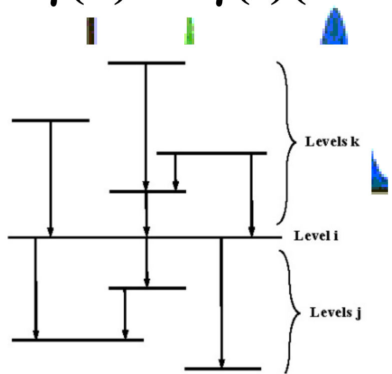

$$\frac{dn_i(t)}{dt} = -\lambda_i n_i(t) + \sum_{k=i+1}^{N} \lambda_k n_k(t) b_{ki},$$

Bateman equation

$$R_i(t) = P_i e^{-t\lambda_i} + \sum_{k=i+1}^{N} M_{ki}\left[(\lambda_i/\lambda_k)e^{-t\lambda_k} - e^{-t\lambda_i}\right],$$

$$M_{ki}(t)(\lambda_i/\lambda_k - 1) = b_{ki}P_k - b_{ki}\sum_{m=k+1}^{N} M_{mk} + \sum_{m=i+1}^{k-1} M_{km} b_{mi}(\lambda_m/\lambda_k)$$

A. Dewald et al. Prog. Part. Nucl. Phys. 67 (2012) 786.

Reduced Transition Probabilities

The square of the transition multipole operator is called Reduced Transition Probability and has not the energy dependence : $B(\lambda, j_i \to j_f) \equiv \sum_{\mu, m_f} |\langle j_f m_f | M(\lambda, \mu) | j_i m_i \rangle|^2$

Relation between the transition probability T and the reduced transition probability B.
(T are in units of sec^{-1} , B(E,λ) in e^2 fm$^{2\lambda}$, B(M,λ) in μ^2_N fm$^{2\lambda-2}$ and E in MeV.

$T(E1)$	=	1.59×10^{15}	E^3	$B(E1)$
$T(E2)$	=	1.22×10^{9}	E^5	$B(E2)$
$T(E3)$	=	5.67×10^{2}	E^7	$B(E3)$
$T(E4)$	=	1.69×10^{-4}	E^9	$B(E4)$
$T(M1)$	=	1.76×10^{13}	E^3	$B(M1)$
$T(M2)$	=	1.35×10^{7}	E^5	$B(M2)$
$T(M3)$	=	6.28×10^{0}	E^7	$B(M3)$
$T(M4)$	=	1.87×10^{-6}	E^9	$B(M4)$

Weisskopf estimates:

When the transition is due to a single proton that changes from one shell-model state to another: EL/ML electric/Magnetic transition probability.

$$T(E1) = 1.0 \times 10^{14} A^{2/3} E^3$$
$$T(E2) = 7.3 \times 10^{7} A^{4/3} E^5$$
$$T(E3) = 34 A^2 E^7$$
$$T(E4) = 1.1 \times 10^{-5} A^{8/3} E^9$$

$$T(M1) = 5.6 \times 10^{13} E^3$$
$$T(M2) = 3.5 \times 10^{7} A^{2/3} E^5$$
$$T(M3) = 16 A^{4/3} E^7$$
$$T(M4) = 4.5 \times 10^{-6} A^2 E^9$$

- e.g. Single particle or multiparticle states in non collective Shell Model Nuclei g.s. E2 up to few W.u.
- e.g.Collective states in quadrupole deformed heavy Nuclei g.s. E2 up to several hundred of W.u.

Forbidden E1 transitions in ^{64}Ge between states with T=0

Studying the violation of isospin symmetry induced by the Coulomb interaction is the observation of E1 transitions in even–even $N = Z$ nuclei. In the long-wavelength limit, the matrix elements of the nuclear E1 operator vanish when both the initial and final states have equal isospin T and $T_3 = 0$

E. Farnea et al. Phys. Lett. B (2002)

^{32}S + ^{40}Ca 125MeV

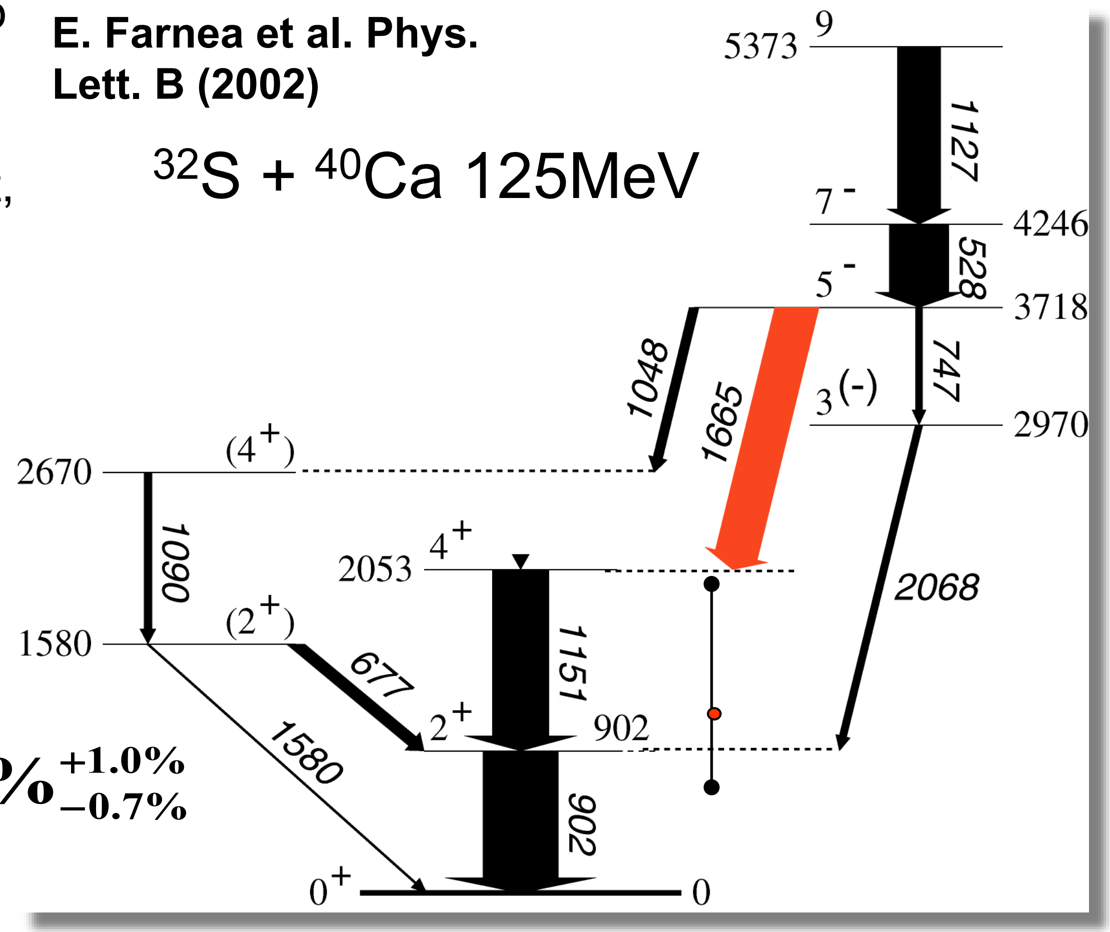

$$\alpha^2 = 2.5\%^{+1.0\%}_{-0.7\%}$$

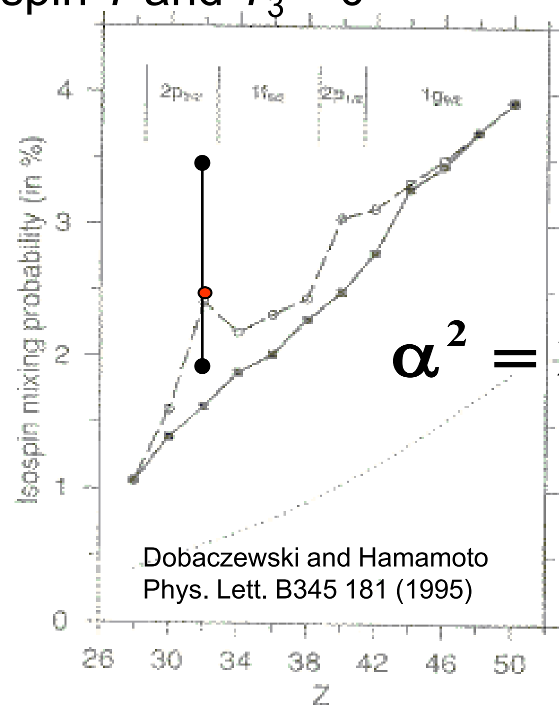

Dobaczewski and Hamamoto Phys. Lett. B345 181 (1995)

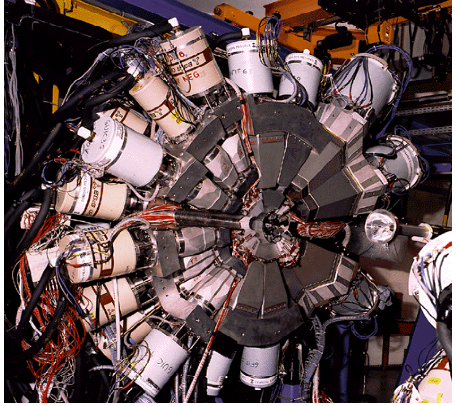

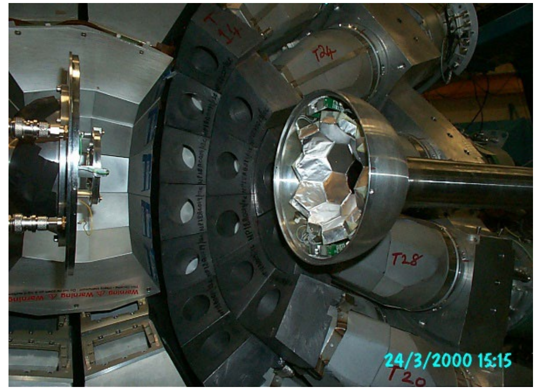

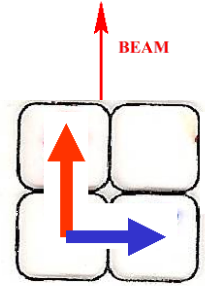

$$A = \frac{N_{\perp} - N_{\parallel}}{N_{\perp} + N_{\parallel}}$$

Angular distribution

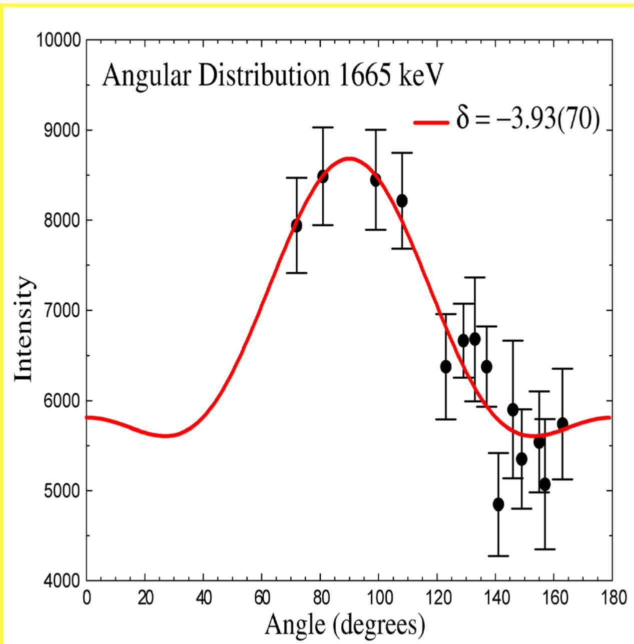

δ = - 3.93 (70)

B(M2) = 6.1(1.6) W.u.

B(E1) = 2.3 (1.3) 10^{-7} W.u.

Lifetime

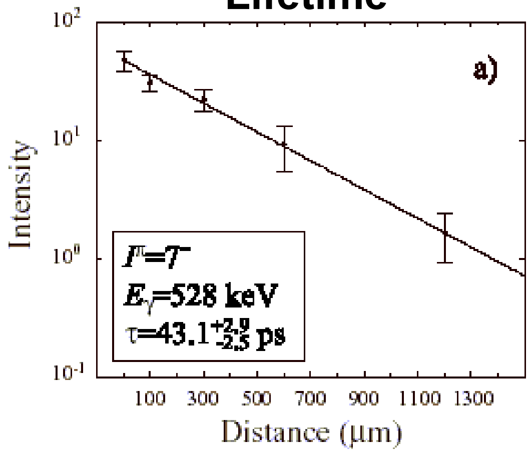

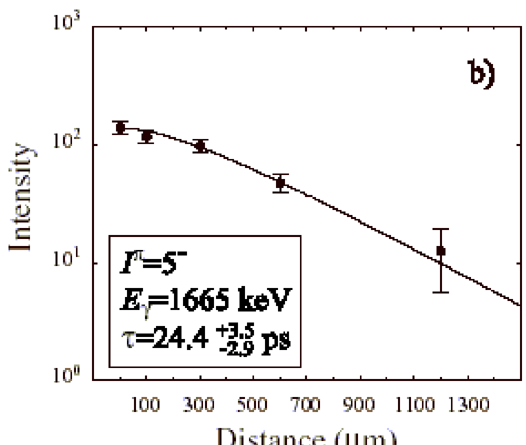

Asymmetry and polarization

A = $N_{\perp}$-$N_{\parallel}$/($N_{\perp}$+$N_{\parallel}$)

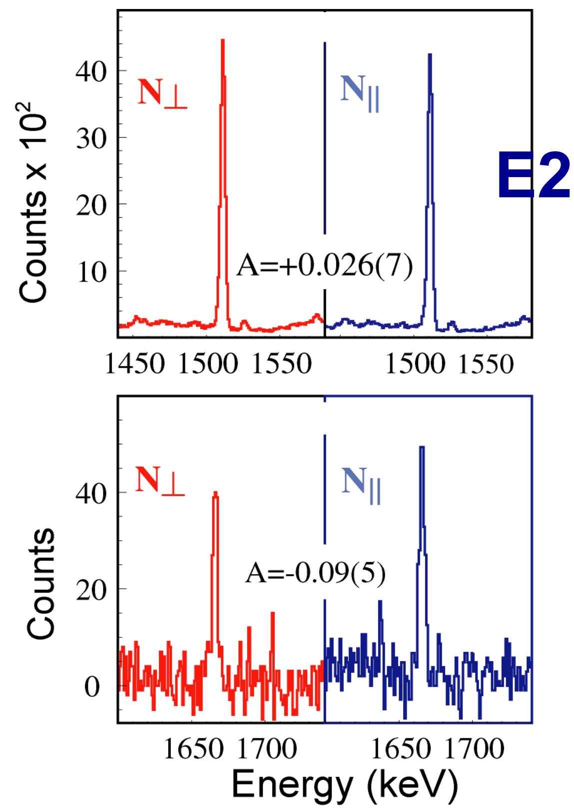

The 1665 keV transition mixed E1/M2 character ~93% quadrupole contents

How Can We Measure It?

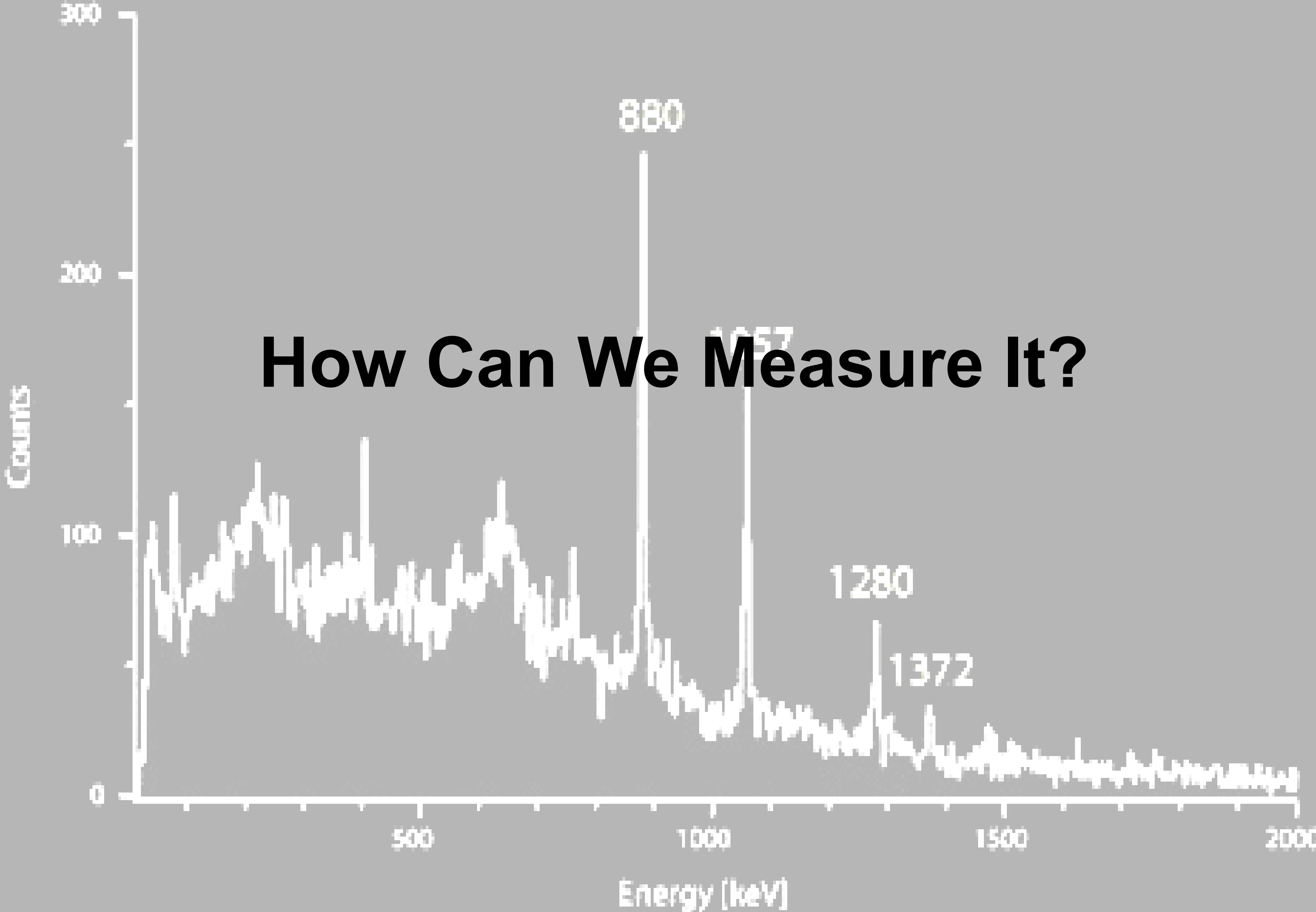

Interaction of the γ-rays with matter

~ 100 keV ~1 MeV ~ 10 MeV γ-ray energy

Photoelectric | **Compton Scattering** | **Pair Production**

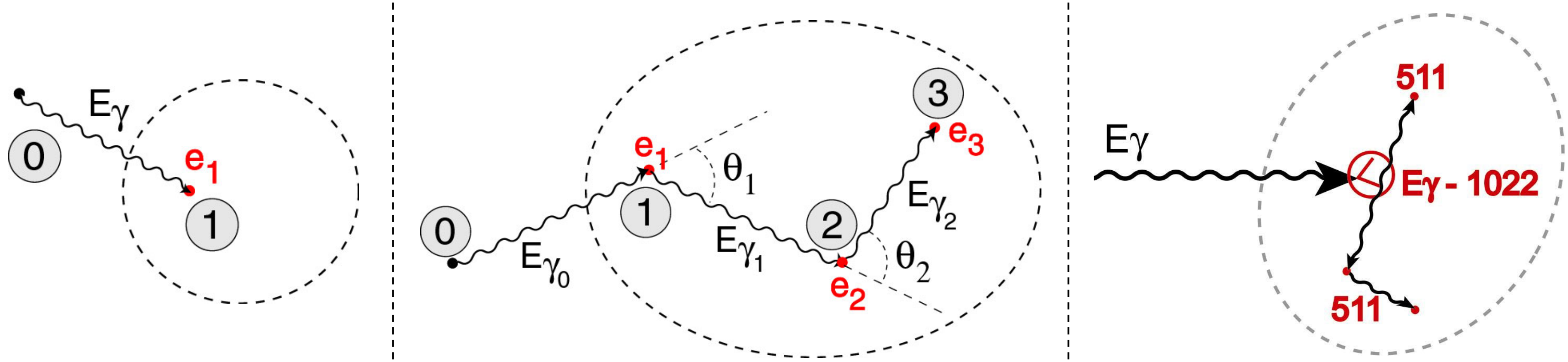

$$E_{\gamma'} = \frac{E_\gamma}{1 + \frac{E_\gamma}{m_0 c^2}\left(1 - \cos\theta\right)}$$

Instrumentation for HR γ-ray spectroscopy

High resolution γ-ray spectroscopy → large volume semiconductor detectors in particular detectors based on HP-Ge (impurities $\sim 10^{-12}$)

Present Ge
>2 kg/crystal

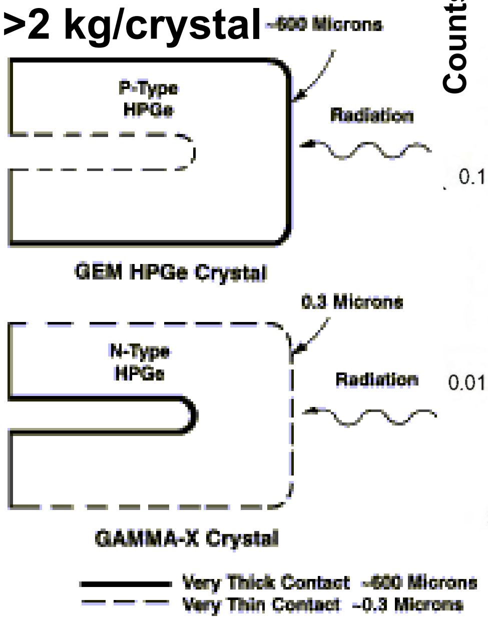

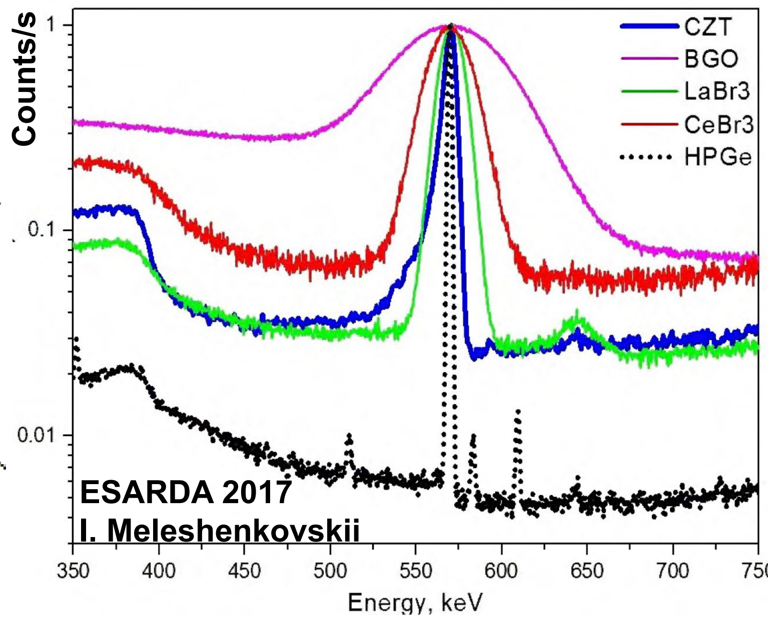

Compton suppressed Ge-detectors → arrays

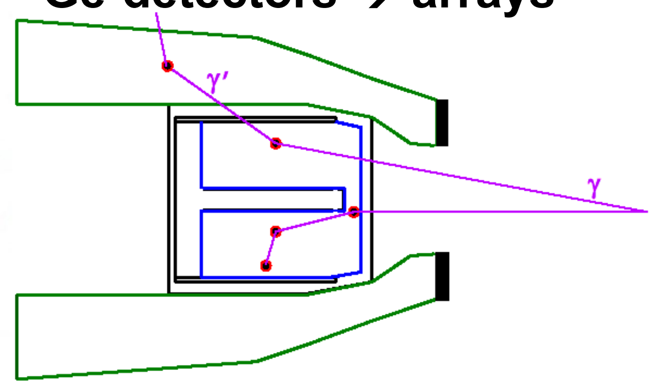

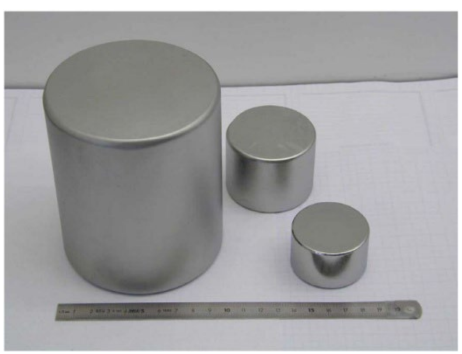

Composite detectors

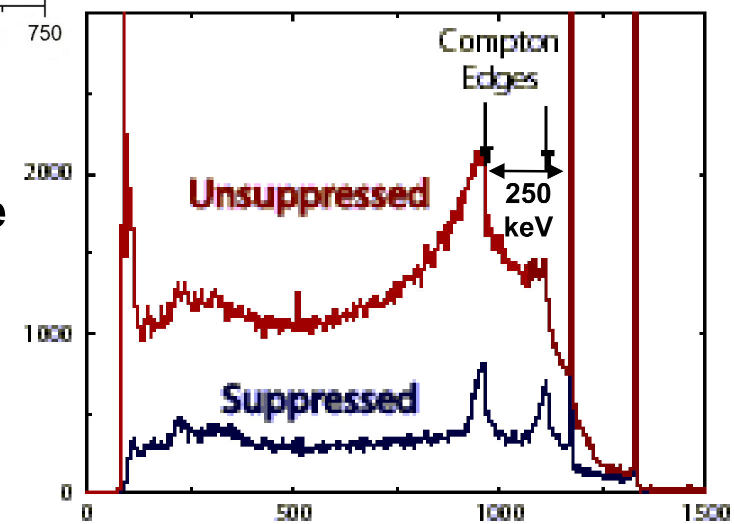

Bibliography: G.F.Knoll, Radiation Detection and Measurement (Wiley)

Instrumentation for HR γ-ray spectroscopy

High resolution γ-ray spectroscopy → large volume semiconductor detectors in particular detectors based on HP-Ge (impurities ~10^{-12})

Present Ge
>2 kg/crystal

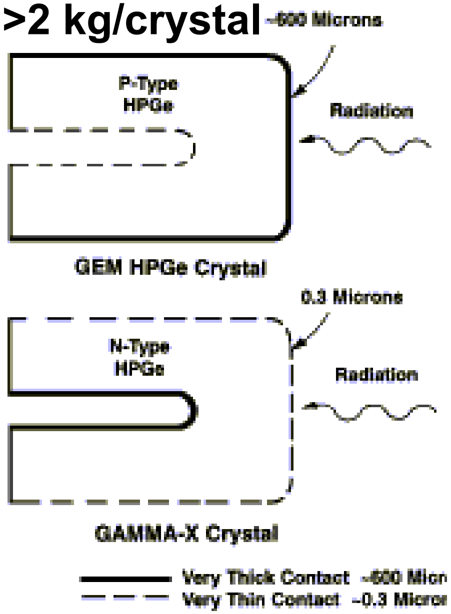

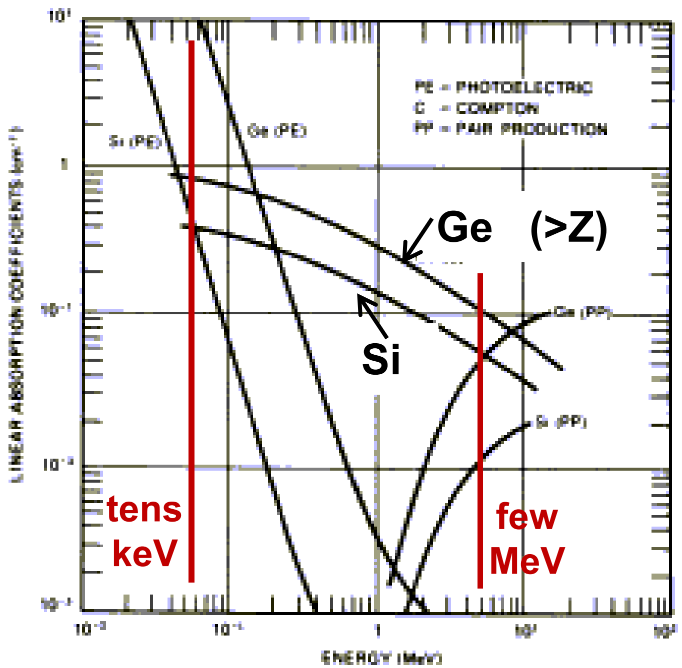

Compton suppressed Ge-detectors → arrays

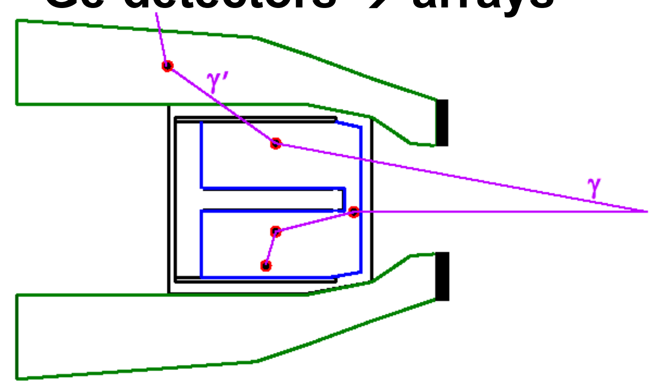

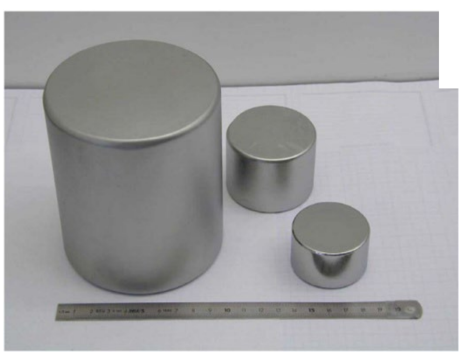

Composite detectors

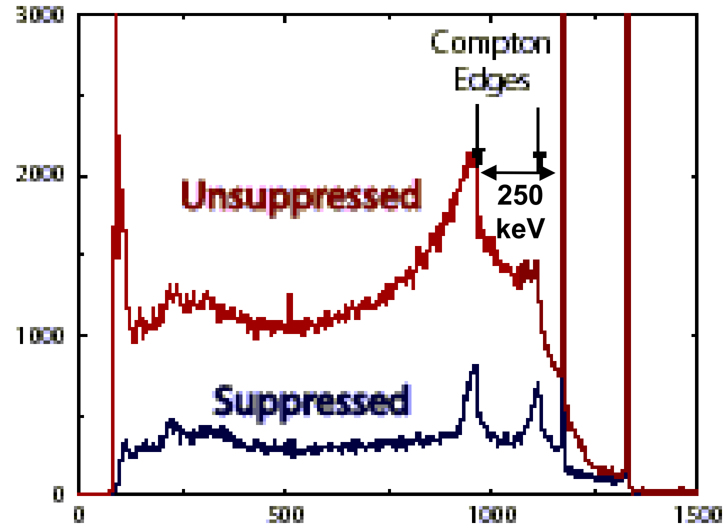

Bibliography: G.F.Knoll, Radiation Detection and Measurement (Wiley)

Germanium detector

Sensitivity factors: Energy Resolution, Peak to Total Ratio

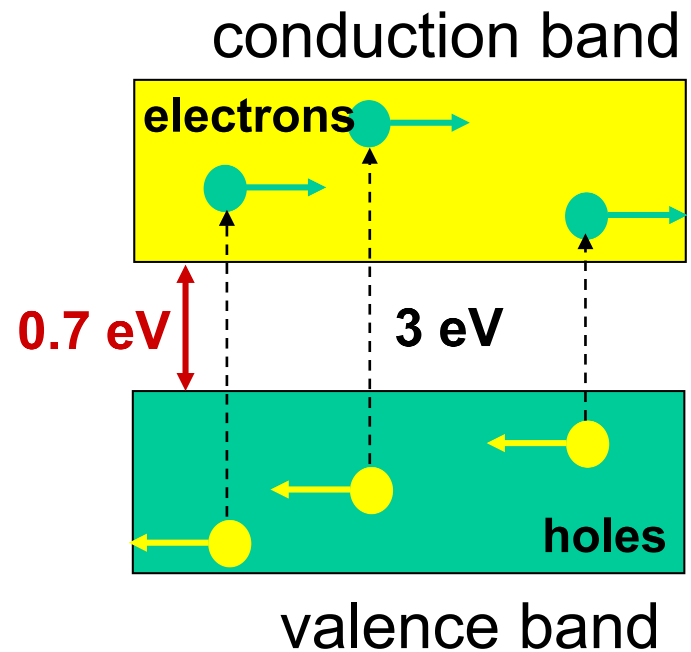

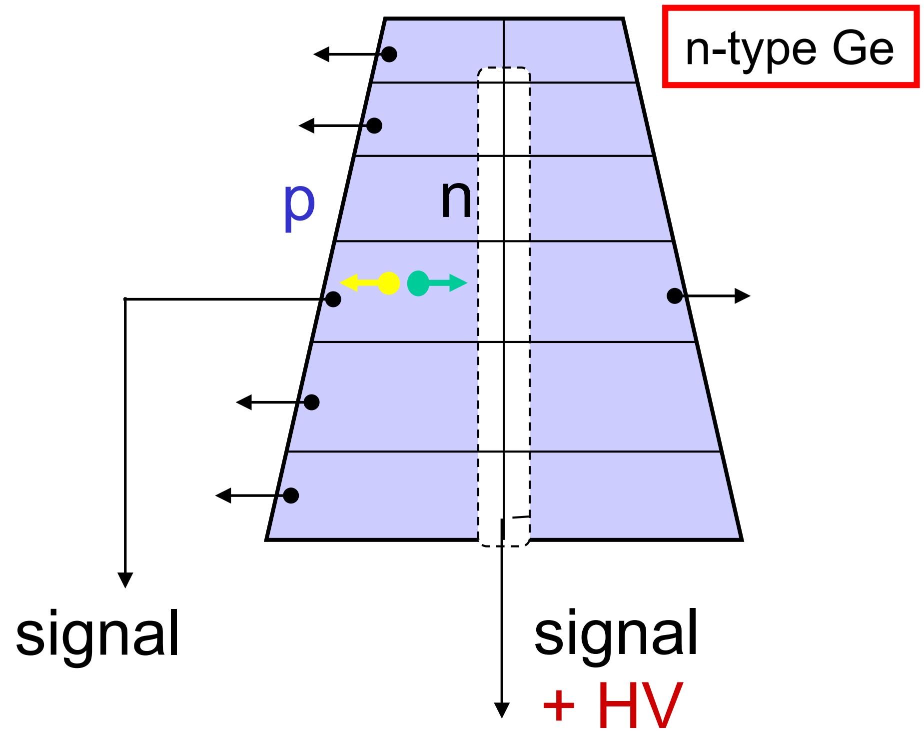

Number of e-h pairs for 1 MeV, $N = 10^6 / 3 = 3 \times 10^5$

Energy resolution (Fano Factor)

$$\sqrt{N}/N = 0.0018 \rightarrow 1.8\,\text{keV}\,(\text{E}_\gamma = 1MeV)$$

Germanium detector Readout

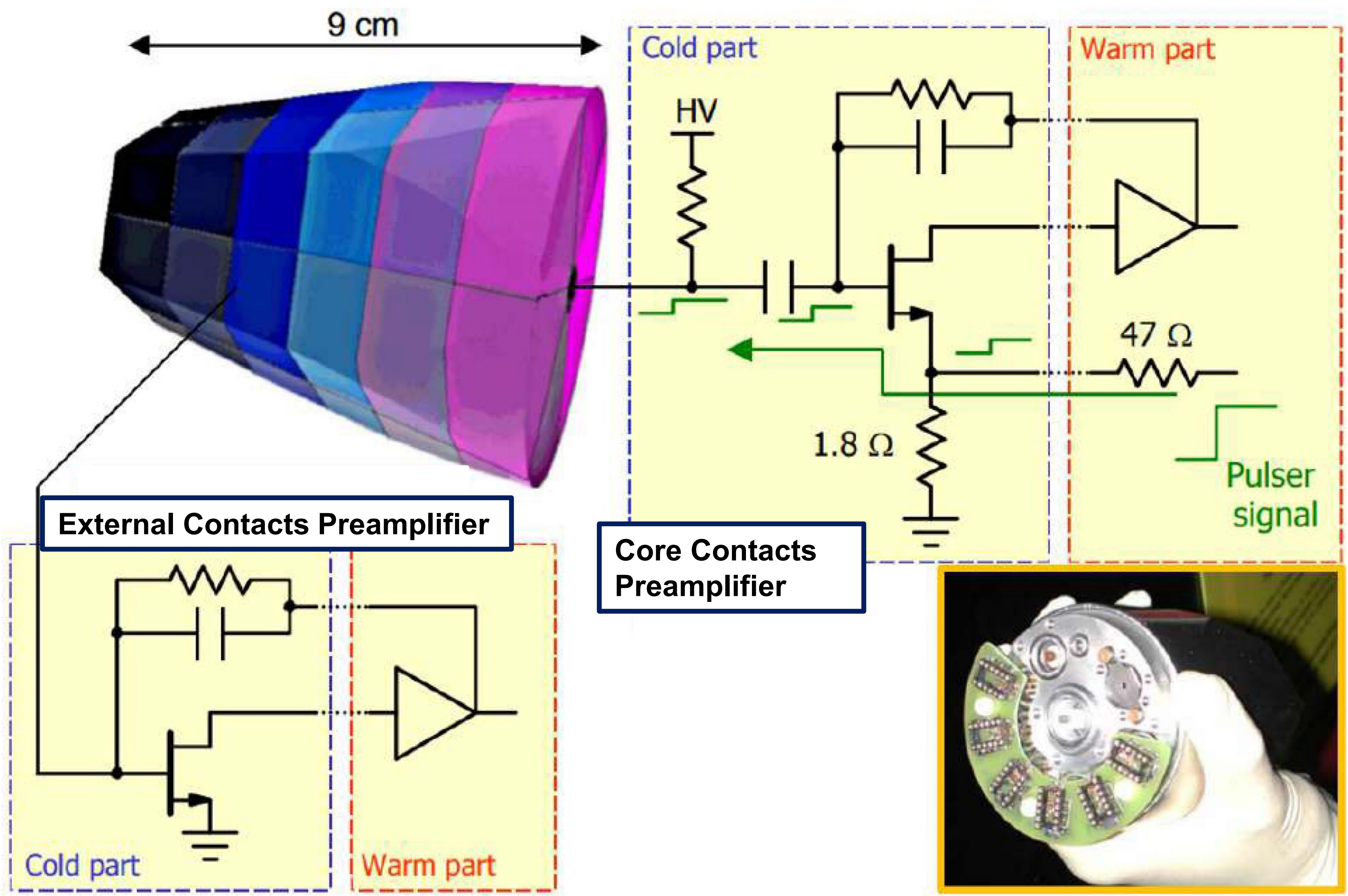

Schematic Readout preamplifier for a detector with multiple external contacts

Thermally activated charge carriers in the conduction band density at room temperature ~ 2.5 10^{13} cm^{-3} for Ge (~ 1.5 10^{10} cm^{-3} for Si)

To reduce the number of free charge carriers :

- => deplete material: np junction
- => increase depletion by applying a reverse bias
- => for Ge, cool detector with LN_2 - 77K

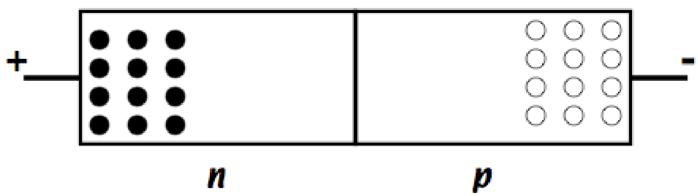

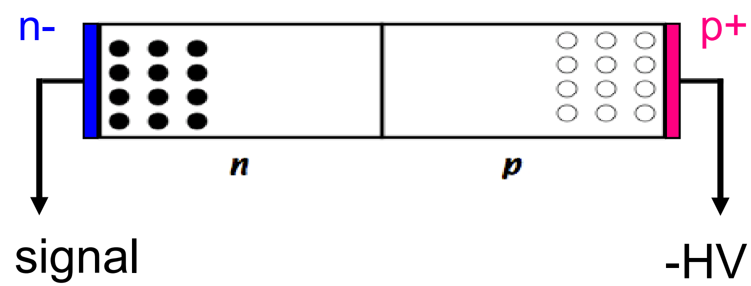

$$FWHM^2 = W^2_D + W^2_X + W^2_E + W^2_{Doppler}$$

$W_D = 2.35\sqrt{F\varepsilon E_\gamma}$ Statistical fluctuations of carriers

ε = 2.96 eV @ 77 K Fano factor F ~ 0.1

(not all the deposited energy goes to create e-h pairs)

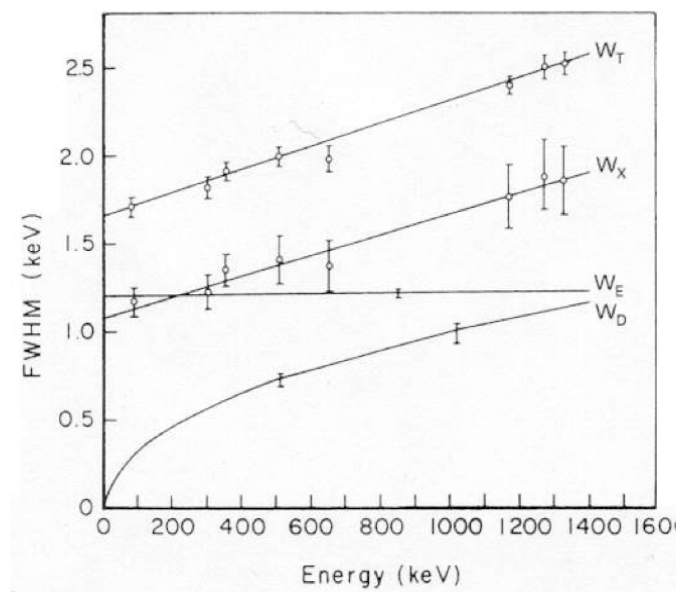

W_X incomplete charge collection

W_E electronic noise

$W_{doppler}$ Doppler broadening

Doppler Broadening

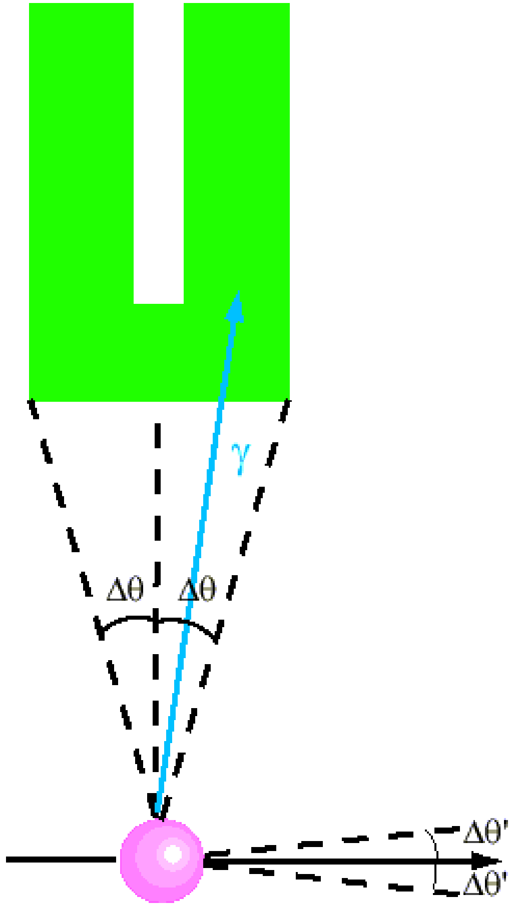

$$E_S = E_0\left(1 + v/c\cos\theta\right)$$

$$\Delta E_S = E_0\, v/c \sin\theta\Delta\theta$$

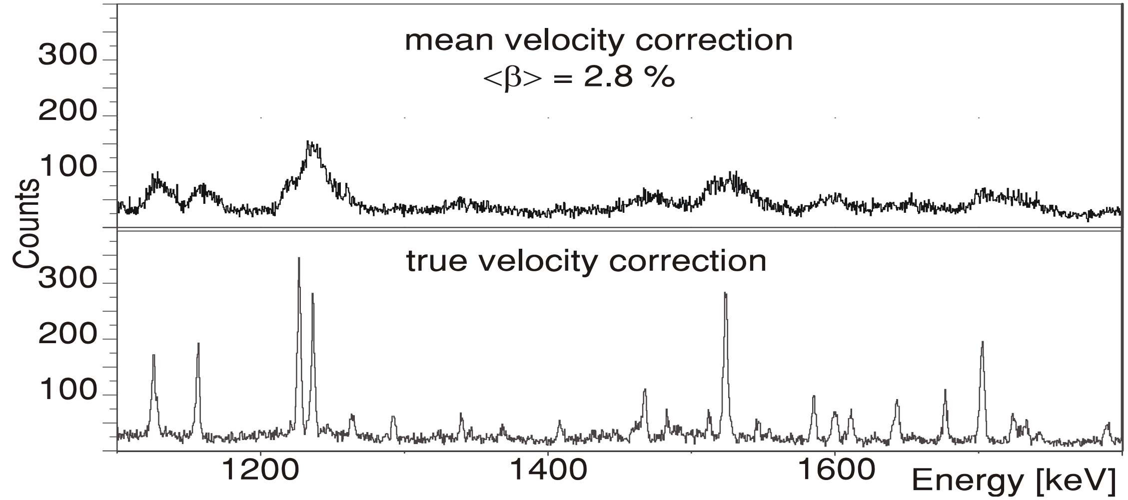

Dedicated ancillary detectors for the determination of the recoil trajectory

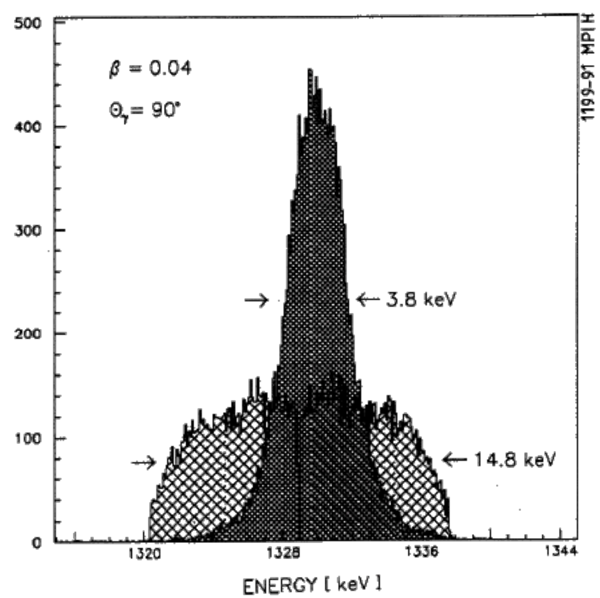

Development of segmented Ge detectors and Pulse Shape Analysis techniques for position determination

Signal-to-noise ratio and Compton suppression

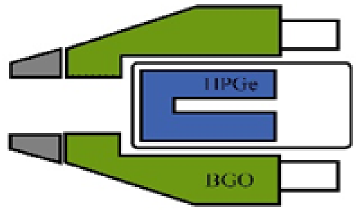

Early arrays made of Ge Detectors with Anti-Compton Shield

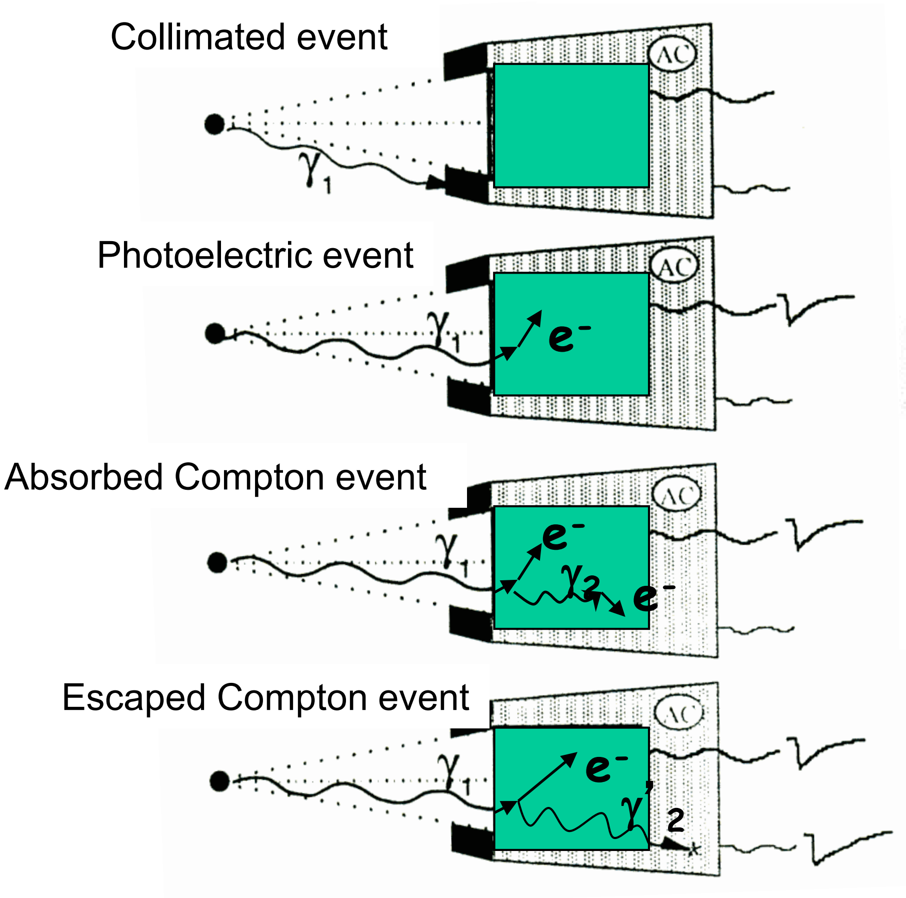

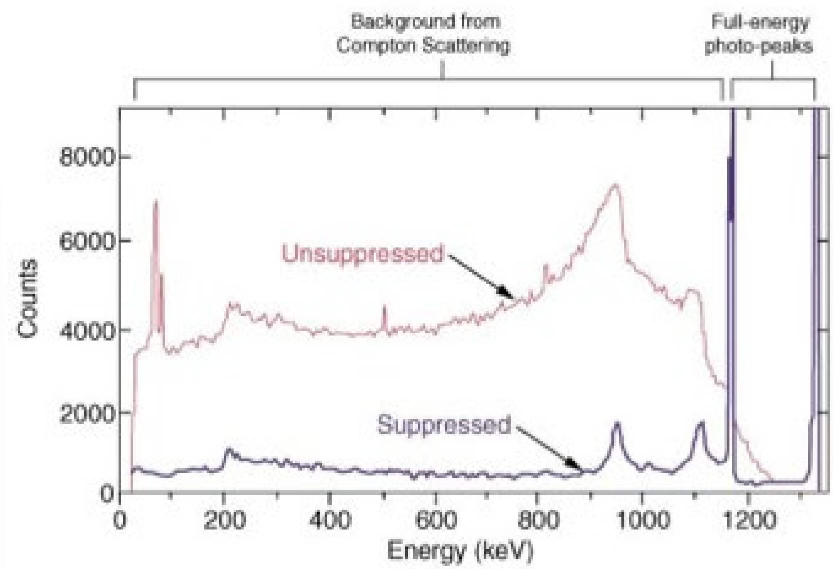

P/T ~ 0.2-0.3 => 0.5-0.6

Composite detectors

=> Reduction of $\Delta\theta_D$

- Eurogam II
- Clovers:

- 4 crystals in 1 cryostat

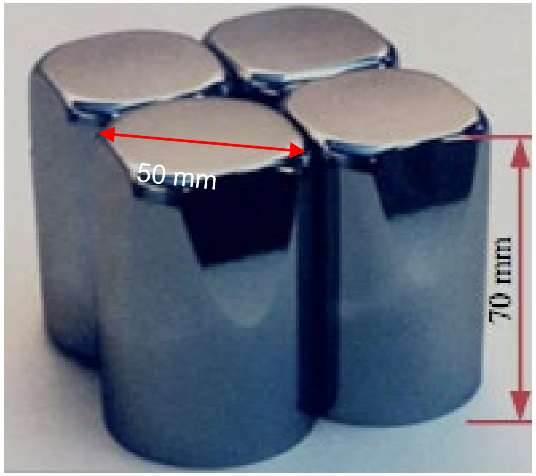

^{30}Si(158 MeV)+^{124}Sn → ^{149}Gd
v/c=2.1%

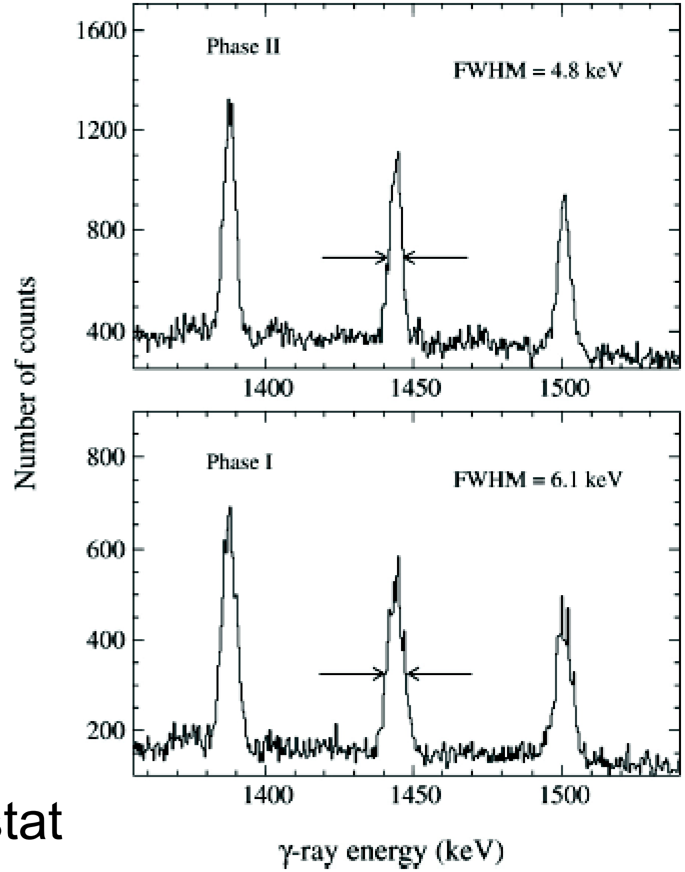

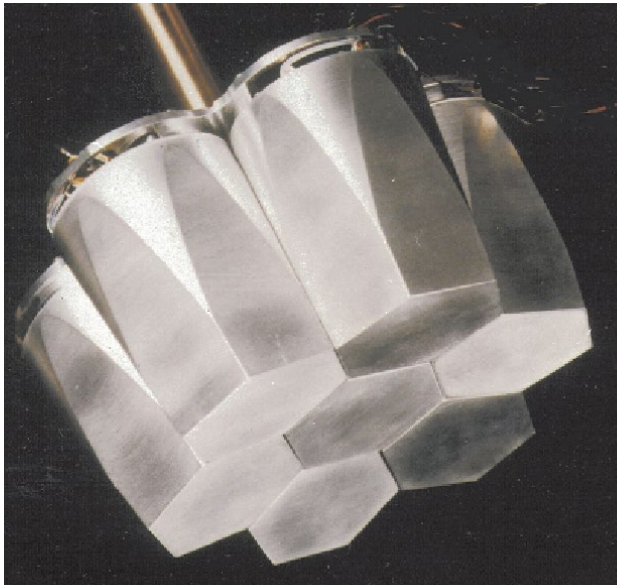

- Euroball
- Clusters:

- 7 crystals in 1 cryostat

Electrical Segmentation of detectors

- Gammasphere segmented detector (2 Fold)
- Exogam at Ganil (Segmented Clover 4 fold)
- Miniball at Isolde (Segmented Clusters 6 fold)
- AGATA ?

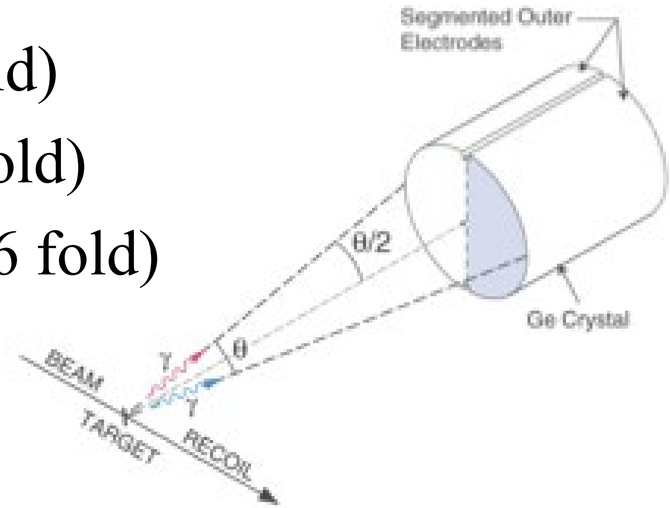

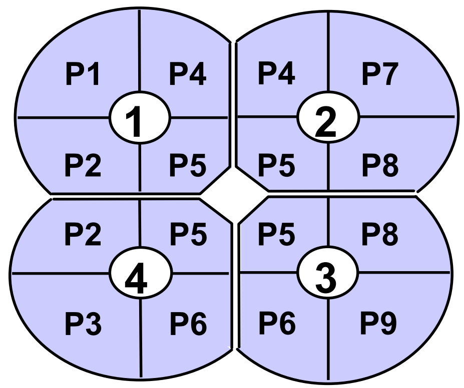

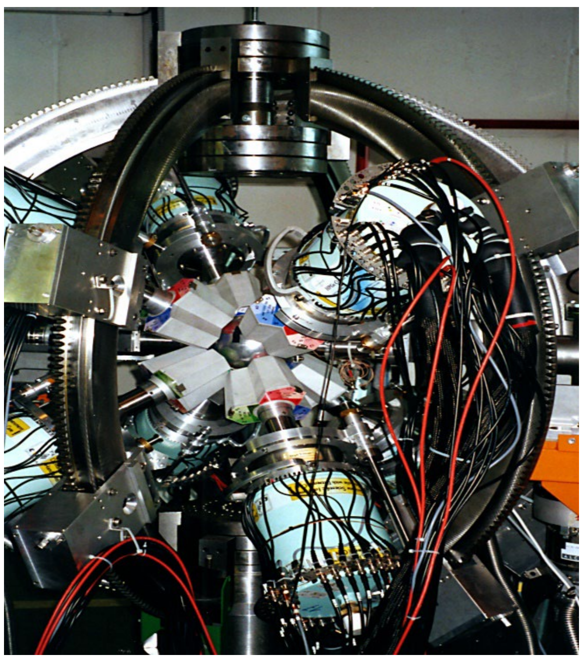

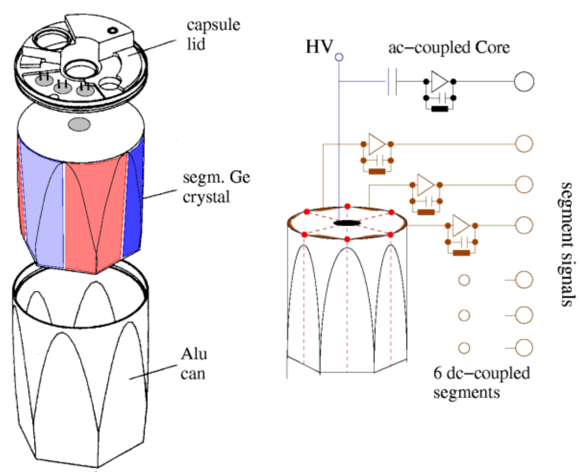

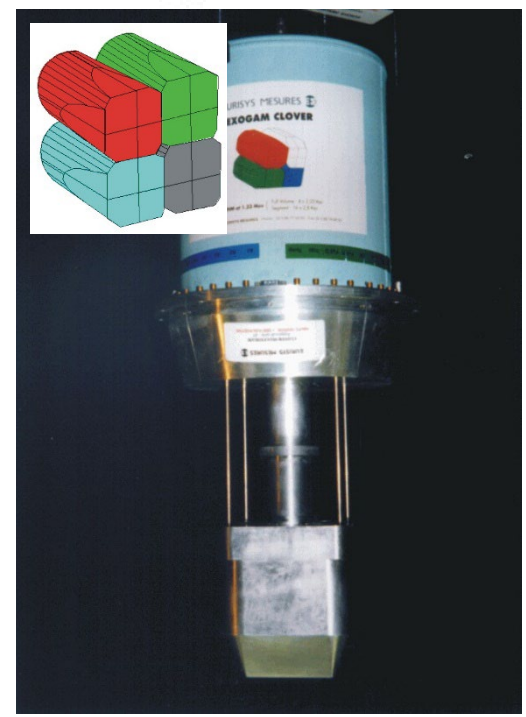

Contemporary HR γ-Spectroscopy Instrumentation

Late 90's
Large γ–Arrays

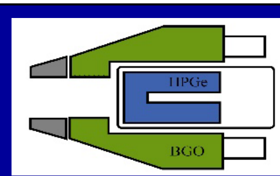

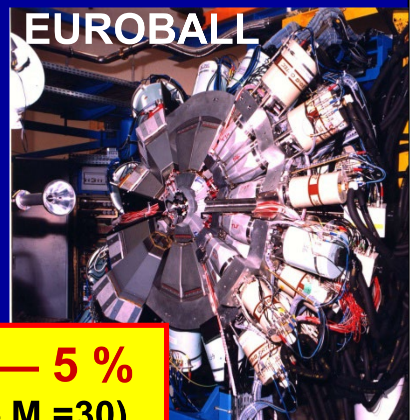

$\varepsilon \sim$ **10 — 5 %**
(M_γ=1 – M_γ=30)

Compact γ–Arrays optimized
Doppler correction, low Mγ

$\varepsilon \sim$ **20 %** **M_γ=1**

Tracking Arrays based on
Position Sensitive Ge Detectors

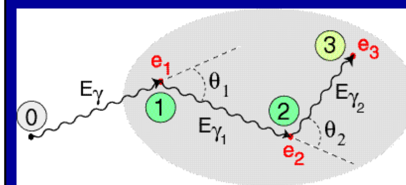

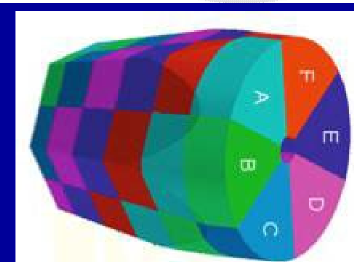

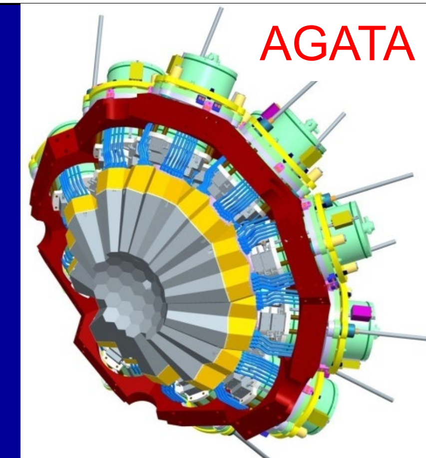

Two Tracking Arrays projects:
GRETA (USA) & AGATA (EU)

>15y R&D

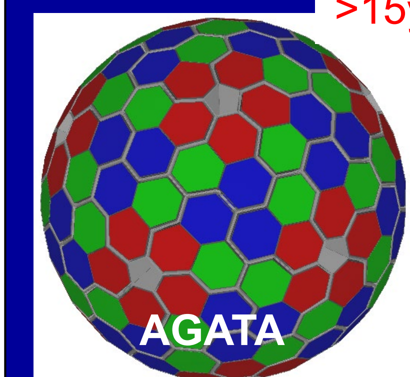

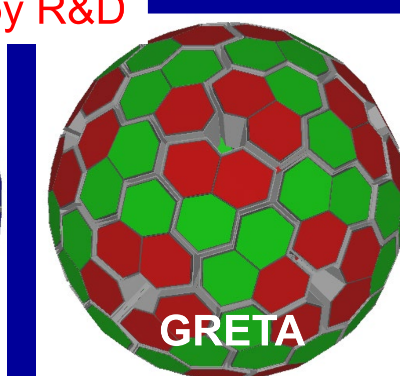

$\varepsilon \sim$ **40 — 20 %**
(M_γ=1 – M_γ=30)

AGATA

(Advanced GAmma Tracking Array)

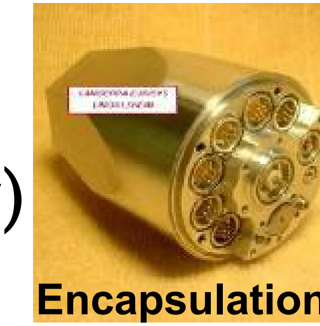

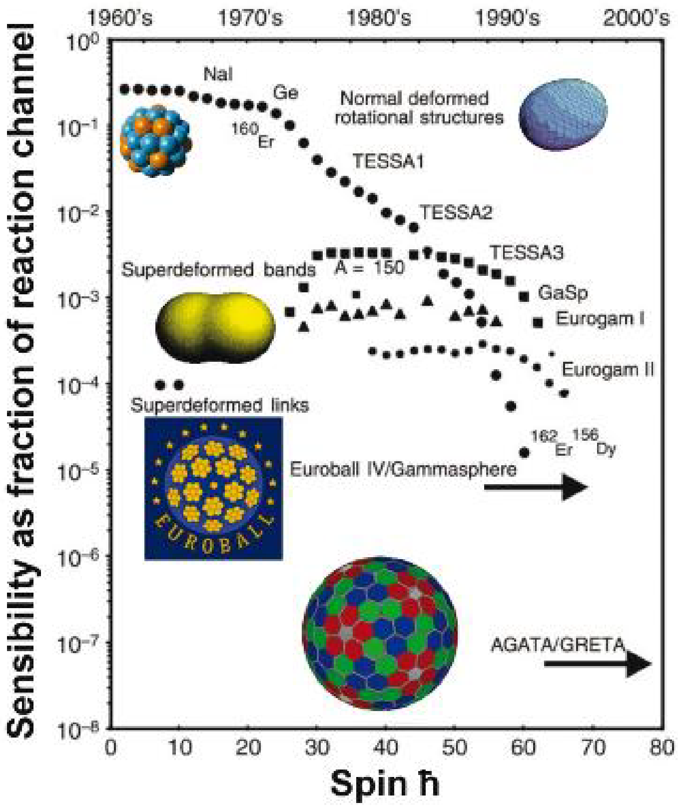

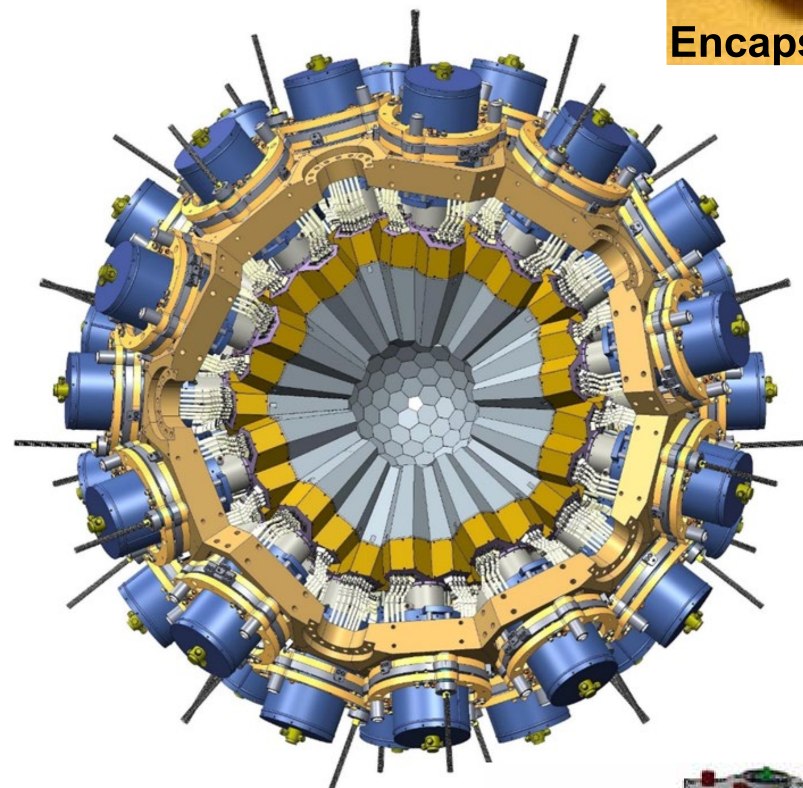

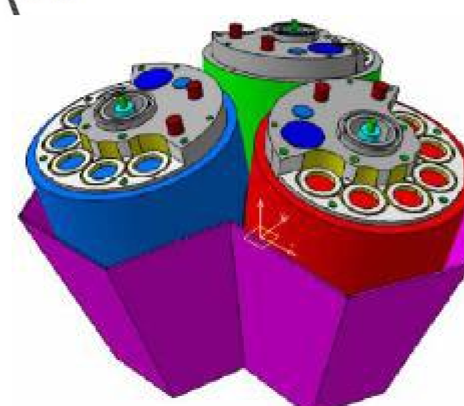

180 Large Volume Encapsulated 36-fold segmented HP-Ge

6660 high-resolution digital electronics channels

High throughput DAQ

Pulse Shape Analysis → position sensitive operation mode

γ-ray tracking algorithms → maximum efficiency and P/T

Tracking Arrays
Aiming for Accuracy

Conditions:
- Low intensity for the nuclei of interest / require high sensitivity
- High background levels
- Large Doppler broadening (specially in in-flight facilities)
- High counting rates (digital FEE)
- High γ-ray multiplicities (Tracking)

$\Omega \sim 40\%$

$\varepsilon_{ph} \sim 10\%$

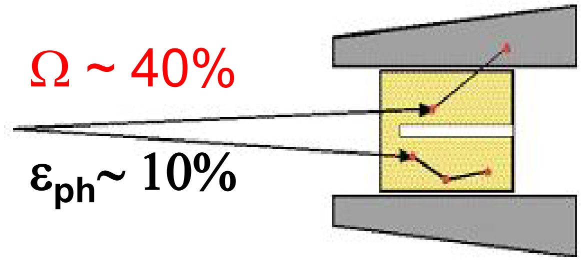

Compton Suppressed
- solid angle taken by the AC shields
- large opening angle ➔ poor energy resolution

$\Omega \sim 80\%$

$\varepsilon_{ph} \sim 40\%$

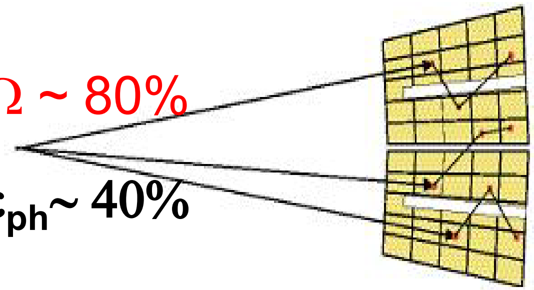

Tracking array
- Large solid angle
- Position sensitive mode using PSA
- Large P/T using tracking for γ-ray reconstruction

Correction of neutron damage

B.Bruyneel EPJ A 49 (2013) 61

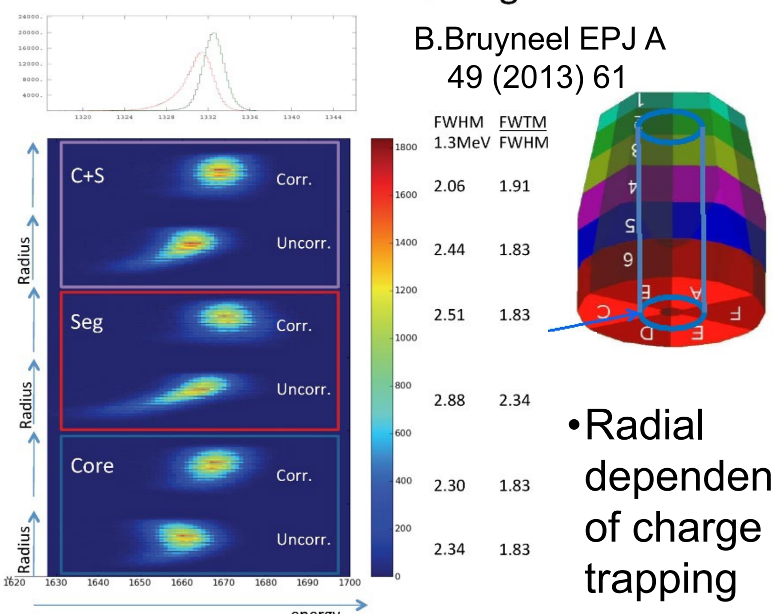

- Radial dependency of charge trapping

Doppler with PSA +Tracking

Total Resolution:

Opening $\Delta\theta$

Recoil $\Delta\beta$

Intrinsic

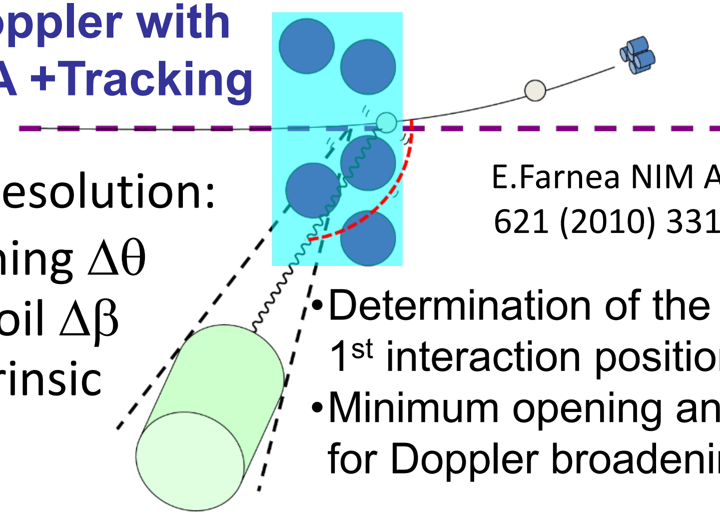

E.Farnea NIM A 621 (2010) 331

- Determination of the 1st interaction position
- Minimum opening angle for Doppler broadening

Position Sensitive Detector for γ-rays

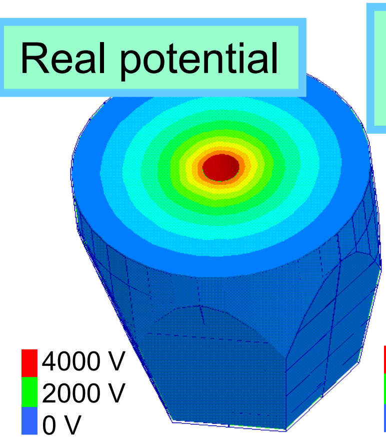

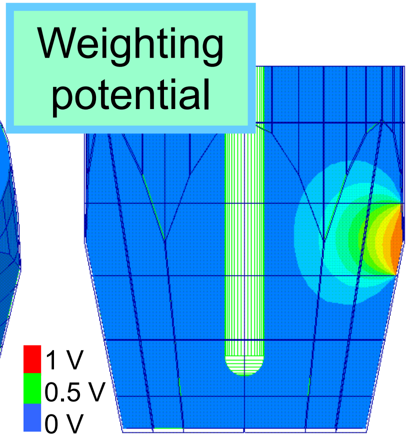

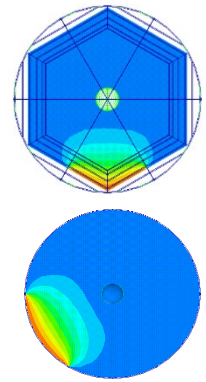

Induced current by the moving charge in the sensing contact → weighting potential Ramo's Theorem.

$$i_k = - q\vec{v} \cdot \vec{\nabla}\phi_k(r_q)$$

E. Gatti, et al. NIM 193 (82) 651

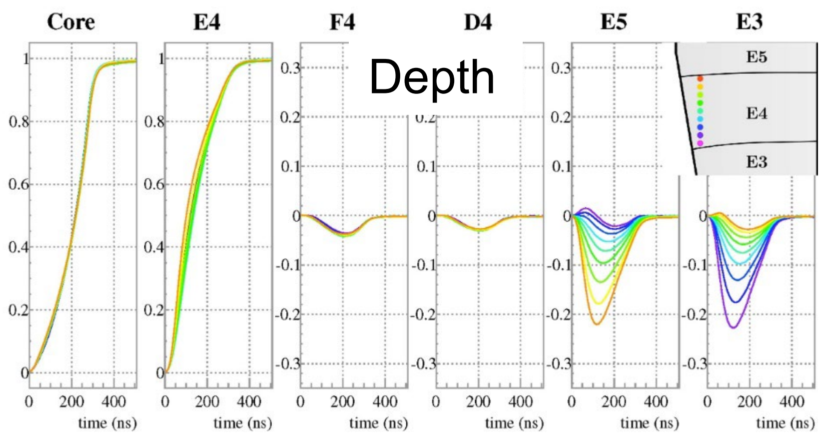

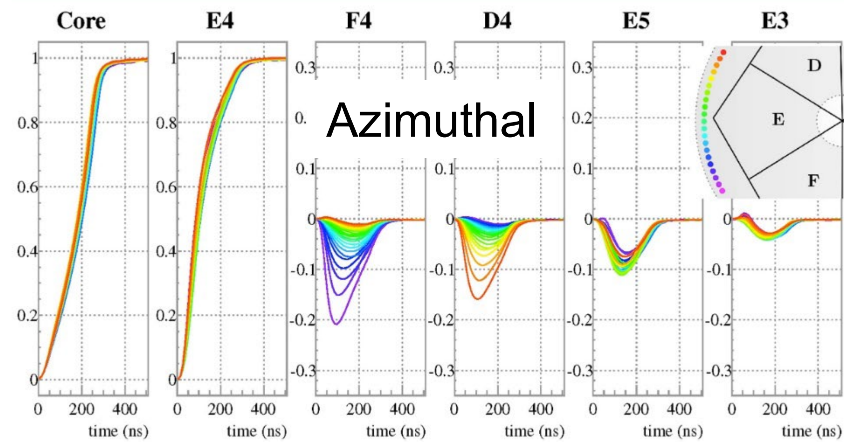

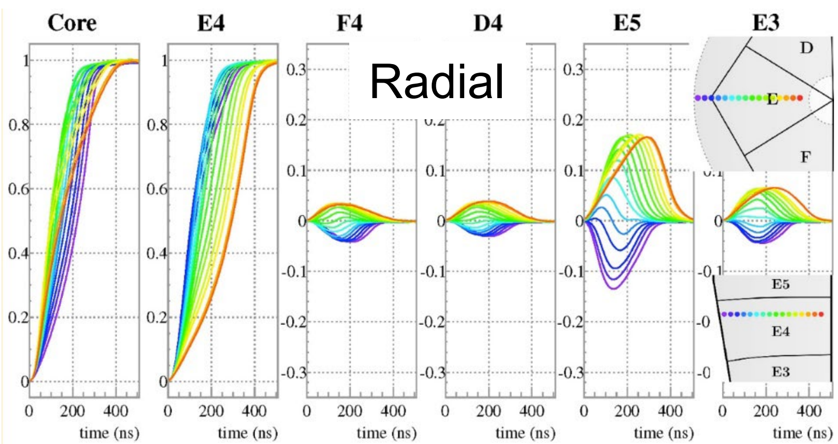

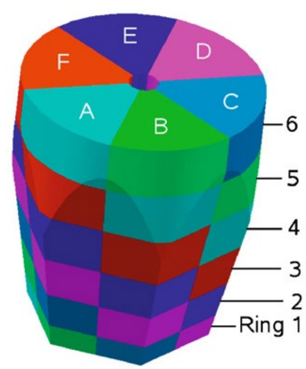

Figures courtesy of M.Ginsz, et al., IPHC Strasbourg

Gamma Tracking Array Concept

AGATA
ADVANCED GAMMA TRACKING ARRAY

Highly segmented HPGe detectors

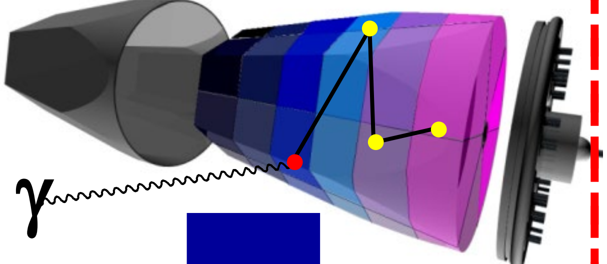

Synchronized digital electronics to digitize (14 bit, 100 MS/s) and process the 37 signals generated by crystals

Readout Raw Data (10 kB/evt/crystal)

HARDWARE

Pulse Shape Analysis of the recorded waves

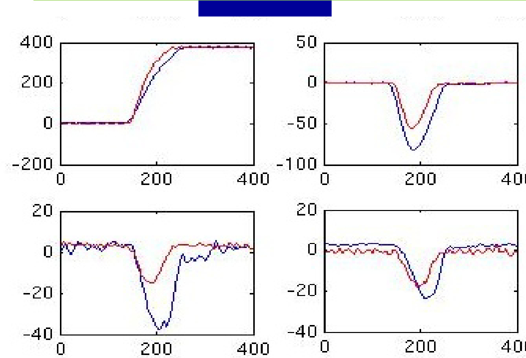

Energies, times, interaction points

$(x,y,z,E,t)_i$

Local level

Global level

Event building time-stamped data

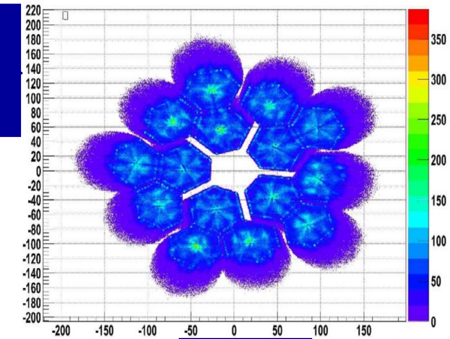

Reconstruction of γ-rays from the hits

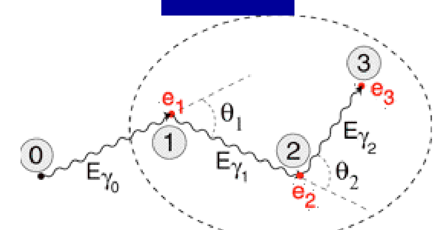

Analysis & correlation with other detectors

SOFTWARE

Analogue vs Digital Electronics

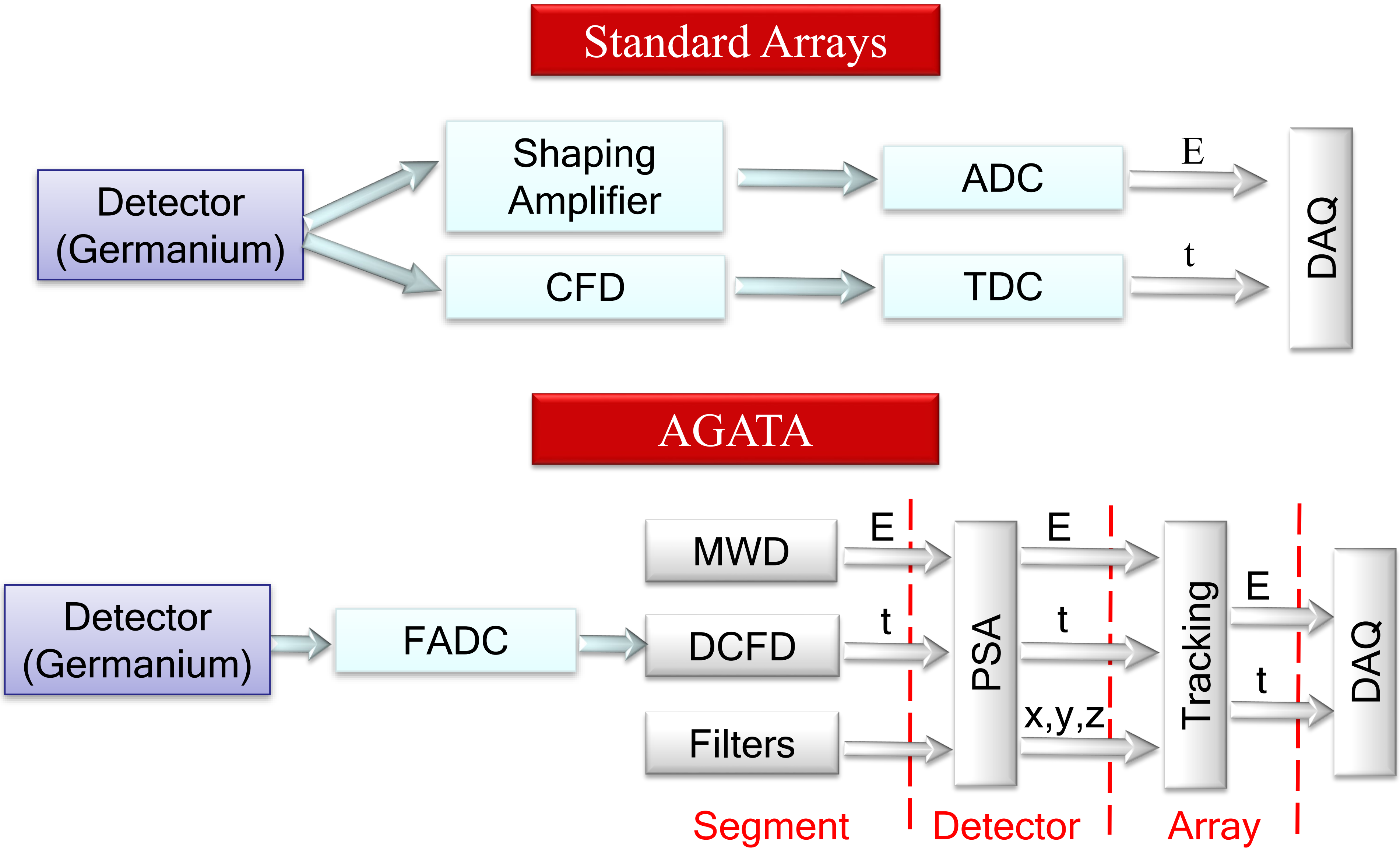

Energy with Digital signals: Moving Window Deconvolution

•removes shaping-effect of preamplifier
⇒current signal recovered
•calculates real collected charge by integrating current signal integration carried out within a moving window to avoid summation of events
•noise-suppression by averaging charge signal
•recursive algorithm

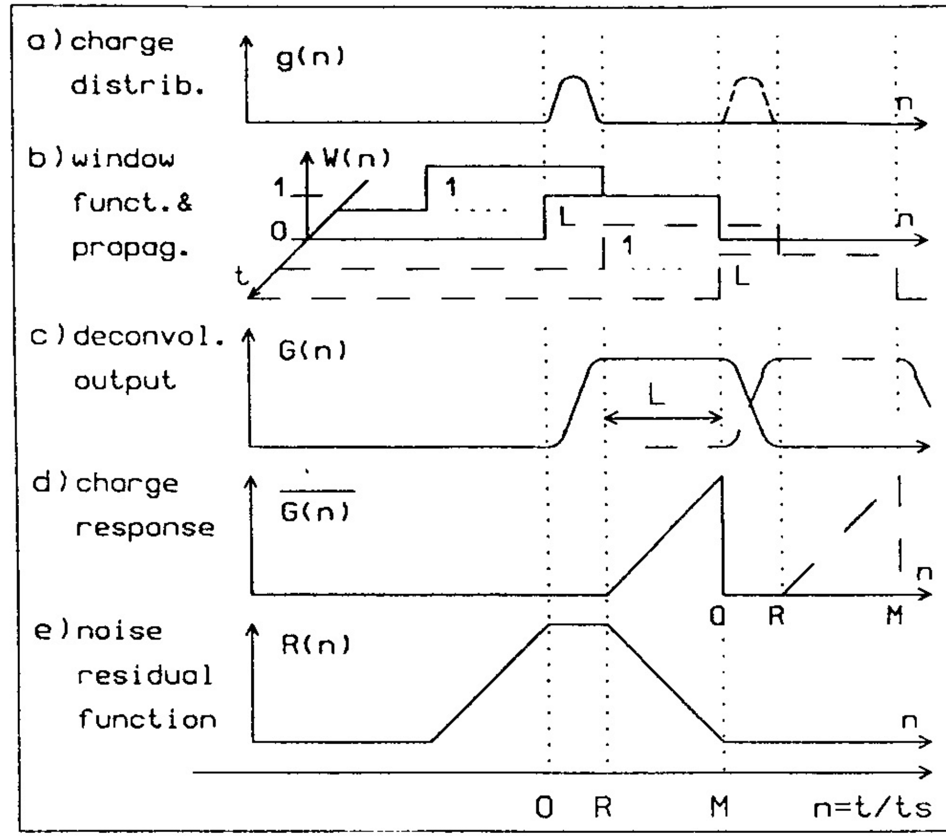

G[n] = G[n – 1] + FADC[n] – k × FADC[n – 1] – FADC[n – L] + k × FADC[n – L – 1]

K = pre-amplifier response ($e^{-\alpha}$)

A.Georgiev & W.Gast IEEE Nucl. Sci. 40 (1993) 770

Energy with Digital signals: Moving Window Deconvolution

•removes shaping-effect of preamplifier
⇒current signal recovered
•calculates real collected charge by integrating current signal integration carried out within a moving window to avoid summation of events
•noise-suppression by averaging charge signal
•recursive algorithm

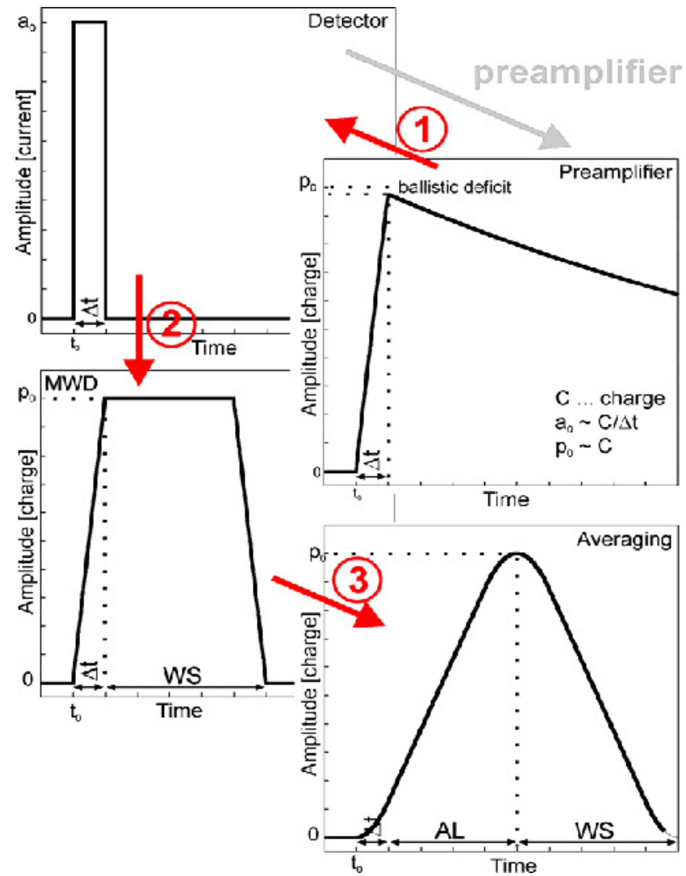

G[n] = G[n – 1] + FADC[n] – k × FADC[n – 1] – FADC[n – L] + k × FADC[n – L – 1]

k = pre-amplifier response (e $^{-\alpha}$)

A.Georgiev & W.Gast IEEE Nucl. Sci. 40 (1993) 770

Digital Pulse Processing for typical functions

- *Leading Edge Discrimination:*
- •y[n]=x[n]-x[n-k](*differentiation*)
- •y[n]= (x[n]+x[n-2]) +x[n-1]<<1(*Gaussian filtering*)
- •Threshold comparison →LED time
- *Constant Fraction Discrimination*:
- •y[n]=x[n]-x[n-k](*differentiation*)
- •y[n]= (x[n]+x[n-2]) +x[n-1]<<1(*Gaussian filtering*)
- •y[n]=x[n-k]<<a-x[n](*constant fraction*)
- •*Zero crossing comparison →CFD time*

J.T. Anderson IEEE Nucl. Sci. 25 (2007) 1751

Pulse Shape Analysis Concept

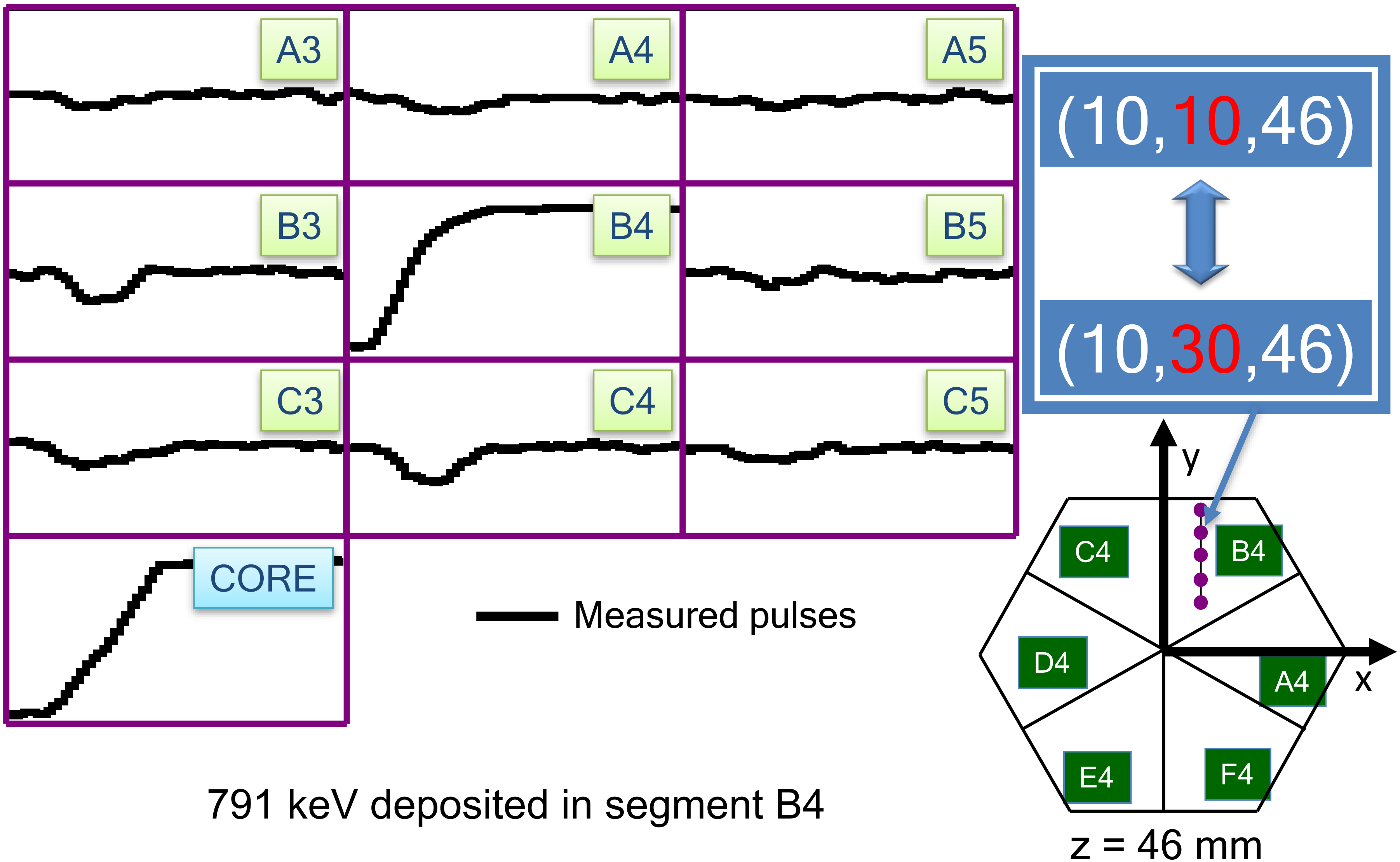

791 keV deposited in segment B4

Very Important: Measured pulses need to be time aligned

R.Venturelli, D.Bazzacco

Pulse Shape Analysis Concept

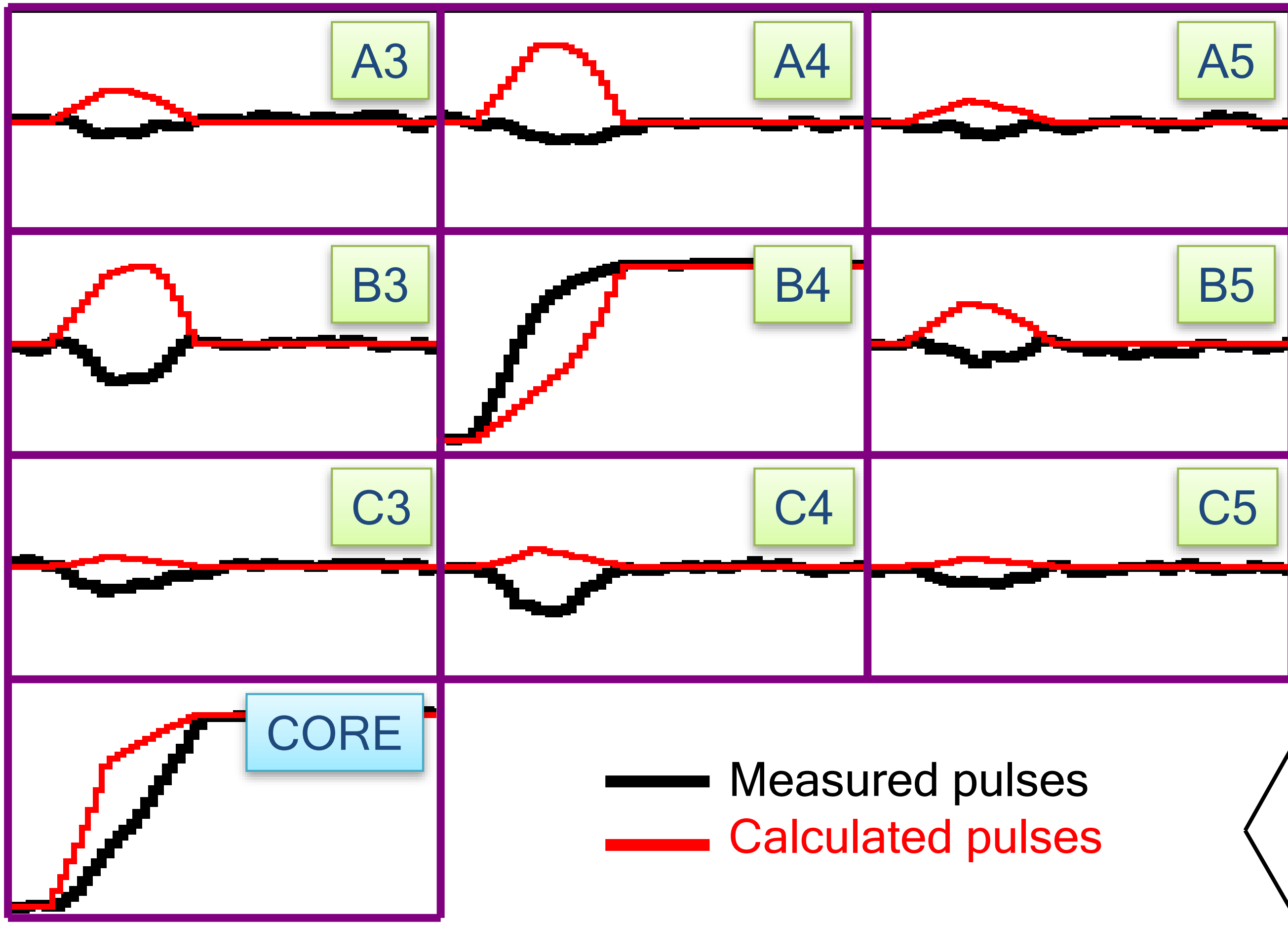

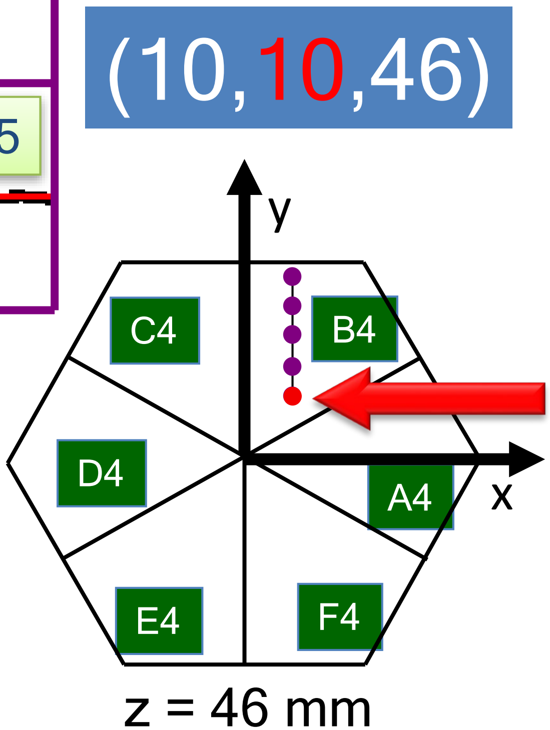

791 keV deposited in segment B4

R.Venturelli, D.Bazzacco

Pulse Shape Analysis Concept

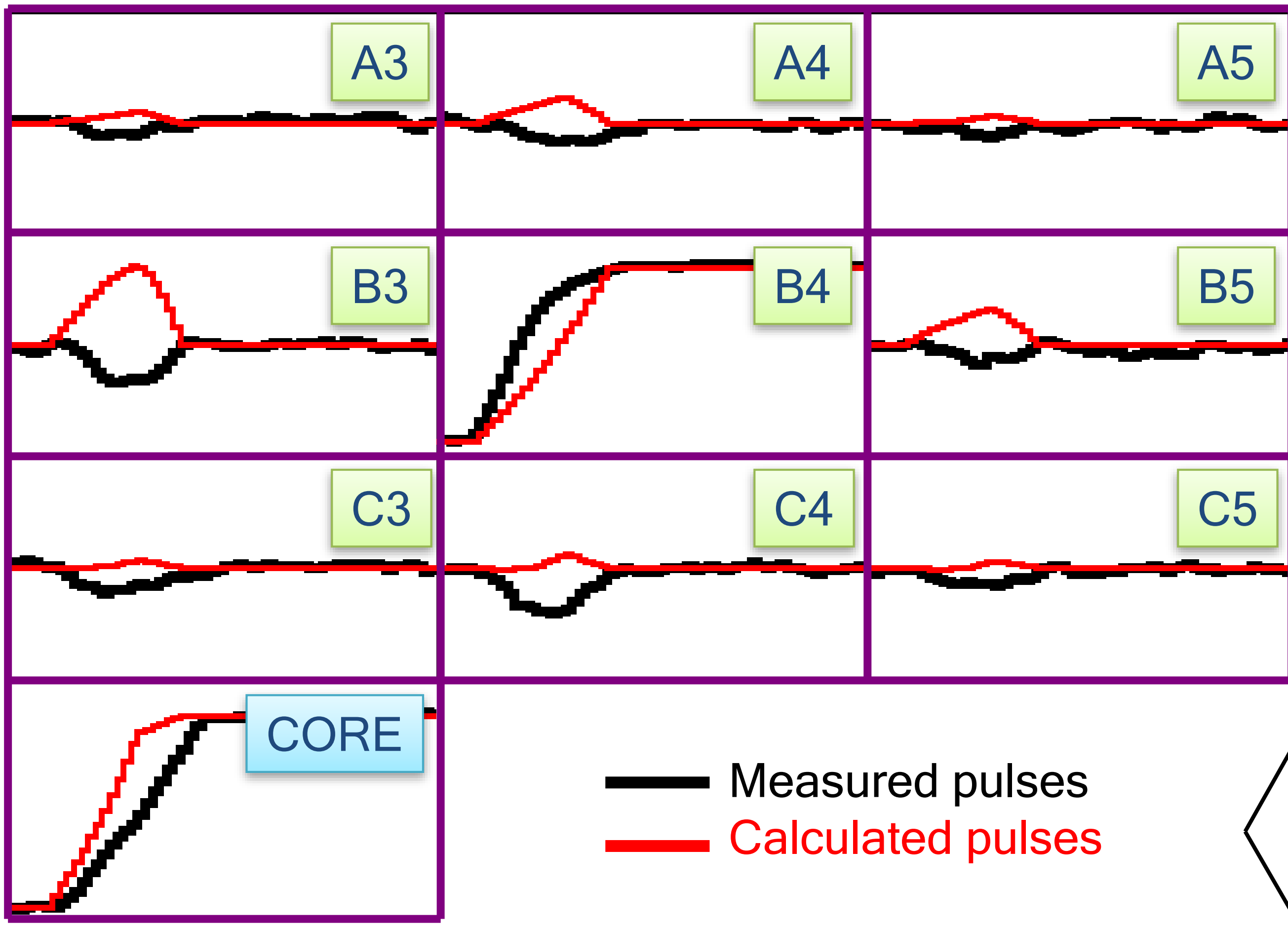

791 keV deposited in segment B4

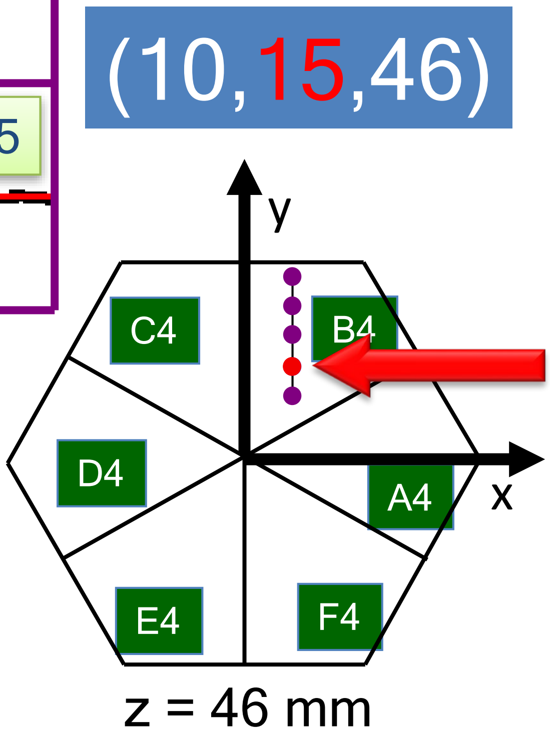

R.Venturelli, D.Bazzacco

Pulse Shape Analysis Concept

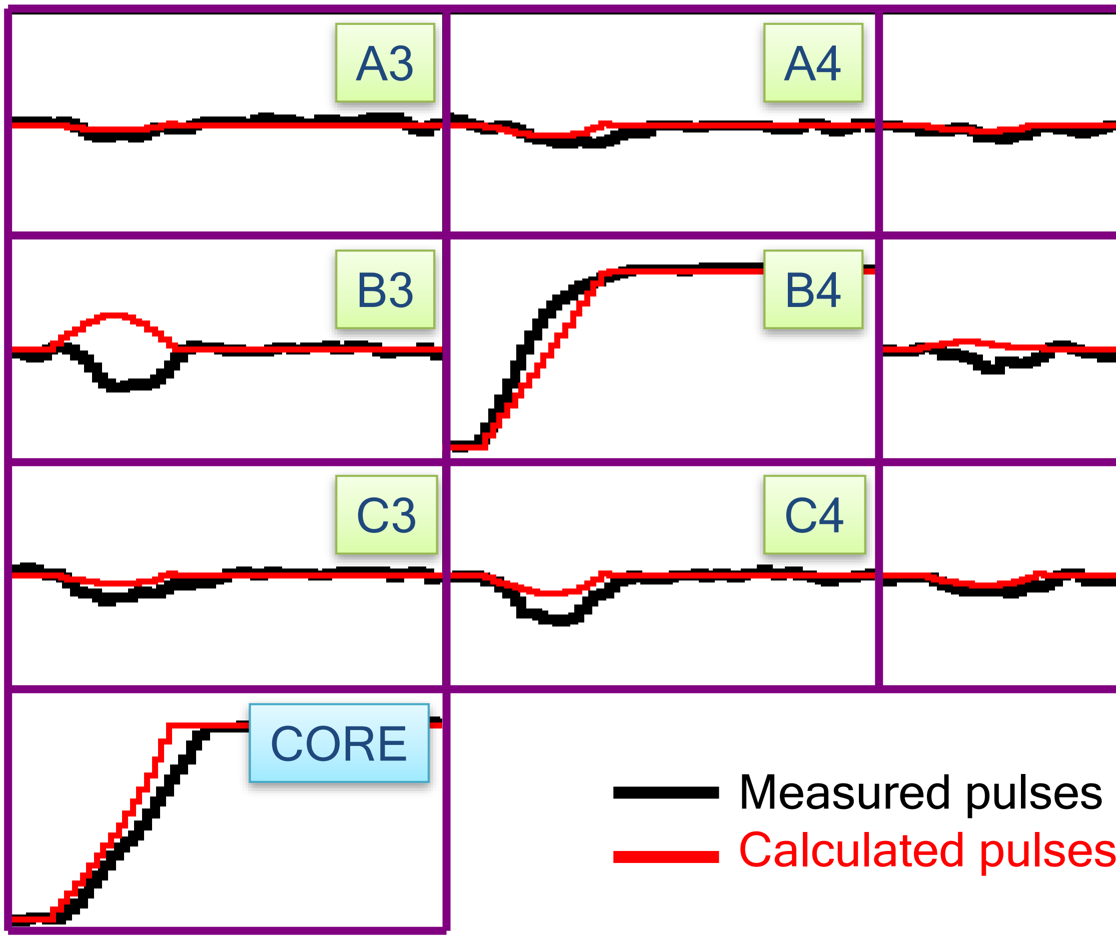

791 keV deposited in segment B4

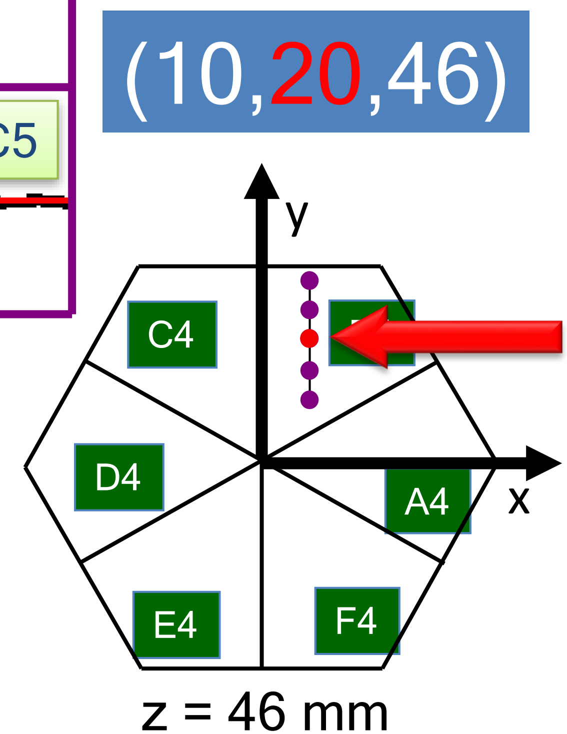

R.Venturelli, D.Bazzacco

Pulse Shape Analysis Concept

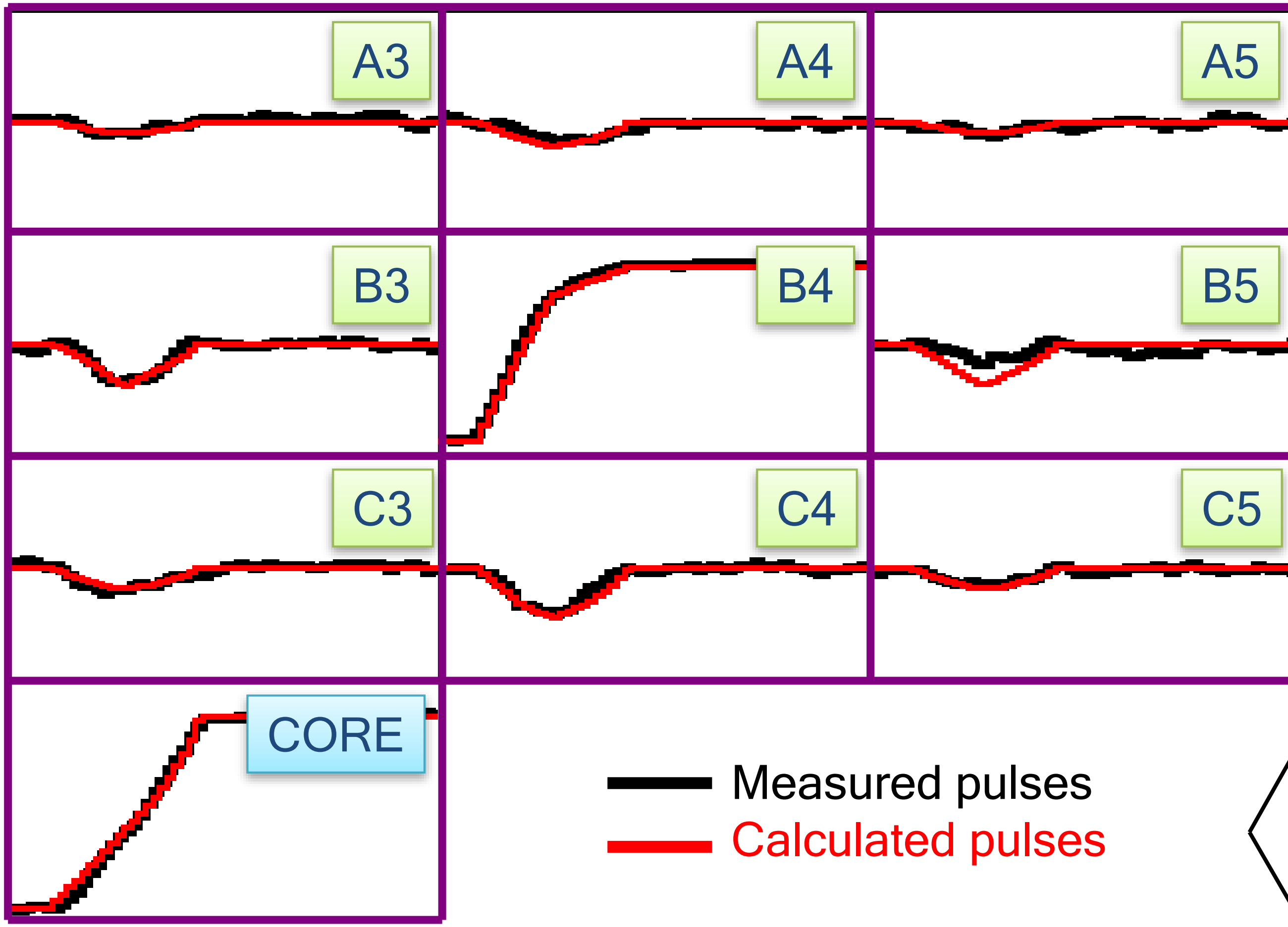

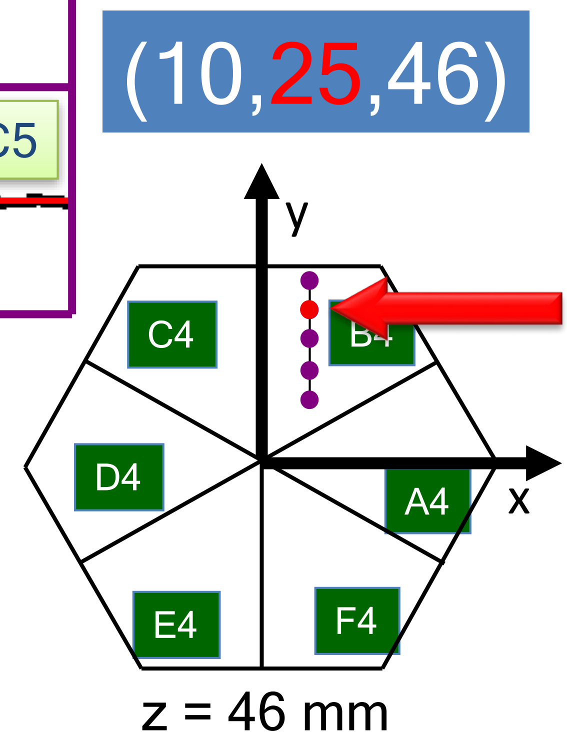

791 keV deposited in segment B4

R.Venturelli, D.Bazzacco

Pulse Shape Analysis Concept

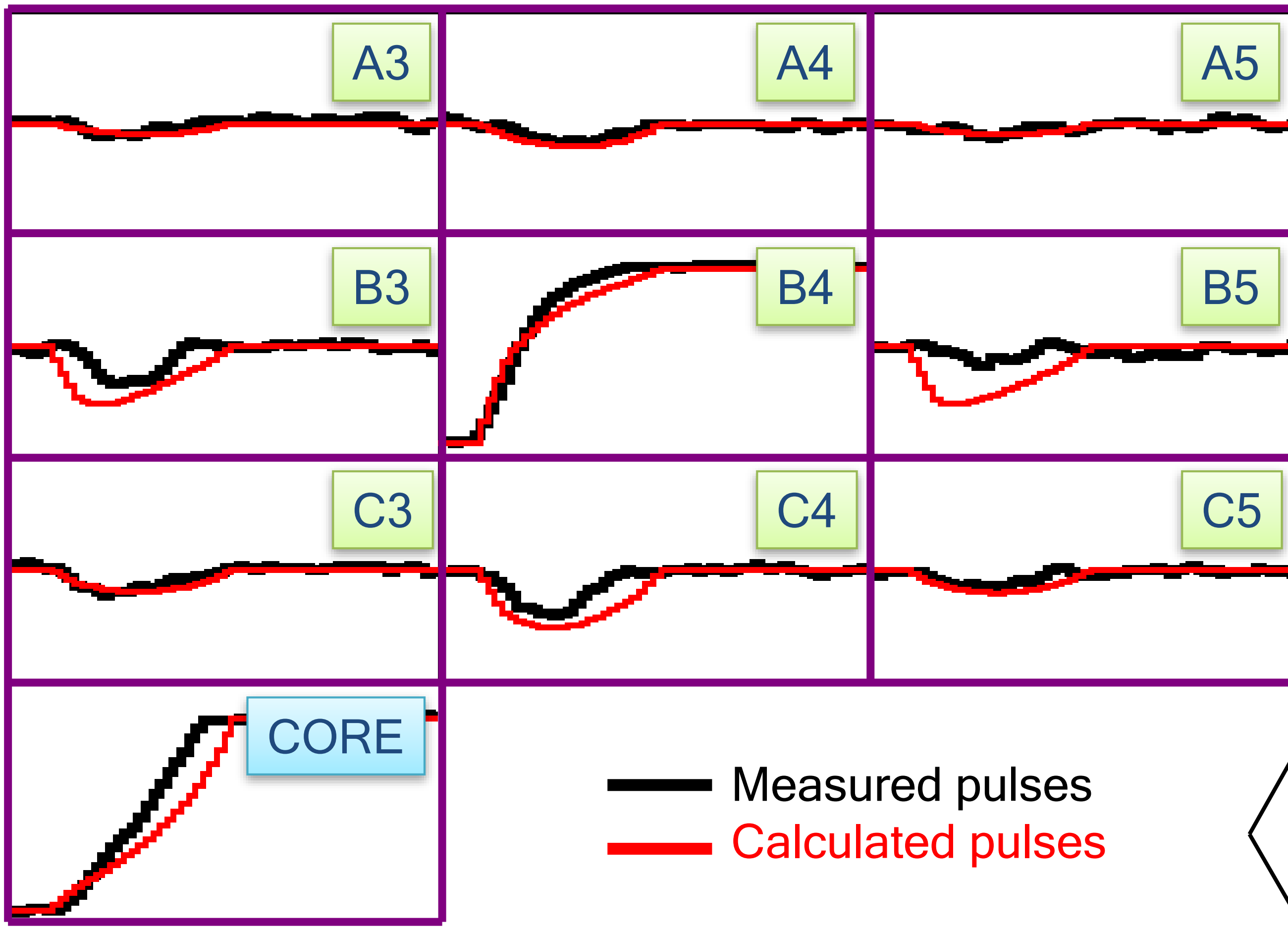

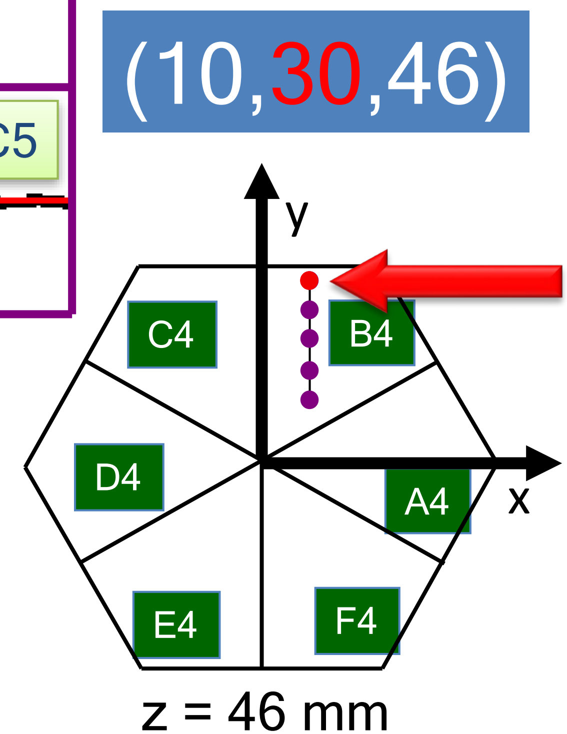

791 keV deposited in segment B4

R.Venturelli, D.Bazzacco

Pulse Shape Analysis Concept

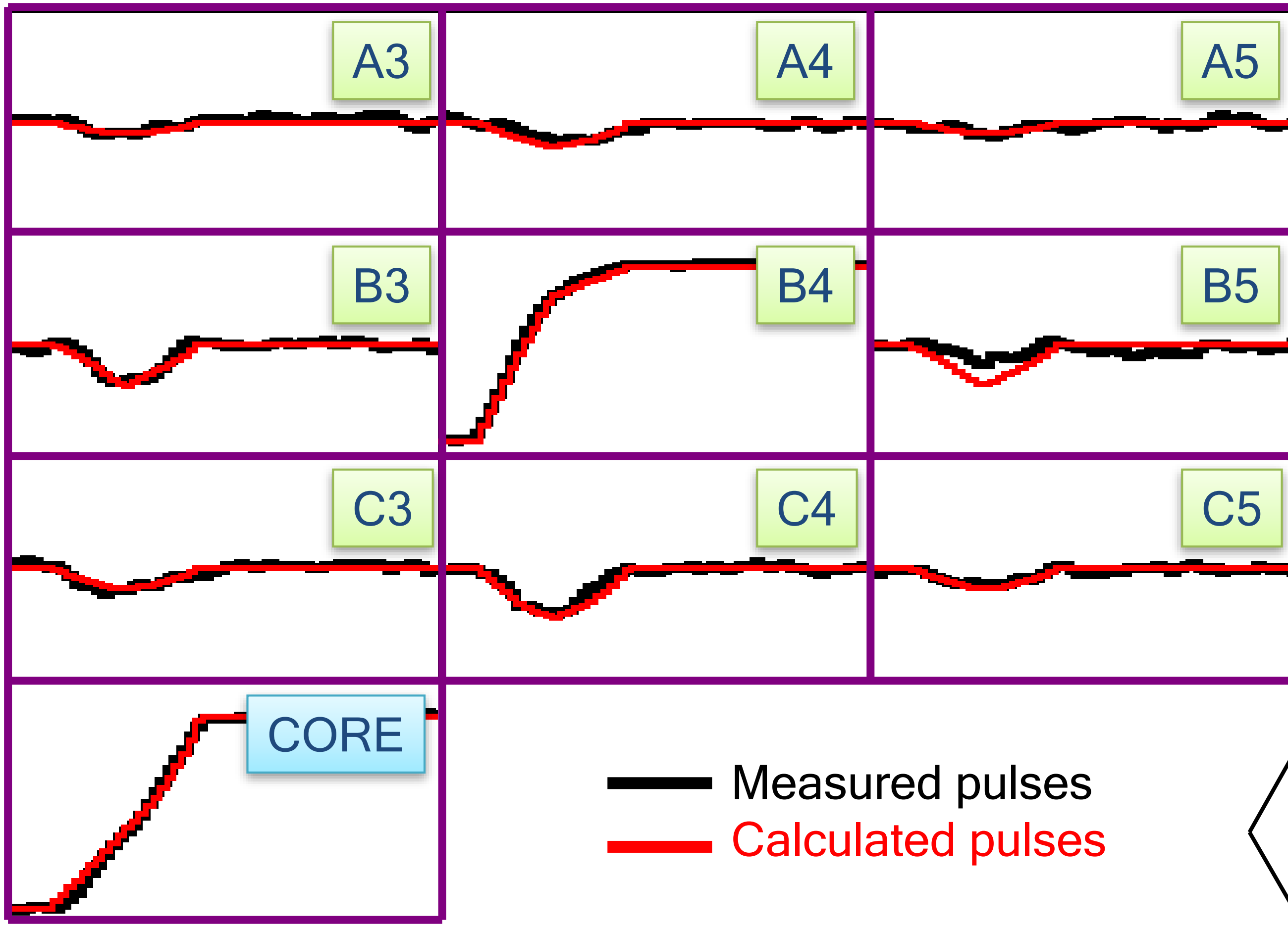

Result of *Grid Search* algorithm

R. Venturelli

(10,25,46)

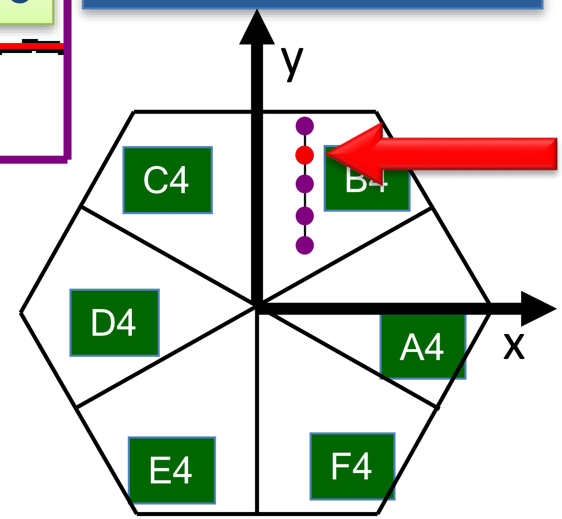

z = 46 mm

791 keV deposited in segment B4

Set of Energies + Interaction Positions → **Tracking**

R.Venturelli, D.Bazzacco

Interaction - Reconstruction Mechanisms

~ 100 keV | ~1 MeV | ~ 10 MeV | γ-ray energy

Photoelectric	Compton Scattering	Pair Production

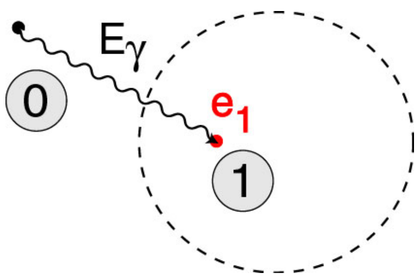

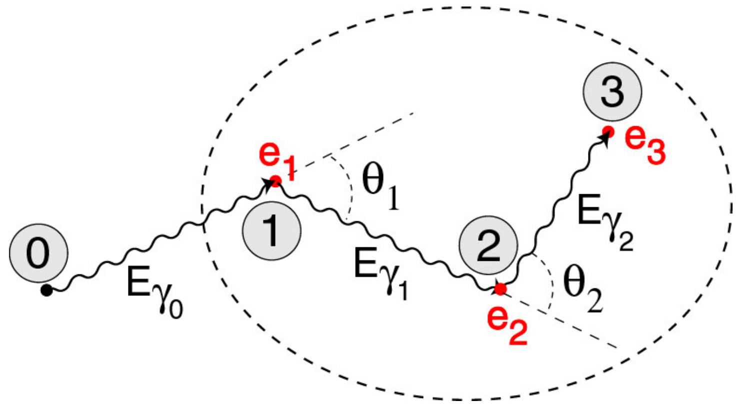

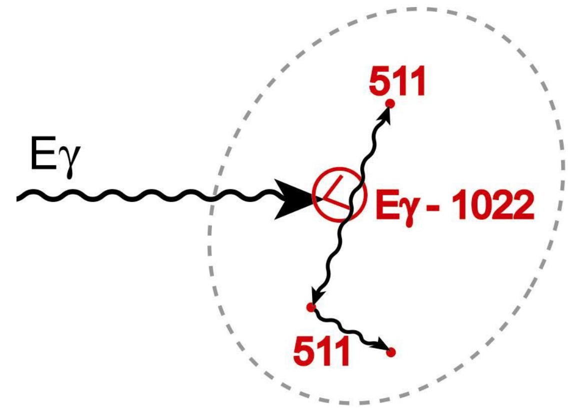

Isolated hits	Angle/Energy	Pattern of hits
Probability of interaction depth	$E_{\gamma'} = \dfrac{E_\gamma}{1+\dfrac{E_\gamma}{m_0c^2}\left(1-\cos\theta\right)}$	$E_{1st} = E_\gamma - 2\,mc^2$

Reconstruction efficiencies are limited by :

Position resolution; Short range scattering; Compton profile.

The tracking Algorithms in AGATA

Two main classes:

- algorithms based on back-tracking
  - **J. Van der Marel, B. Cederwall, NIMA 437 (1999) 538.**
  - **J. Van der Marel, B. Cederwall, NIMA 447 (2002) 391.**
  - **L. Milechina, B. Cederwall, NIMA 508 (2003) 394.**
- algorithms based on clusterisation and forward-tracking
  - **G.J. Schmid, et al., NIMA 430 (1999) 69.**
  - **D. Bazzacco, MGT code developed within the TMR program 'Gamma-ray tracking detectors'**
  - **I. Piqueras, et al. NIMA 516 (2004) 122**

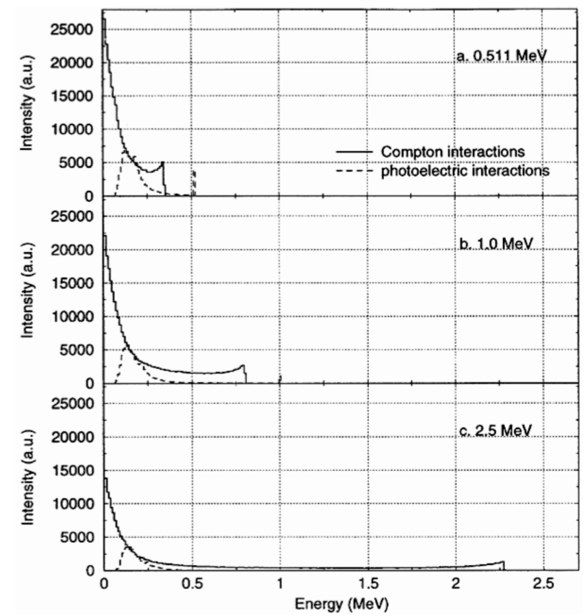

$$E_{\mathrm{s,p}} = \frac{E_t}{1 + E_t/m_e c^2 (1 - \cos\theta_\mathrm{p})}$$

Forward-tracking

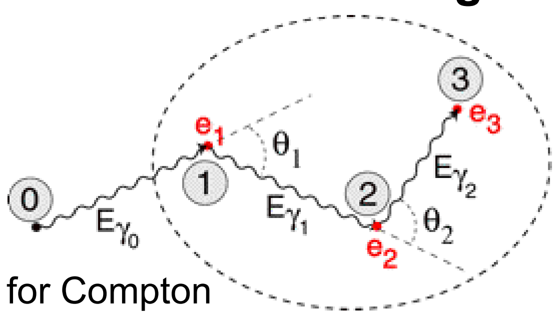

Probability for Compton or photoelectric and for the path in Germanium

$$L = \prod_{n=1}^{N} P_n \exp - \left[\frac{E_{\gamma n} - E_{\gamma n,pos}}{\sigma_E} \right]^2$$

Likelihood

Back-tracking

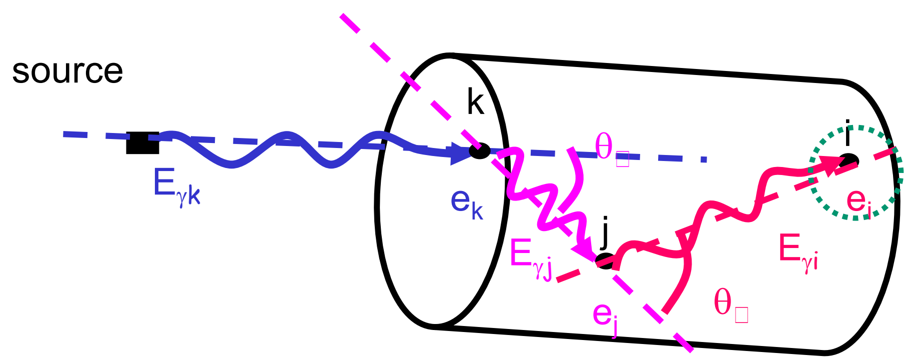

$$\cos(\theta) = 1 - m_e c^2 (1/E_{sc} - 1/E_{inc})$$

A.Lopez-Mertens et al. NIMA 533 (2004) 454

PSA and Tracking

P.-A.Söderström et al. NIM A 638(2011)96

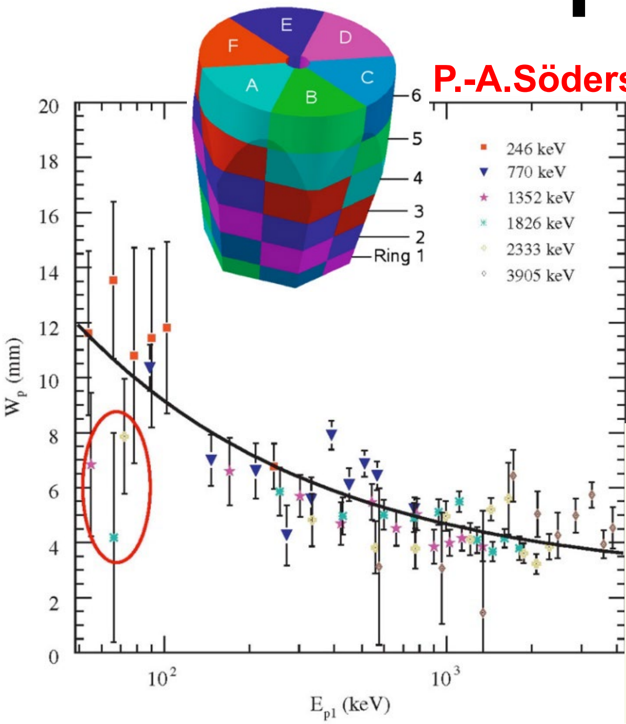

Induced current by the moving charge in the sensing contact: Ramo's Theorem.

E. Gatti, et al. NIM 193 (82) 651

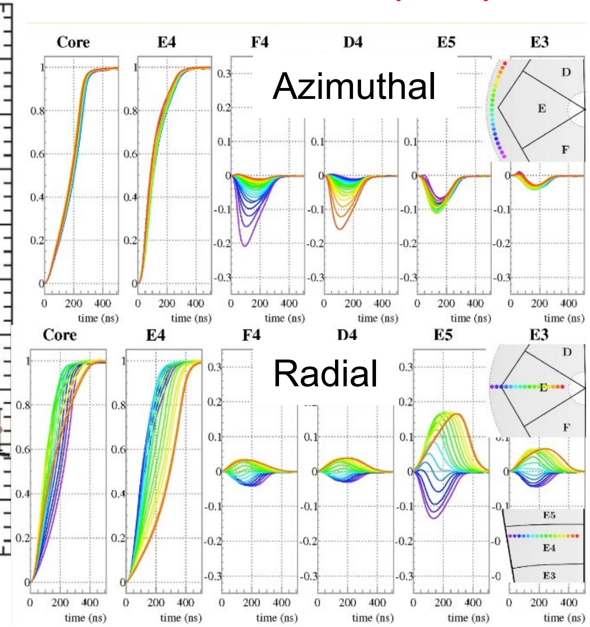

Figures courtesy of M.Ginsz, et al., IPHC Strasbourg

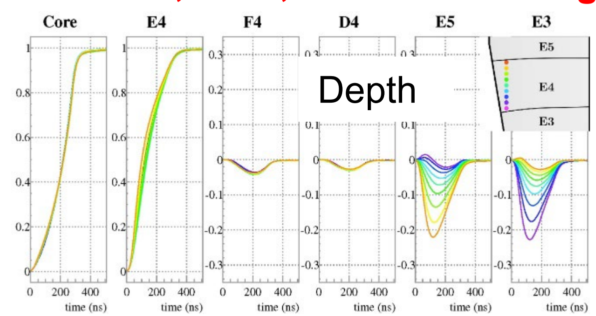

Photoelectric	**Compton Scattering**	**Pair Production**

Photoelectric — **$\sim 10^2$ keV**

Range in Ge

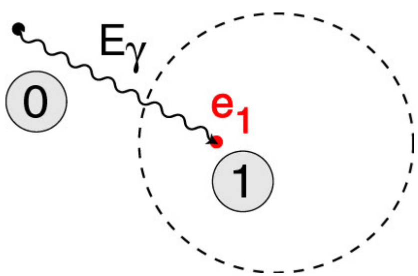

Compton Scattering — **$\sim 10^3$ keV**

$$E_{\gamma'} = \frac{E_\gamma}{1 + \frac{E_\gamma}{m_0 c^2}(1-\cos\theta)}$$

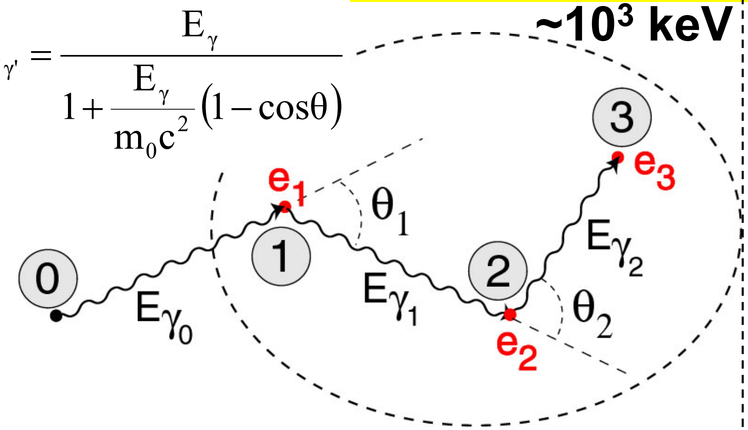

Pair Production — **$\gg 10^3$ keV**

$E_{1st} = E_\gamma - 2\,mc^2$

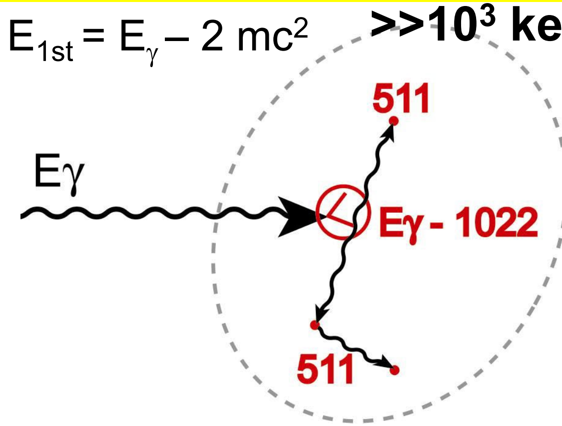

Isolated hits	Angle/Energy	Pattern of hits

AGATA 4π Performance simulations

Efficiency and P/T Monte Carlo simulations for the 180 Capsules set-up with Tracking

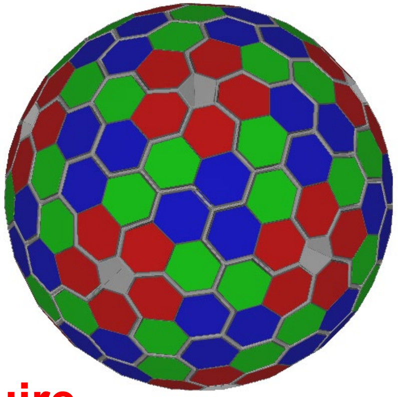

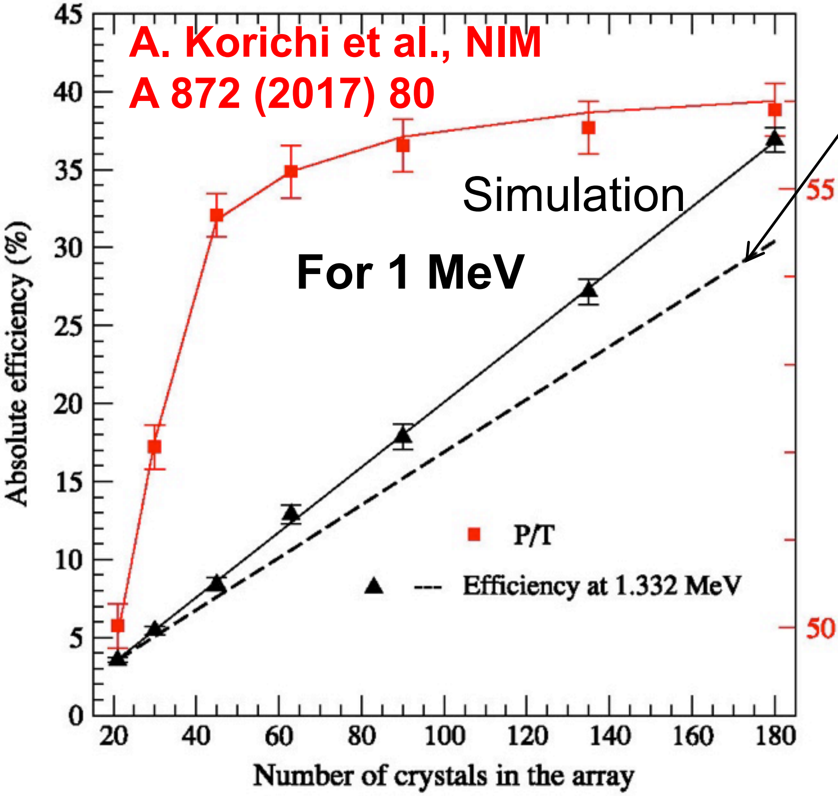

Linear Scaling from known efficiencies

These expectations require the PSA improvements regarding multiple interactions in one segment.

Efficiency depends as well on the γ-ray multiplicity
Recent Upgraded Simulations by M.Labiche (STFC)

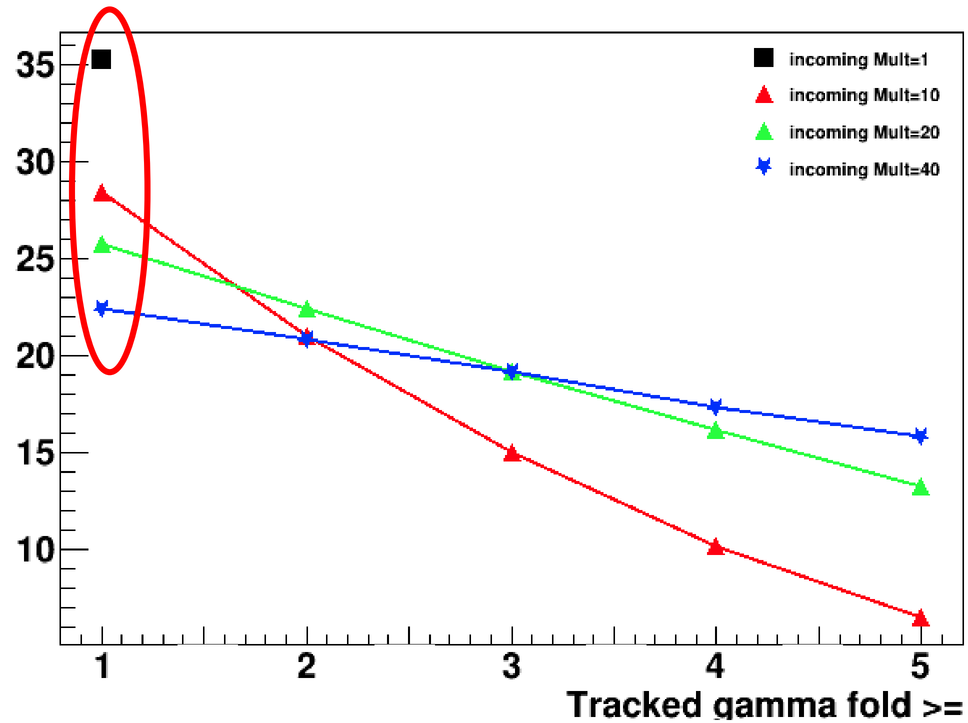

CSNSM-Orsay, STFC-Daresbury

Linear Polarization measurements with AGATA

$$\frac{d\sigma}{d\Omega} = \frac{r_0^2}{2}\left(\frac{E'}{E}\right)^2 \left[\frac{E'}{E} + \frac{E}{E'} + \sin^2(\theta)(1 + P\cos(2\varphi)\right]$$

O. Klein and Y. Nishina – Z. Phys. 52 (1929) 853

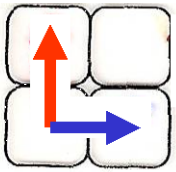

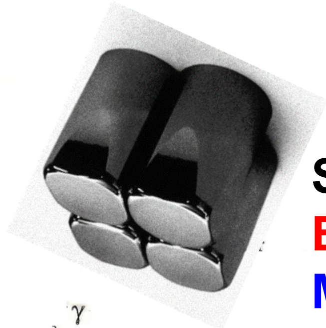

Stretched
Eλ positive &
Mλ negative
asymmetry

$$A = \frac{N_\perp - N_{||}}{N_\perp + N_{||}}$$

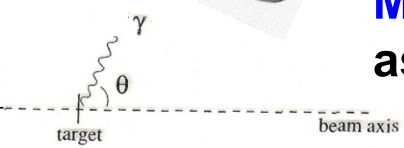

Sensitivity Q
average Σ on θ

P.G. Bizzeti et al., EPJ A 51 (2015) 49

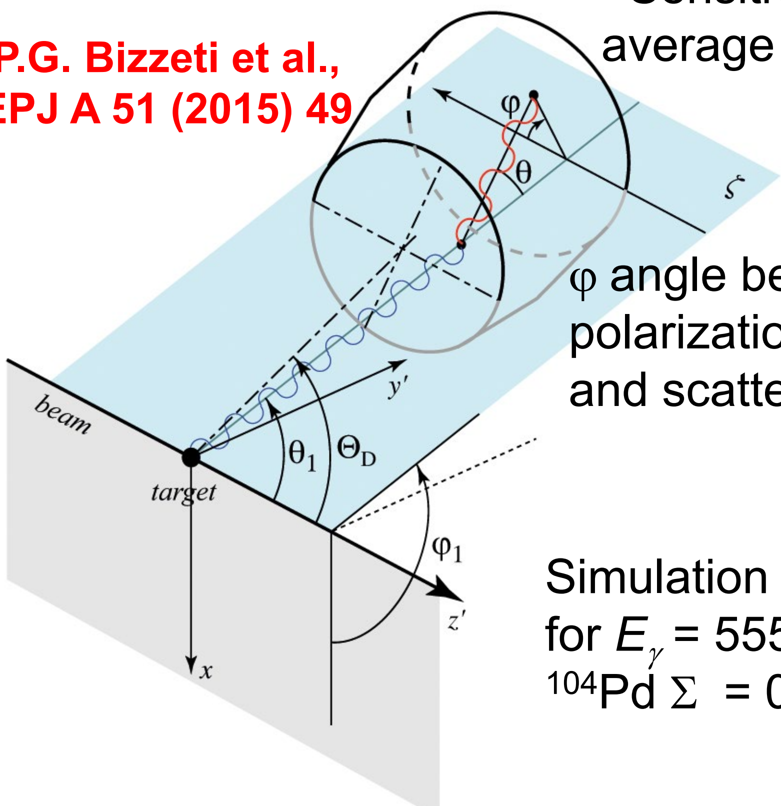

φ angle between polarization plane and scattering plane

Simulation value for E_γ = 555.8 keV ^{104}Pd Σ = 0.439

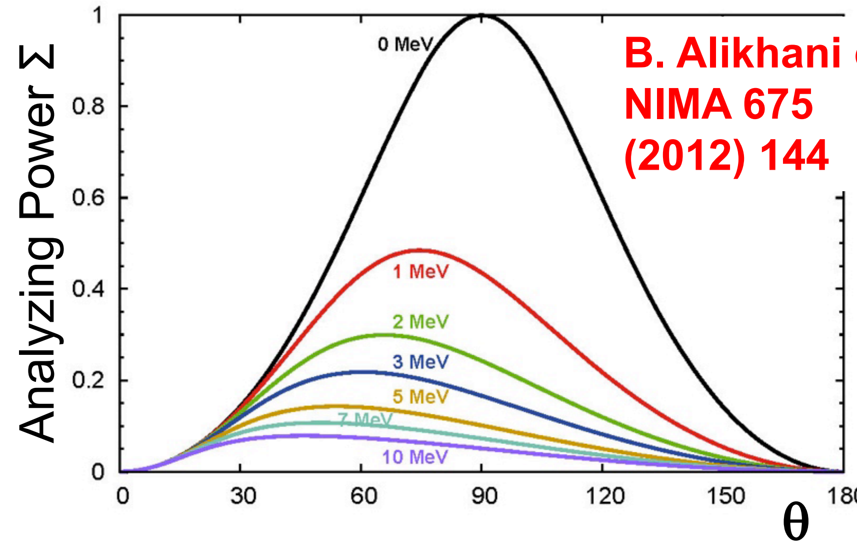

B. Alikhani et al. NIMA 675 (2012) 144

N_c	Experimental asymmetry A_s	Calculated polarization P	Analyzing power A_{exp}
3	-0.136 ± 0.014	-0.262	0.520 ± 0.053
4	-0.132 ± 0.014	-0.273	0.483 ± 0.052
5	-0.157 ± 0.014	-0.286	0.547 ± 0.049
6	-0.070 ± 0.014	-0.208	0.338 ± 0.067
7	-0.079 ± 0.014	-0.157	0.506 ± 0.089
8	-0.102 ± 0.014	-0.227	0.450 ± 0.062
Average			0.484 ± 0.024

In-Flight Geometrical Line-Shape Lifetime Measurement Techniques

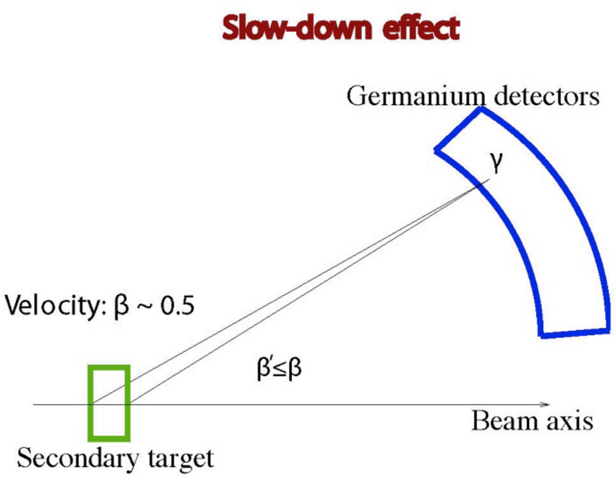

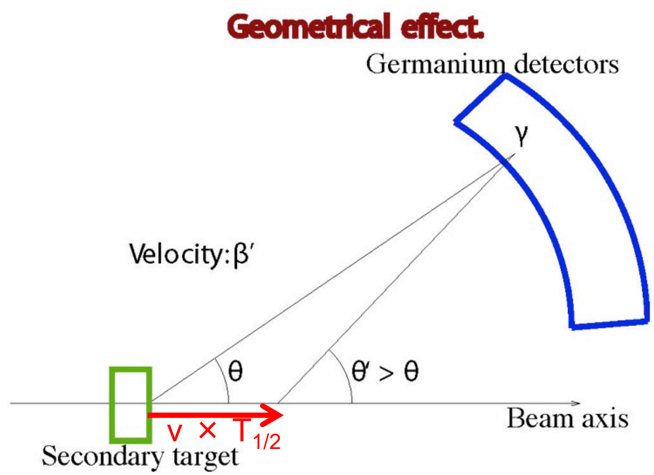

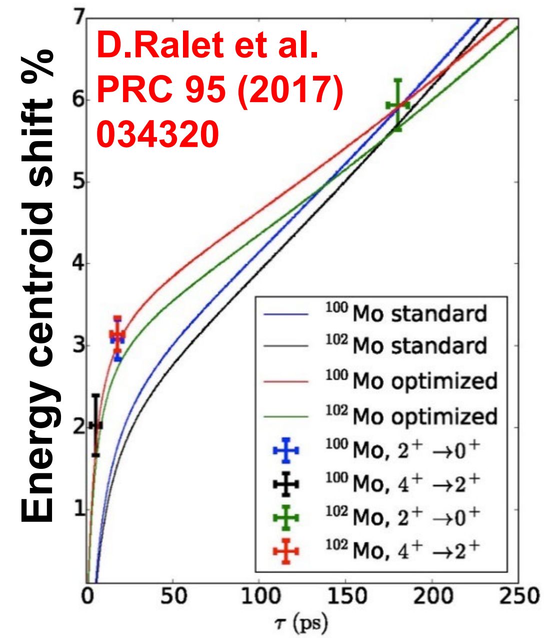

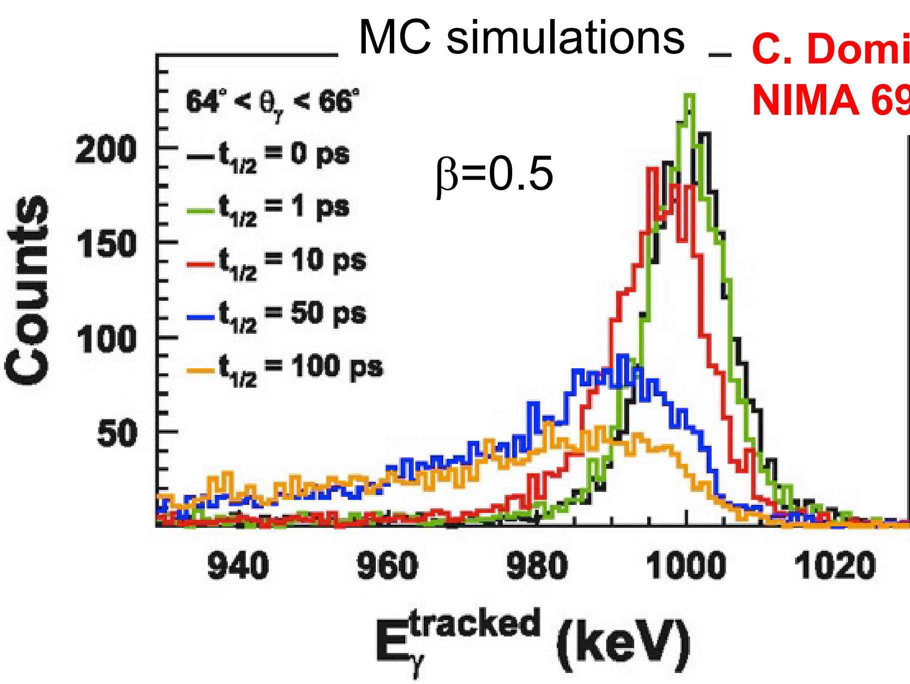

C. Domingo-Pardo et al, NIMA 694 (2012) 297

- New “DSAM-like” technique based on the position sensitivity and the Doppler correction.
- Possible to measure down to 1 to 10 ps lifetimes with relativistic RIBs.

D.Ralet PhD Thesis

Continuous-Angle DSAM

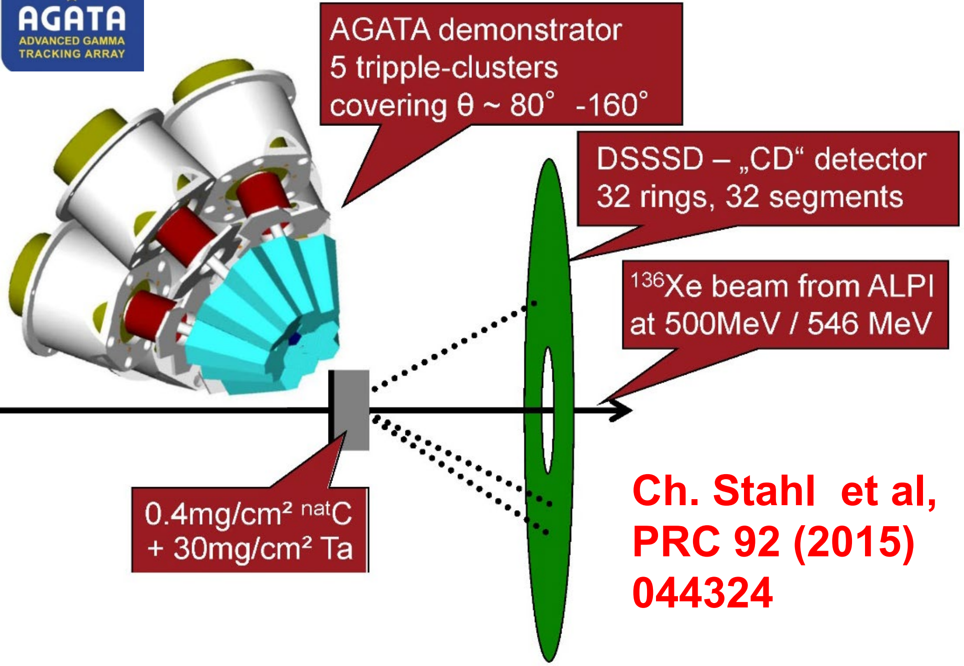

Ch. Stahl et al, PRC 92 (2015) 044324

The continuous-angle DSAM represents an advancement of the "conventional" DSAM. It extends the γ-ray lineshapes analysis as a function of γ -ray energy to a lineshape analysis as a function of both γ-ray energy and polar angle of the γ-ray detection.

Also the Geometrical Line-Shape lifetime measurement available for long lifetimes

Firstly used with the AGATA –Demonstrator at LNL with a 136Xe beam impinging on a ^{nat}C + Ta target.

^{136}Xe Coulex

LNL-data, 546 MeV run

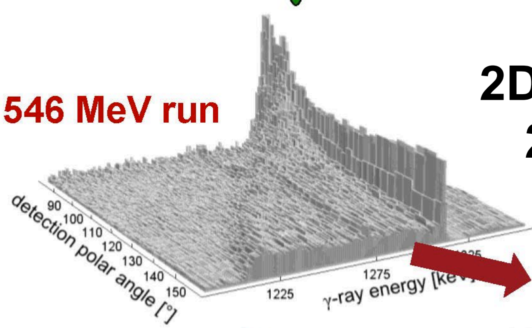

Fit-Function

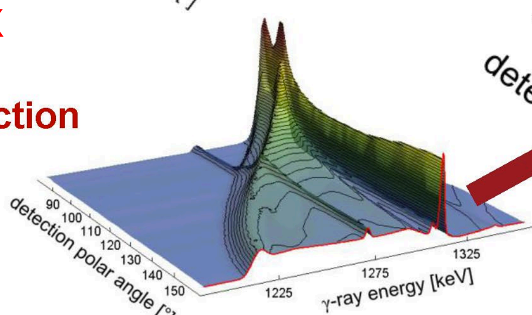

2D-data fitted with 2D fit-function

Preliminary spectrum!

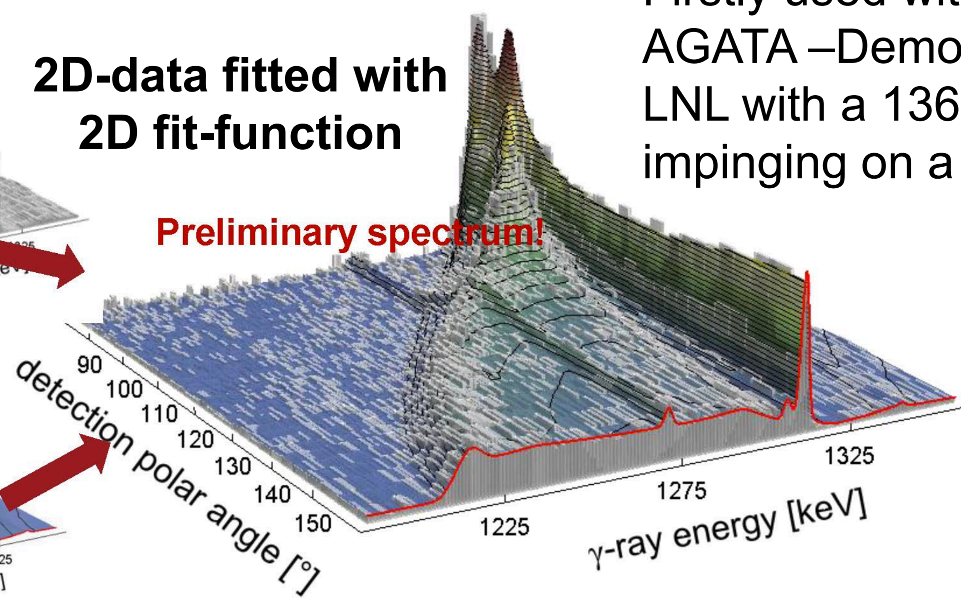

Ch. Stahl et al, CPC 214 (2017) 174

How to Produce Excited or Excite a Nucleus?

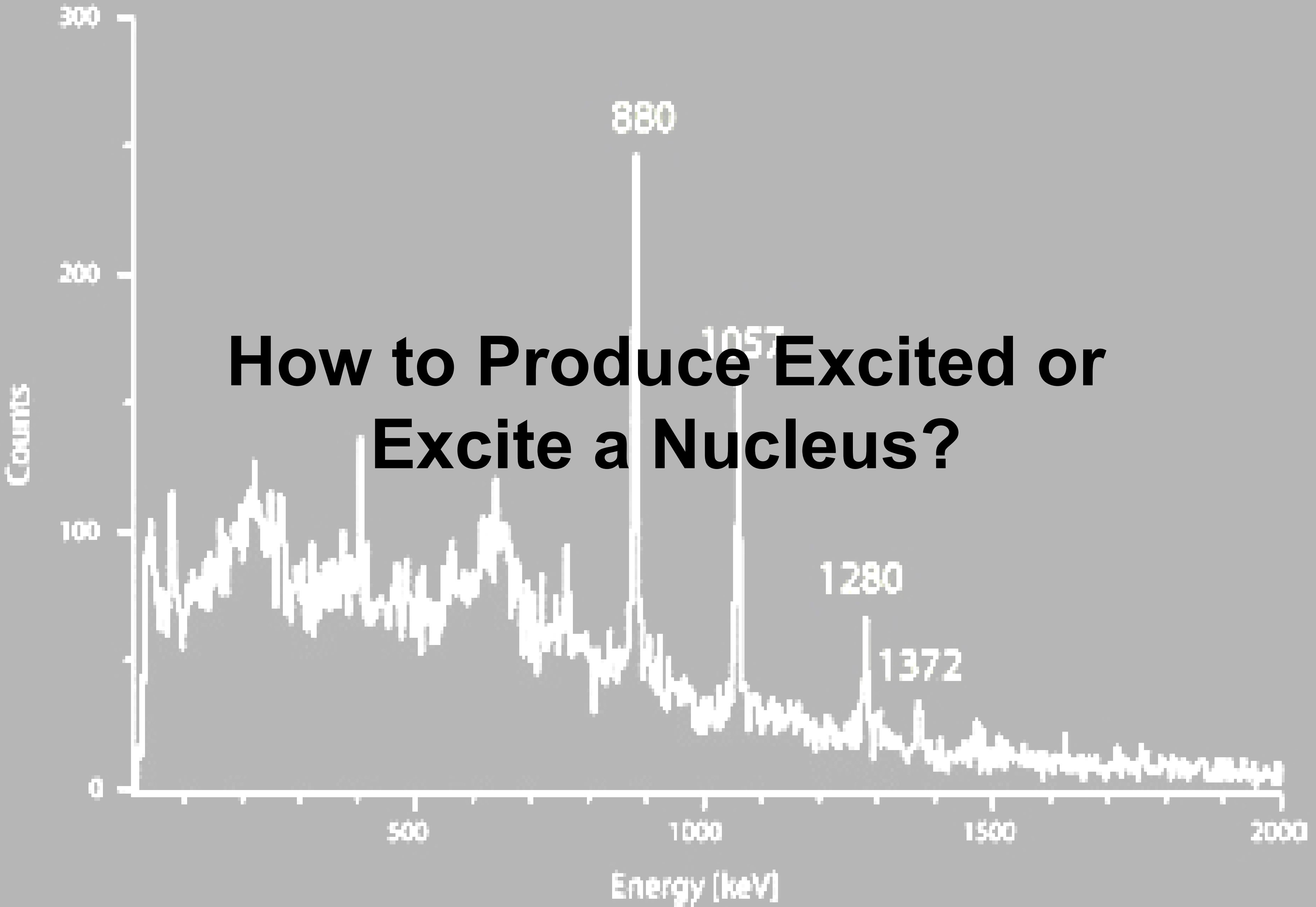

Types of Nuclear Reactions

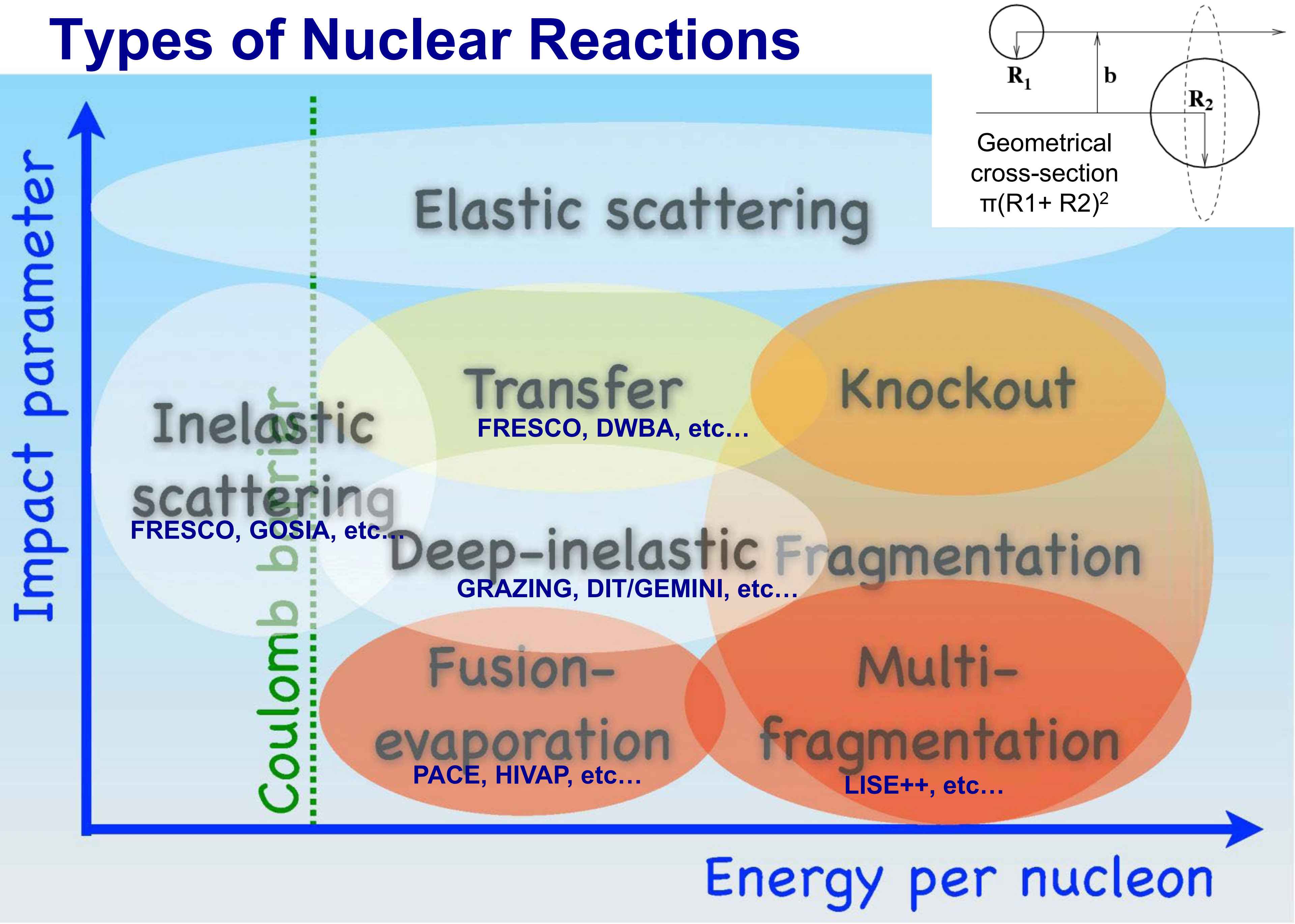

Low Energy reaction mechanisms used for γ-Spectroscopy (up to ~10 MeV.A)

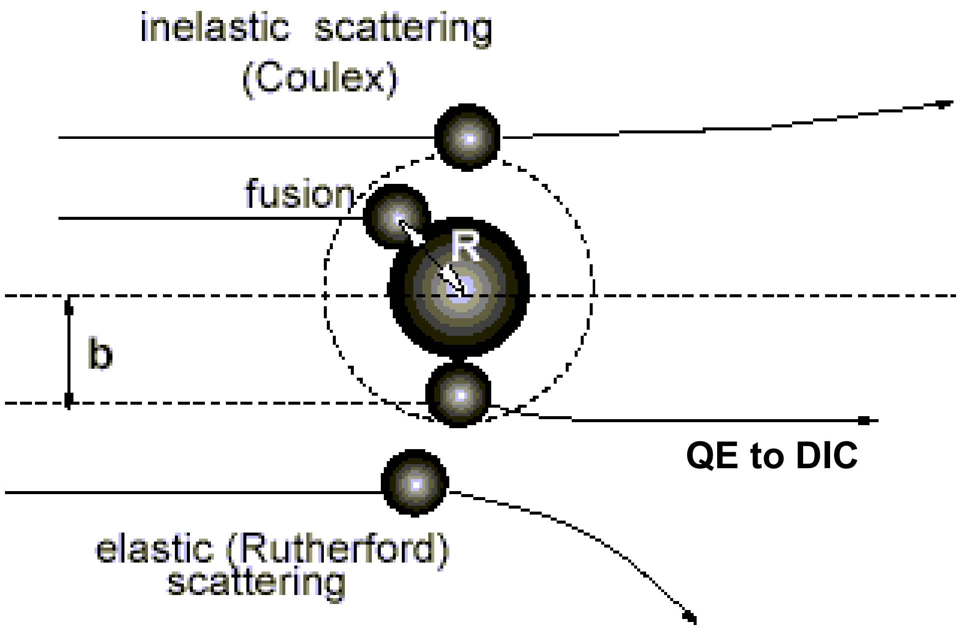

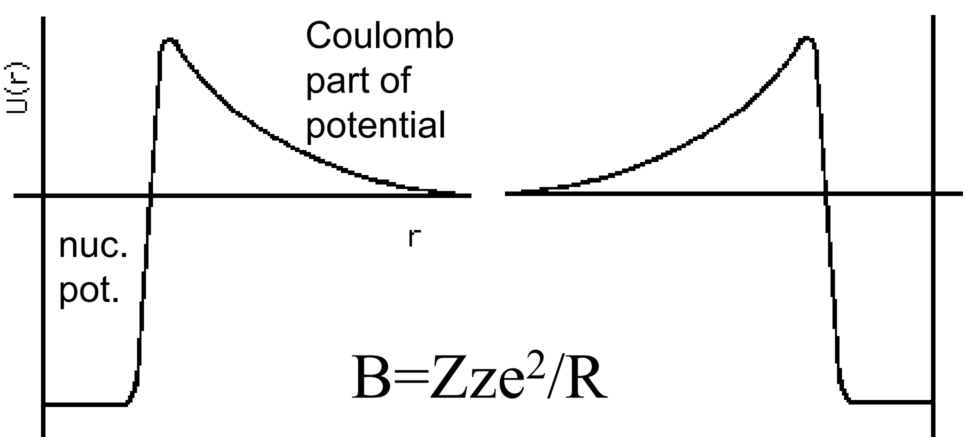

$$B=Zze^2/R$$

Smaller impact parameter "b"

- Coulomb excitation and Inelastic scattering.
- Transfer and quasi-elastic processes (p,n capture...).
- Multi-nucleon transfer.
- Deep Inelastic Collisions.
- Quasi-fusion reactions.
- Fusion with light particles evaporation .
- Fusion with evaporation of Massive Fragments (IMF)
- Fusion-fission

Cross sections up to few barns typically from tens of mb to μb

Yields from Cross-Section Estimates

- The Cross-Section estimate σ is given in barn i.e. 10^{-28} m^2 = 100fm

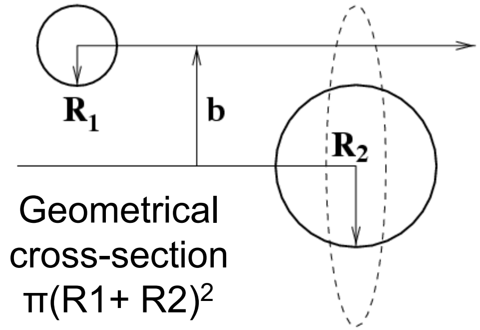

- The yield of a reaction is proportional to the Cross-section, the number of atoms in the target and the atoms per second in the beam:
  - Cross-section are given in barn's (10^{-24}cm^2)
  - Target thicknesses are usually given in mg/cm^2
  - The beam intensity is given in particles per second (pps) or in particle nA (pnA).

$$yield = \sigma\,(barn) \cdot 10^{-24}\left(\frac{cm^2}{barn}\right) \cdot \frac{Target\ \left(\frac{g}{cm^2}\right)}{Mol\ weight\ (g)} \cdot N_A \cdot Beam\left(\frac{Atoms}{s}\right)$$

The production cross-section does not imply that a transition or particular phenomena will be observed with such intensity, e.g. superdeformed bands 1/100 yield

Example Coulomb Excitation: Deformation in ^{42}Ca

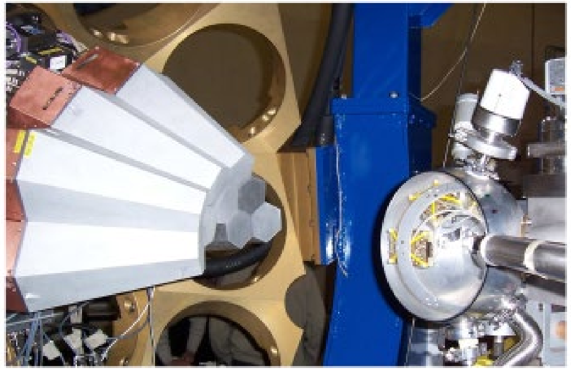

Beam:
^{42}Ca, E=170 MeV
Targets:
^{208}Pb, 1 mg/cm
^{197}Au, 1 mg/cm

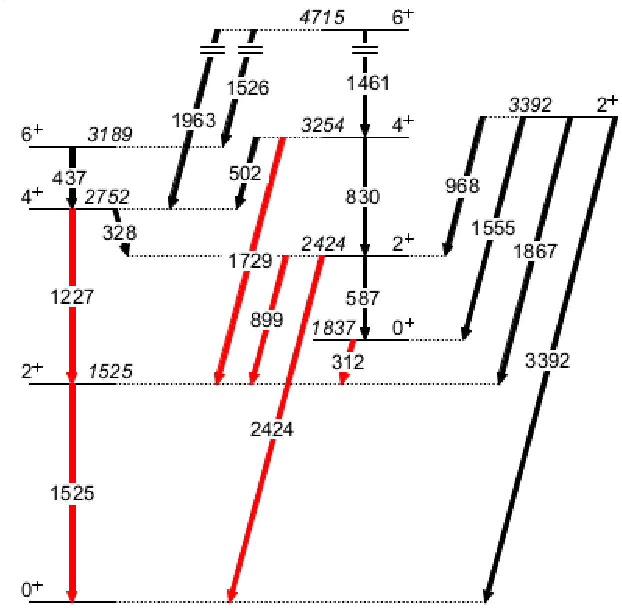

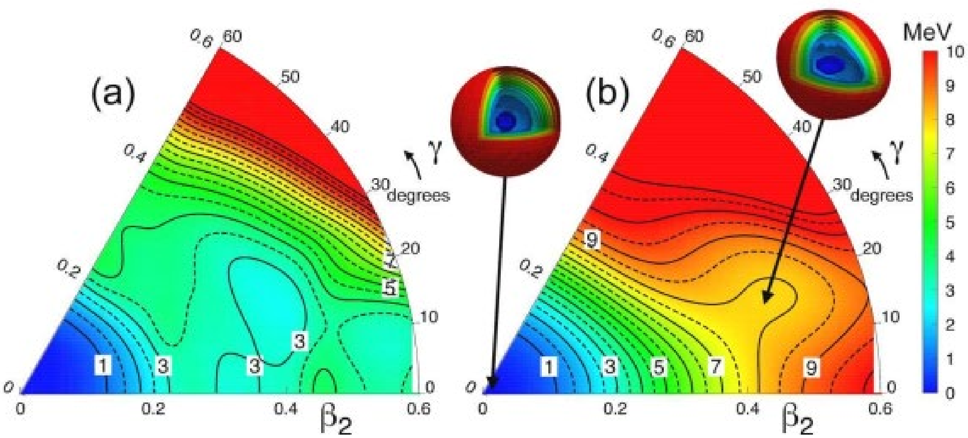

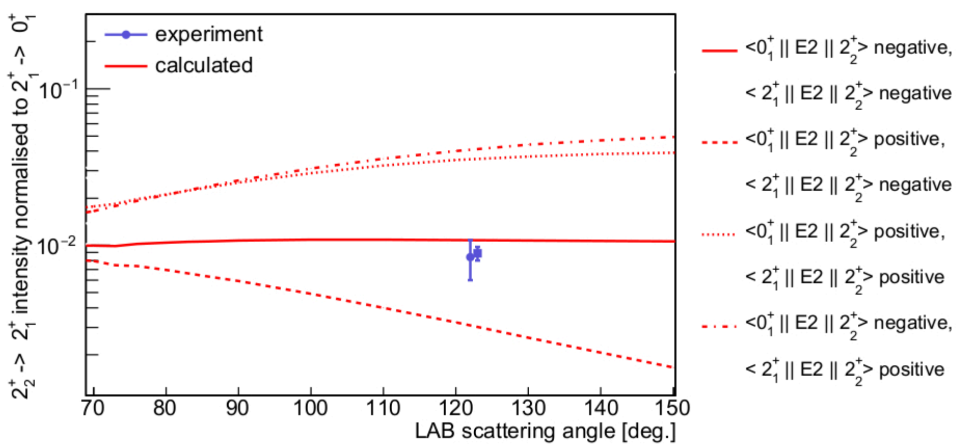

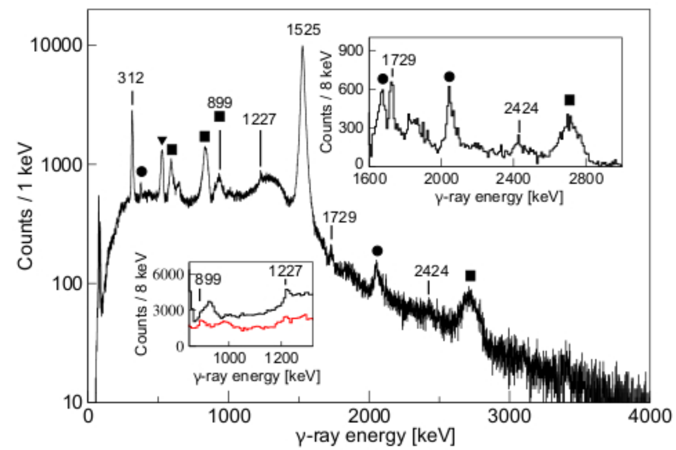

Kasia Hadynska-Kleck
PRL 117 (2016)

An exceptionally low alpha capture reaction rate on oxygen-15 and its impact as X-ray burst trigger Reaction

Relevant in Accreting Neutron Stars & X-ray Bursts

Light curves are extremely sensitive to alpha capture on ^{15}O.
Dominated by 4033 keV state in ^{19}Ne.

Ch. Diget, J.S. Rojo et al.,

$$N_A\langle\sigma v\rangle_r \propto \omega\gamma_r \exp\left(-\frac{E_r}{k_b T}\right)$$

$$\omega\gamma_r = \frac{2J_r+1}{(2J_i+1)(2J_f+1)}\frac{\Gamma_\alpha\Gamma_\gamma}{\Gamma_{tot}}$$

Extremely low cross section of $^{15}O(\alpha, \gamma)^{19}Ne$.

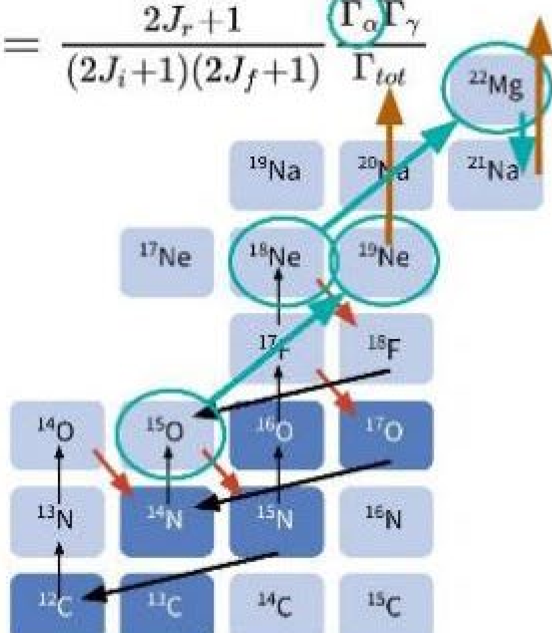

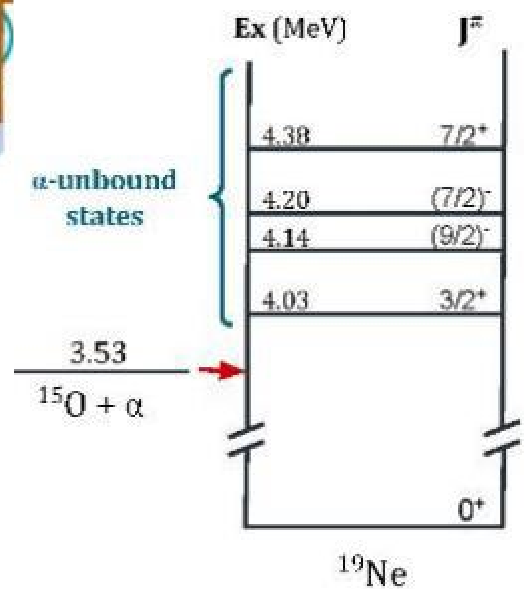

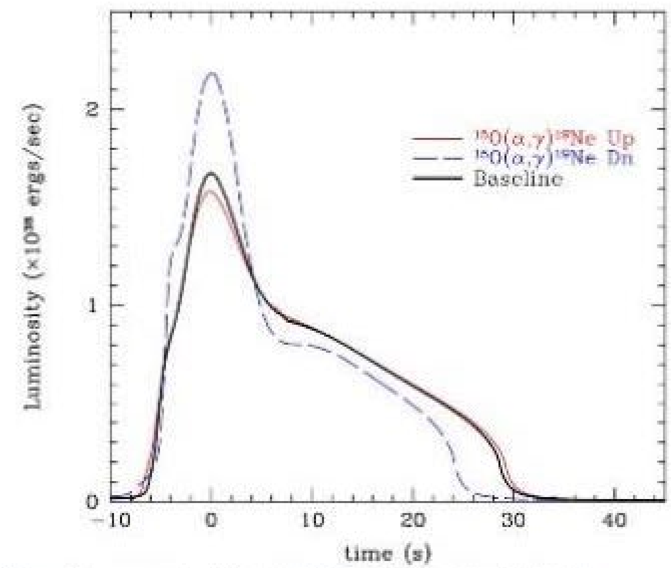

Single-zone X-ray burst sensitivity study Cyburt et al., APJ 830:55 (2016)

Hot-CNO Breakout points:
$^{15}O(\alpha, \gamma)^{19}Ne$ alpha capture
$^{18}Ne(\alpha, p)^{21}Na$ alpha capture

$$^{15}O + {}^{7}Li \rightarrow t + {}^{19}Ne^{*} \rightarrow t + {}^{19}Ne + \gamma$$

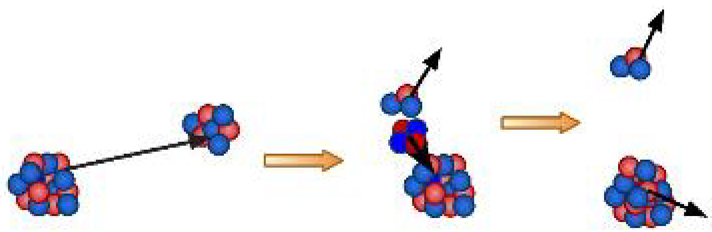

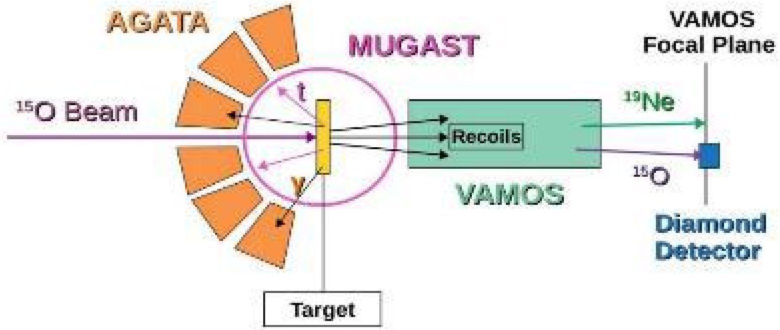

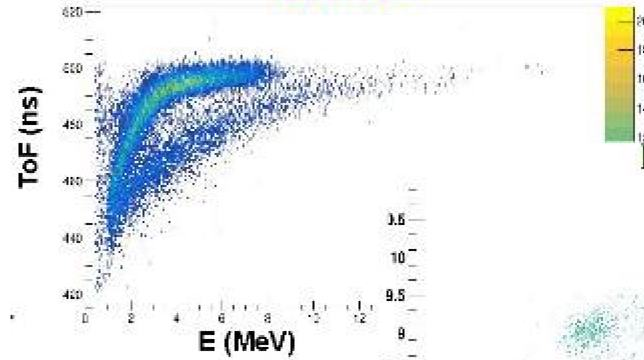

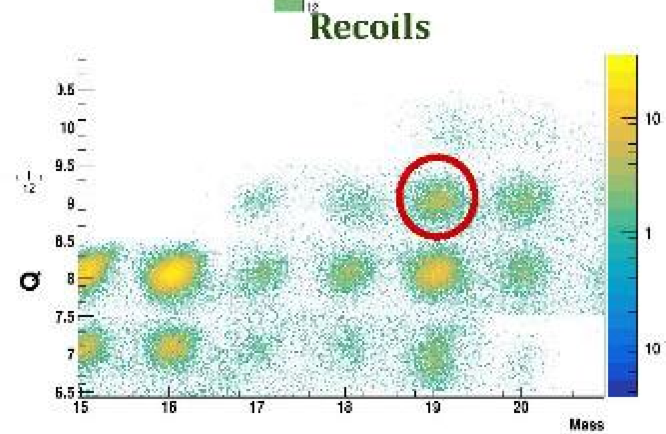

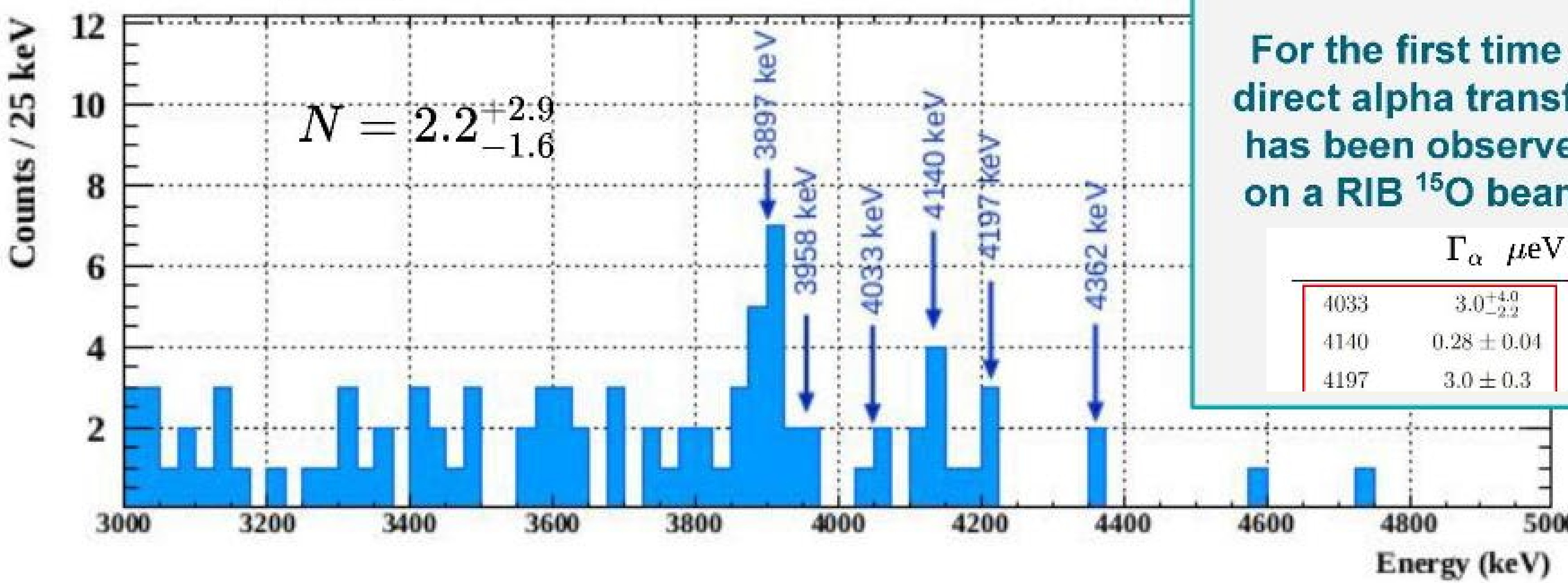

For the first time a direct alpha transfer has been observed on a RIB ^{15}O beam!

	Γ_α μeV
4033	$3.0^{+4.0}_{-2.2}$
4140	0.28 ± 0.04
4197	3.0 ± 0.3

Ch. Diget, J.S. Rojo et al.,

Example: GRAZING REACTIONS

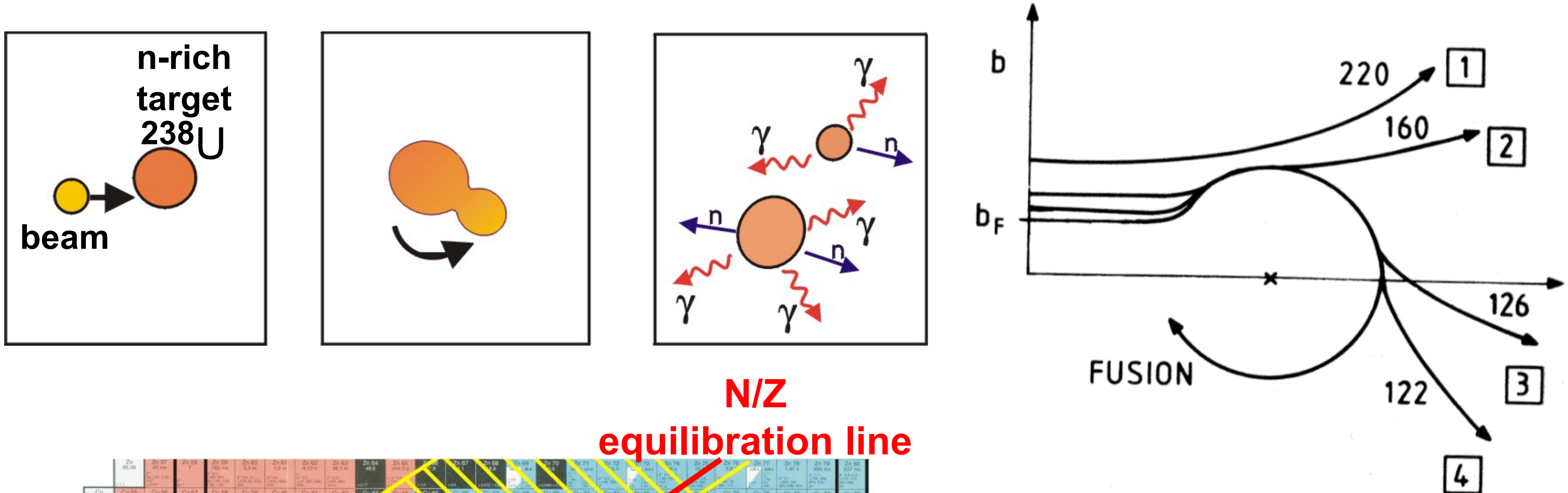

N/Z
equilibration line

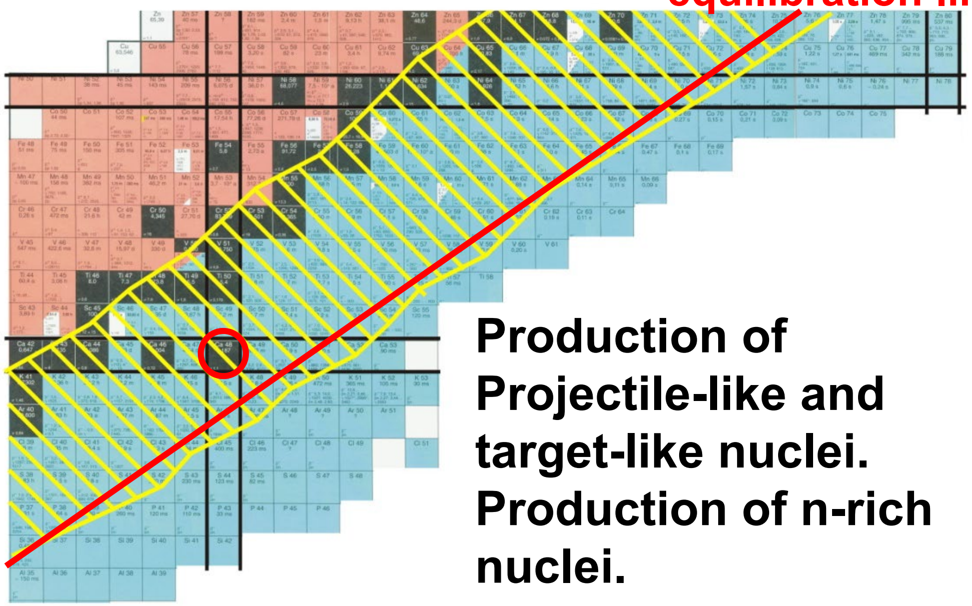

Production of Projectile-like and target-like nuclei. Production of n-rich nuclei.

J. Wilczynski, Phys. Lett. 47B(1973) 484

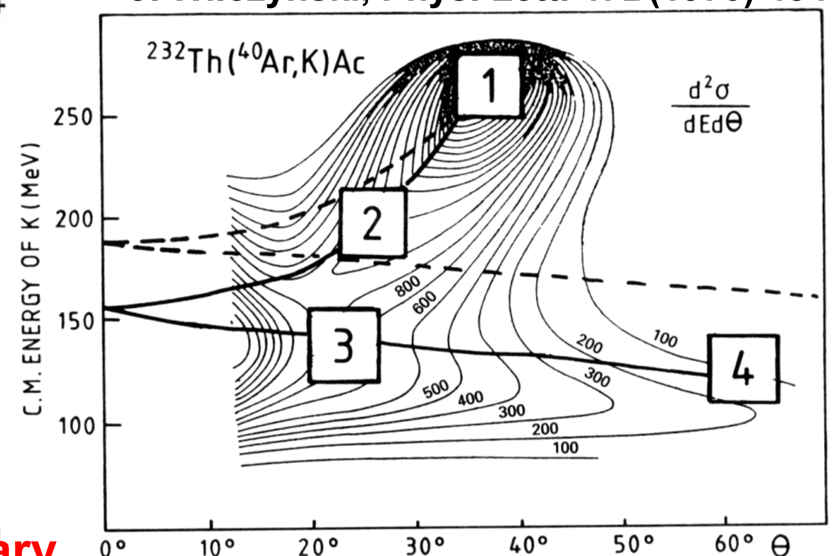

Identification of products with complementary detectors or by γ-spectroscopy of the partners is required

Multi-Nucleon Transfer GRAZING REACTIONS

Analysis

^{94}Ru Gamma Tracked Spectrum

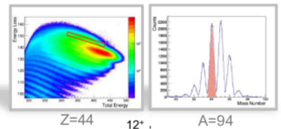

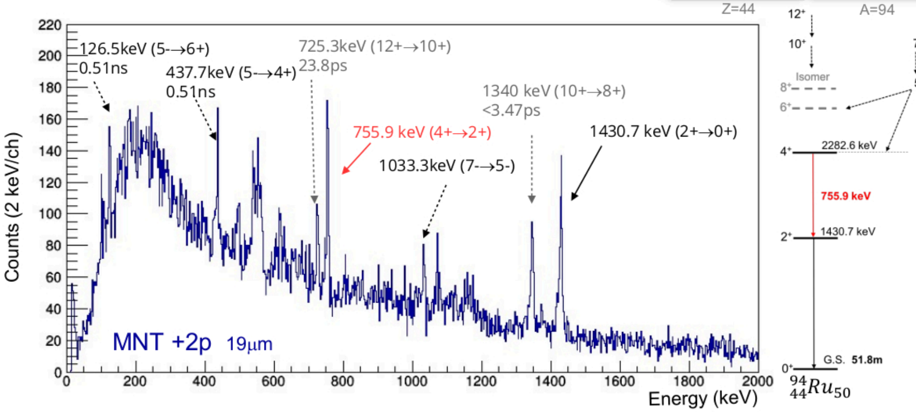

Reaction $^{92}Mo+^{92}Mo$:
-Beam-energy: 716,9MeV
-Grazing angle LAB: ~23 º

Rosa Perez Vidal PhD Thesis

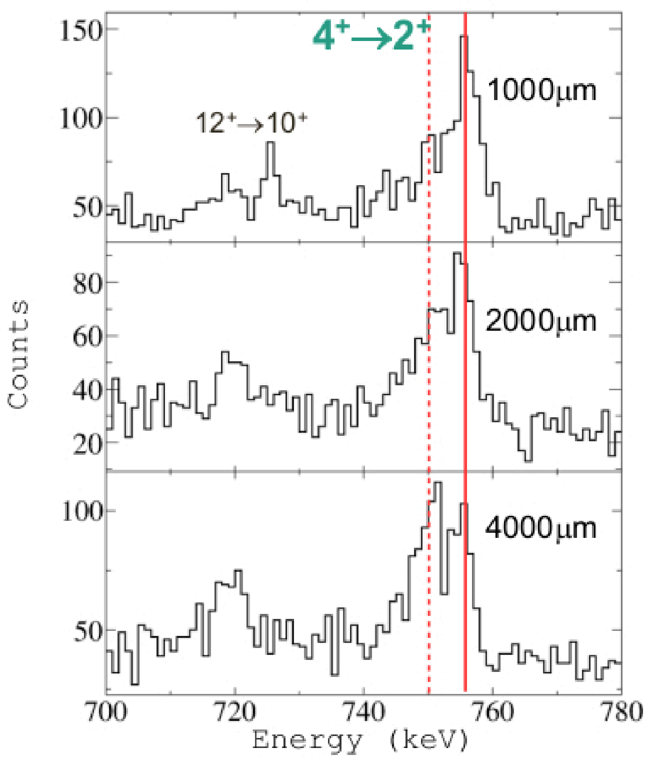

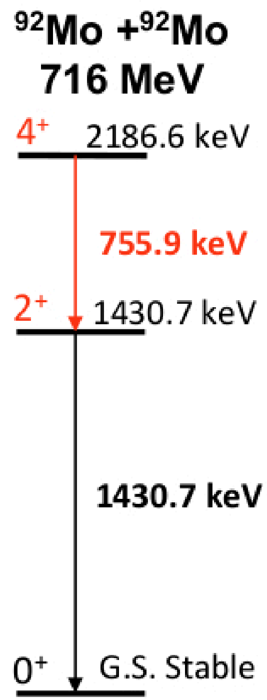

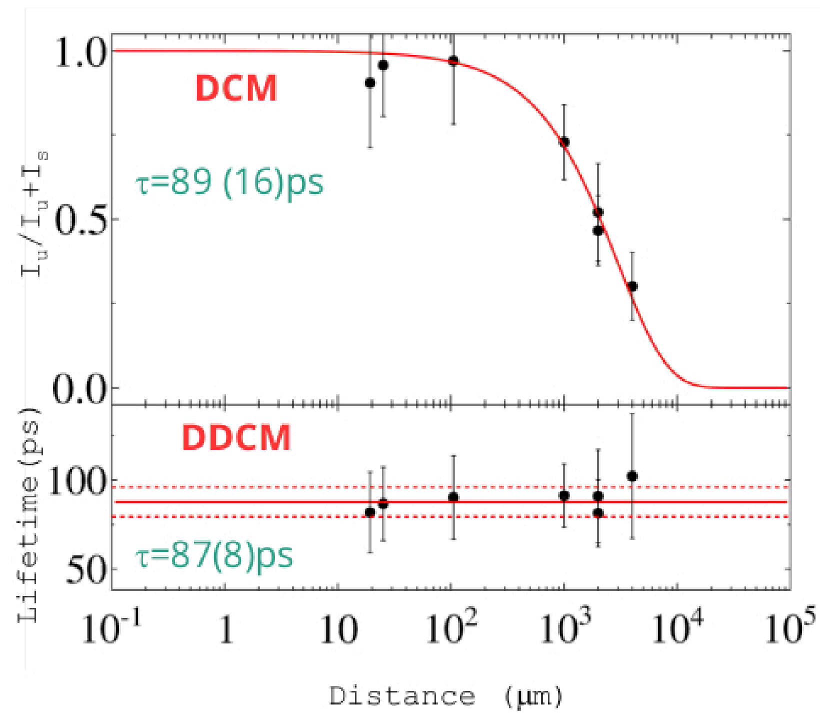

Example: FUSION-EVAPORATION REACTIONS

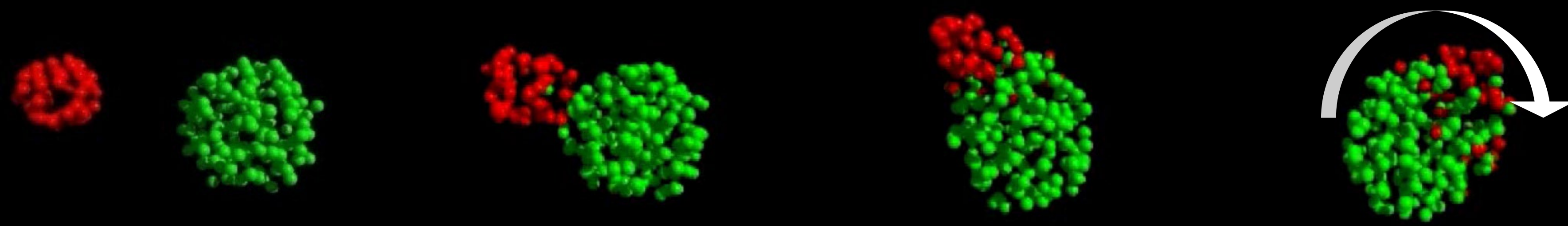

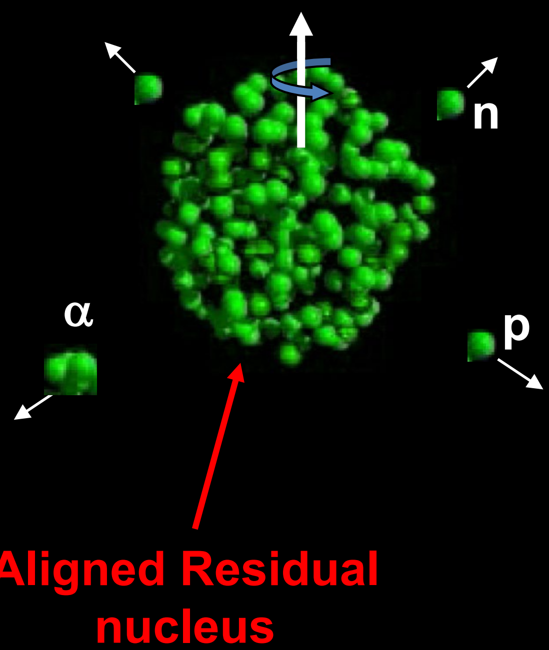

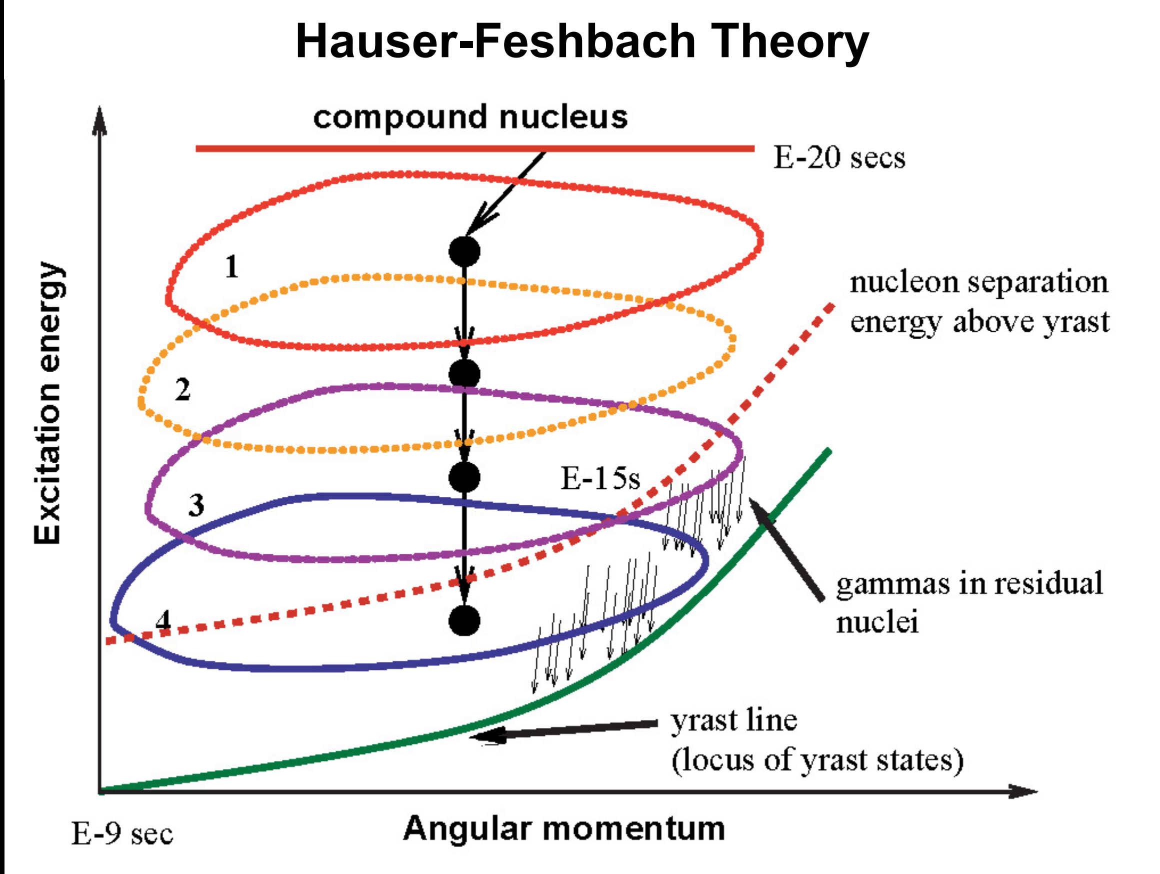

Example: Spectroscopy with Fusion-Evaporation Reactions

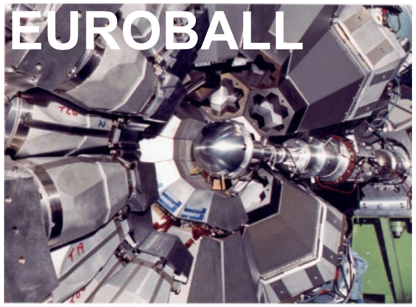

$^{40}Ca(^{40}Ca,4pn)^{75}Kr^{*}$

States identified up to J=57/2
and 19 MeV excitation energy

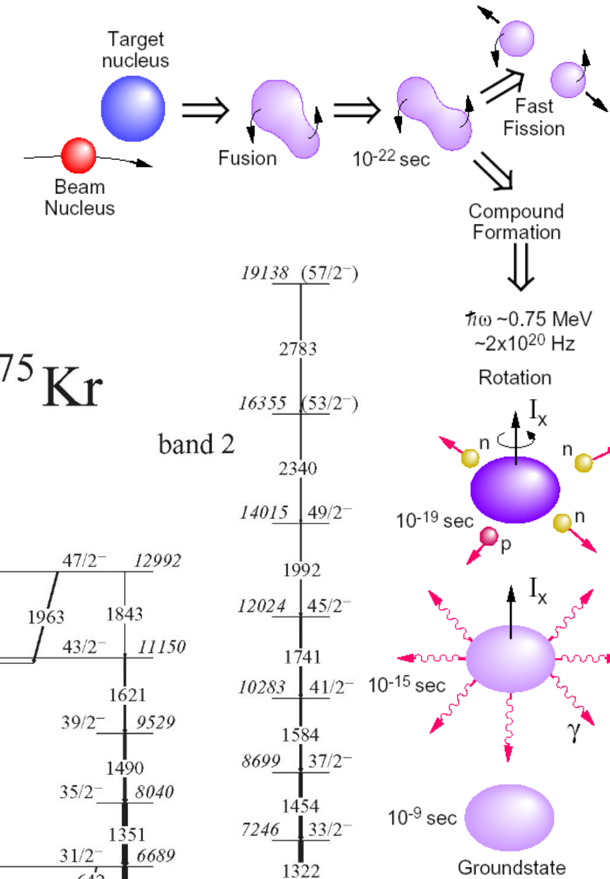

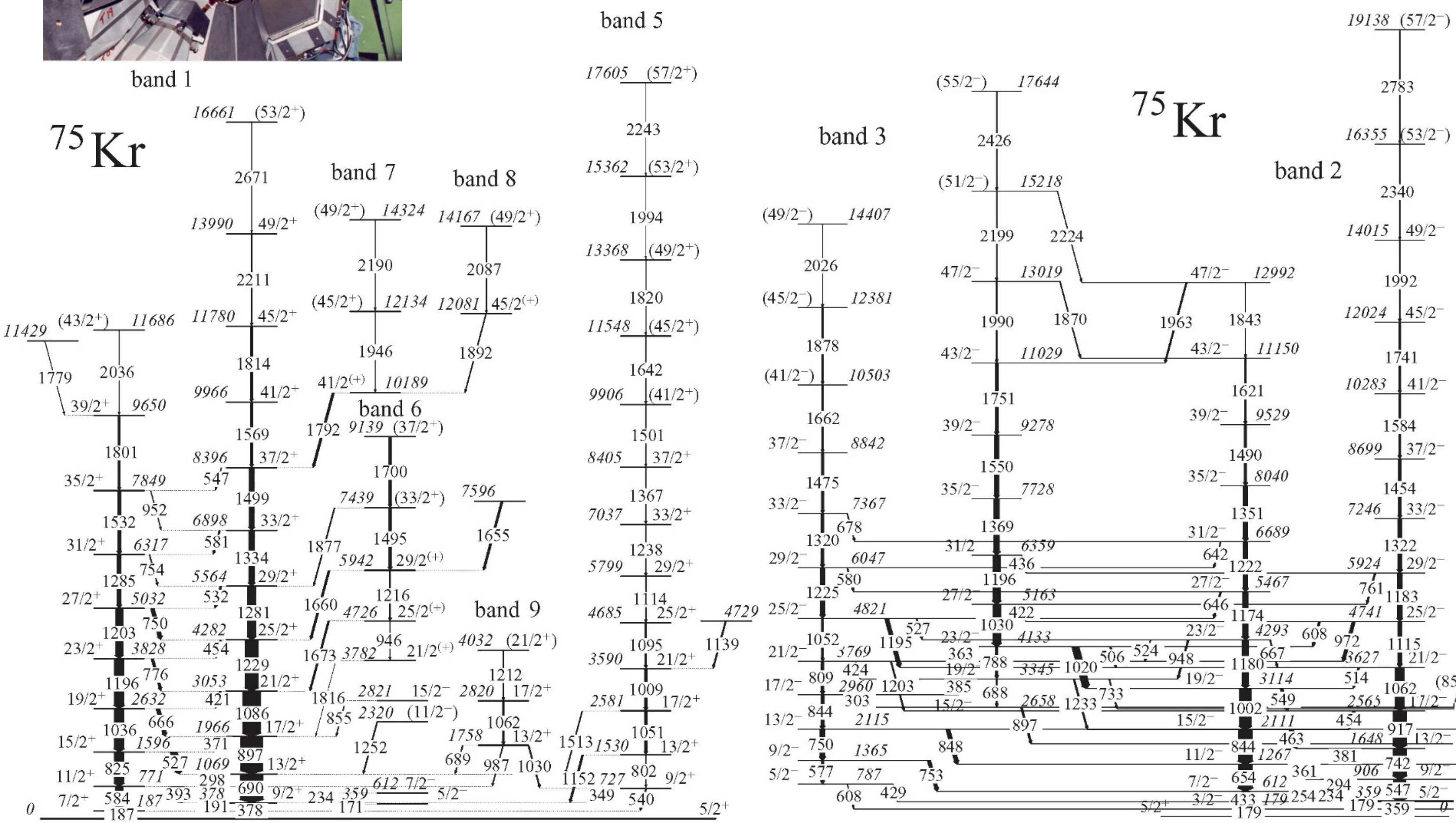

Th. Steinhardt, et al., Phys. Rev. C **86**, 064310 (2012)

High energy reaction mechanisms used for γ-Spectroscopy (above ~40 MeV.A)

Generally used with exotic ion beams produced by fragmentation or fission at relativistic energies

- Relativistic (single step) Coulomb excitation
- Inverse proton scattering
- Knockout reactions
- Fragmentation reactions

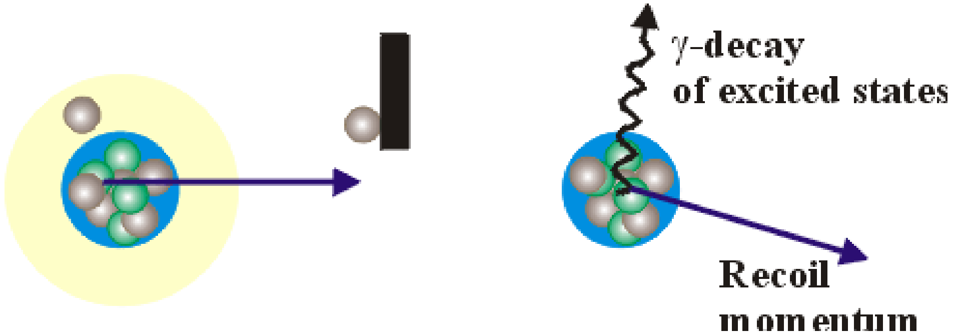

Knockout reaction

Cross sections :

- up to1 barn for Coulex (large Z nuclei)
- tens of mbarn for proton scattering and 1 nucleon knockout,
- down to few mb for 2 nucleons knockout.
- smaller cross sections for fragmentation

Fragmentation reaction

Quadrupole collectivity in 52Fe AGATA@GSI/FRS

Production of the 52Fe beam by fragmentation of 600 MeV.A ^{58}Ni on a ^{9}Be 4g/cm^{2} primary target of GSI-FRS. Three seconds Spill Secondary Target 400mg/cm2 Au. AGATA-PRESPEC setup

T.Hüyük PhD thesis & article in preparation

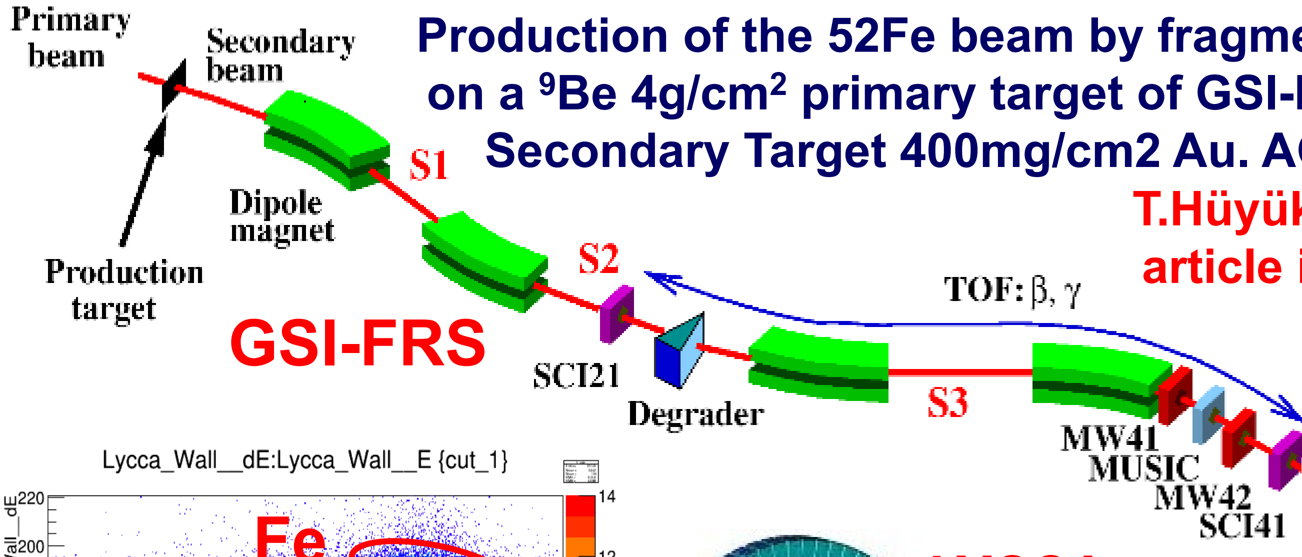

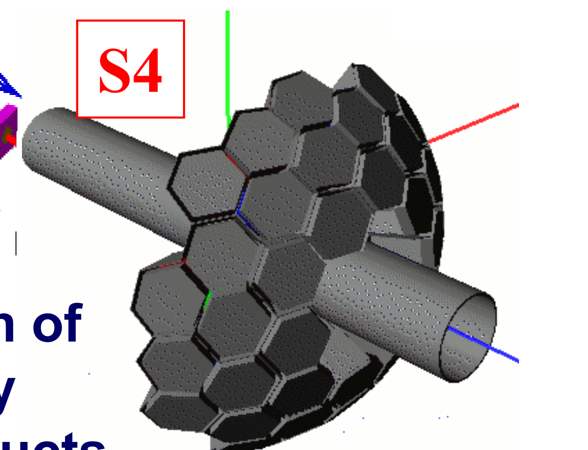

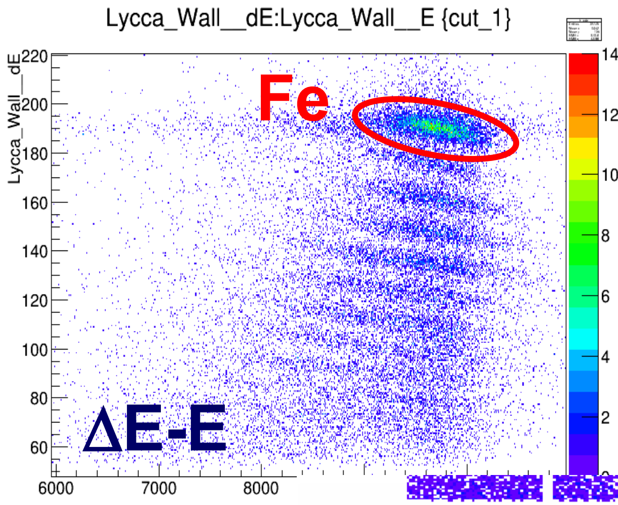

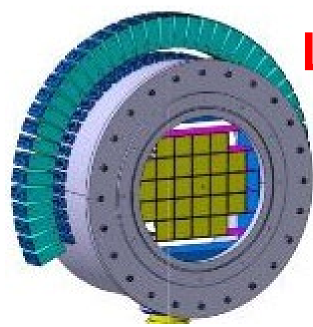

LYCCA

Identification of secondary reaction products

$$E_0 = \frac{E_S}{\gamma\left(1+\frac{v}{c}\cos\theta_\gamma\right)}$$

β=0.51
Target-AGATA distance 8cm

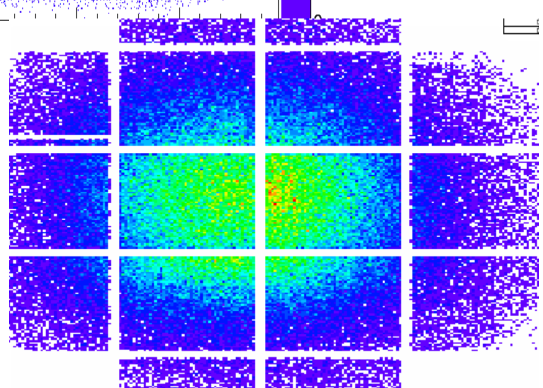

Z identification
Scattering angle

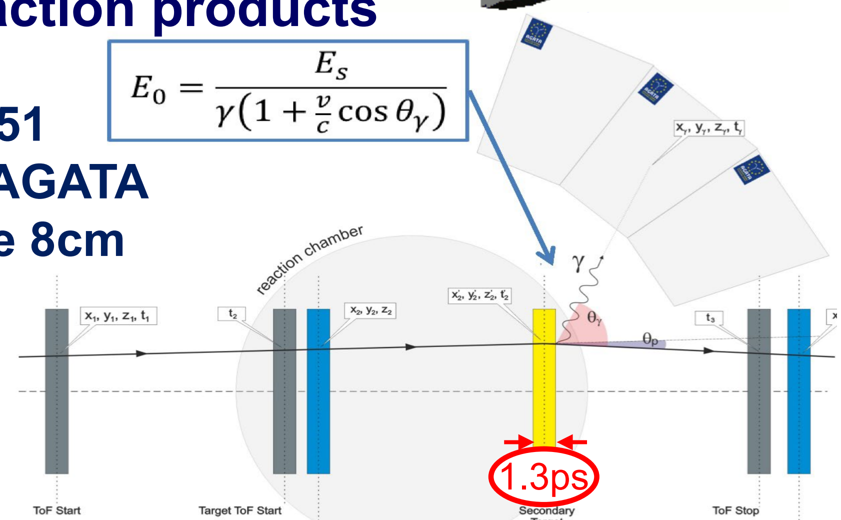

^{52}Fe Relativistic Coulomb Excitation Results

With Empirical Indirect Feeding 14%

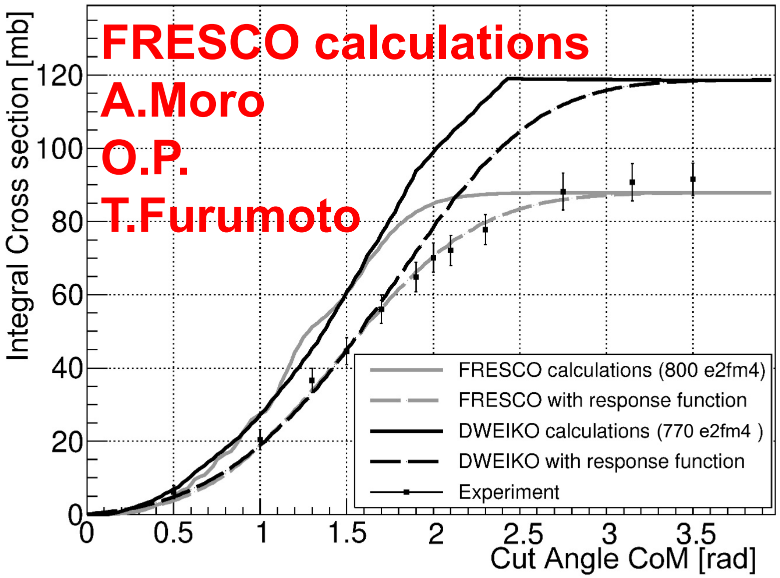

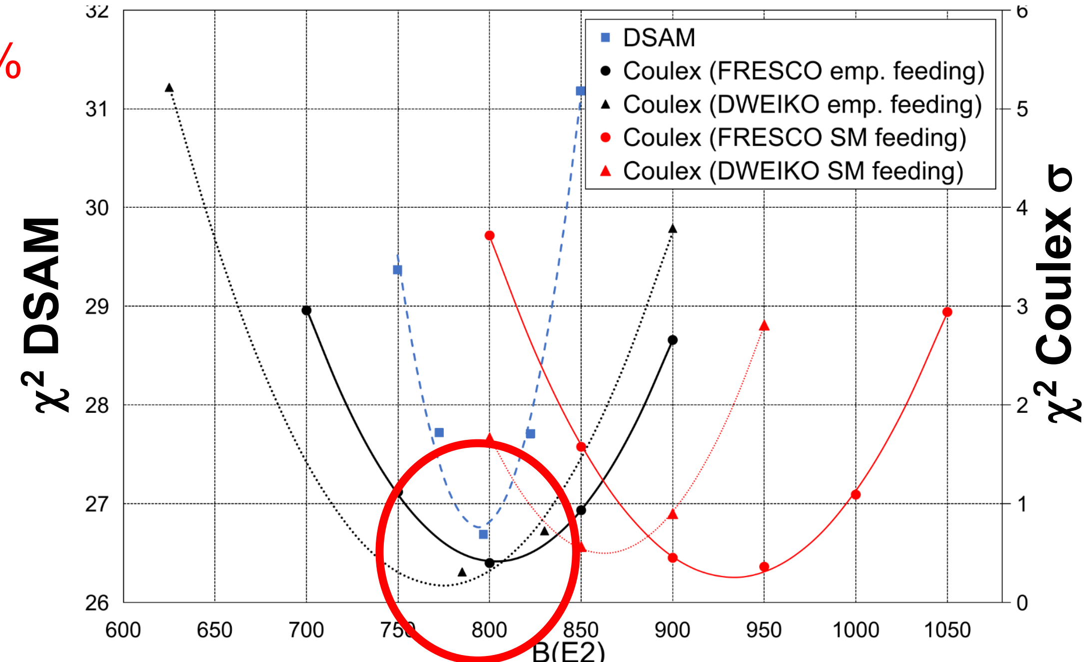

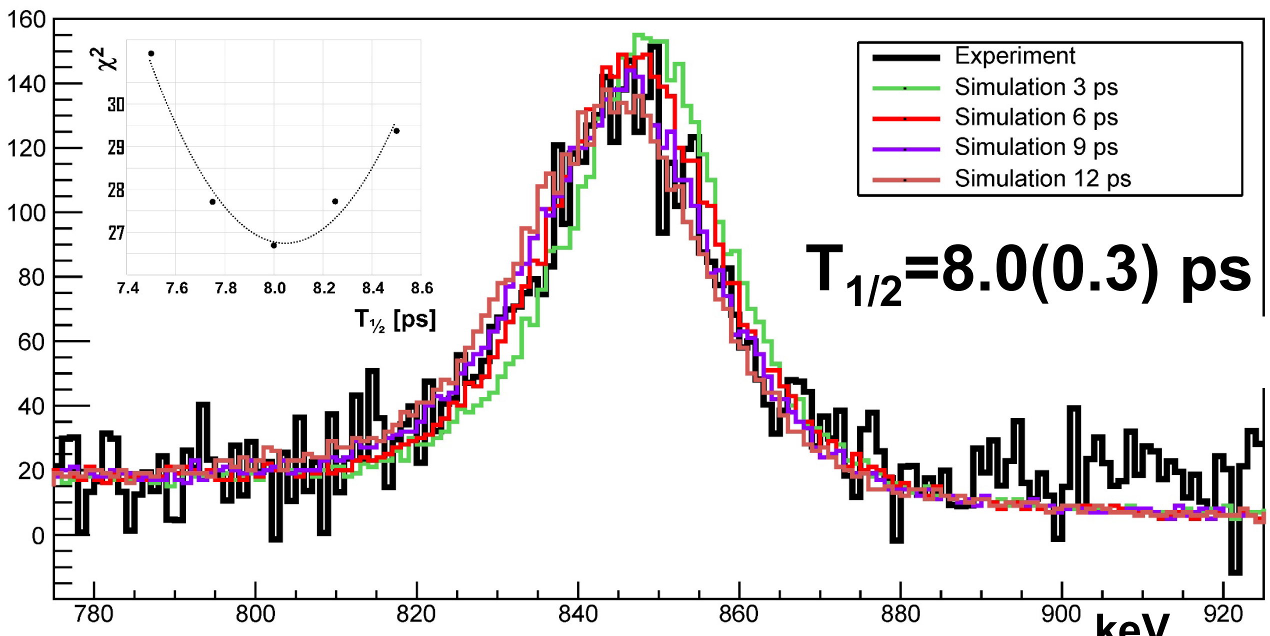

Adopted Value

$B(E2, 0^+ \rightarrow 2^+_1)$=
800(60) e^2fm^4

LSSM Calculations ANTOINE	B(E2)
KB3G	847 e^2fm^4
GXPF1	863 e^2fm^4

LSSM: S.Lenzi eπ=1.31 eν=0.46

In agreement with B(E2)= 817(102) e^2fm^4 by K.L.Yurkewicz, PRC 70 (2004) 034301. Not observed enhanced collectivity K.Arnswald PLB. 772 (2017) 599

Further Information on Reactions Cross-Section Determination:

- Inelastic, Transfer Reactions, Grazing etc…
  - http://nrv.jinr.ru/nrv/
- GOSIA (Coulomb excitation
  - http://www.pas.rochester.edu/~cline/Gosia/
- GRAZING MNT

- Fusion-Evaporation Reactions
  - PACE in LISE++: http://lise.nscl.msu.edu/lise.html
  - HIVAP: W. Reisdorf, Z. Phys. A 300, 227 (1981)
- Relativistic Coulomb Excitation
  - DWEIKO: C.Bertulani et al. Comput. Phys. Commun. 152 (2003) 317.
- Fragmentation, Knock-out etc..
  - LISE++: http://lise.nscl.msu.edu/lise.html

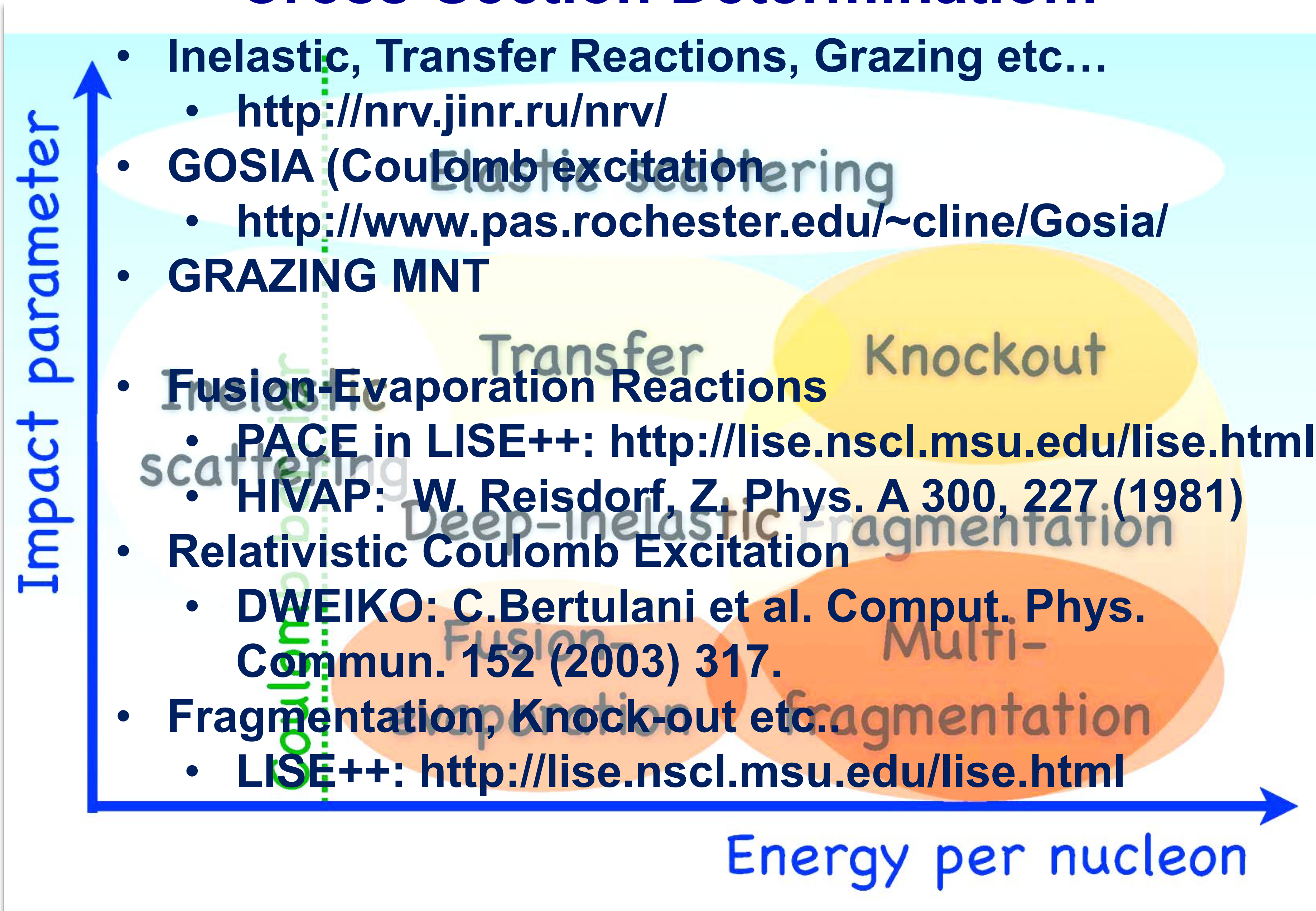

Complementary Instrumentation!

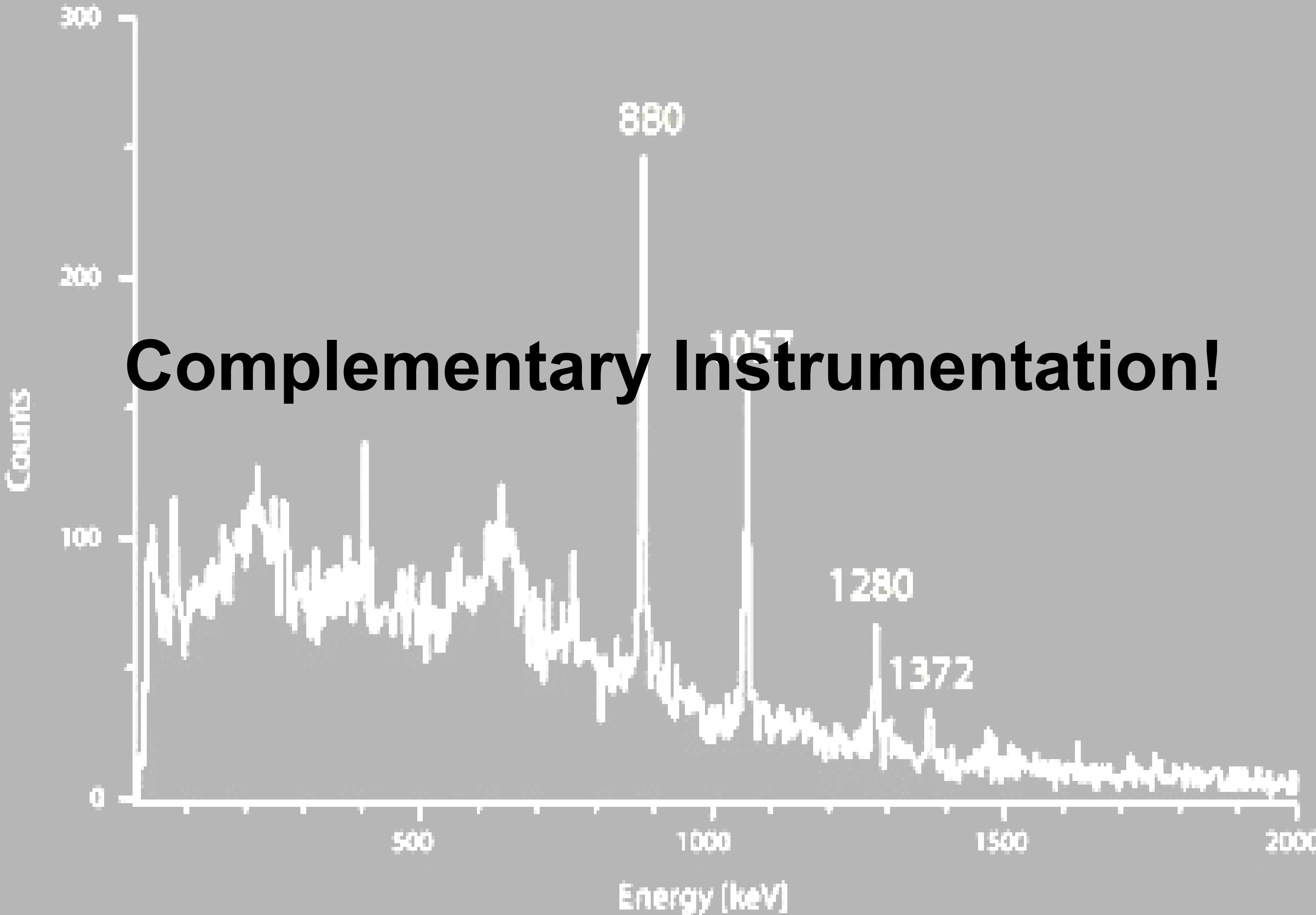

Complementary Instrumentation

- Fundamental to increase the sensitivity of the γ-ray detector. Identifying the reaction channel or reaction products:
  - Particle detectors (Light charged particles or neutrons)
  - Spectrometers (Identification of the reaction products)
  - Beam Trackers (for relativistic experiments)
  - etc…
- Fundamental to perform some measurements
  - Plunger devices for RDDS measurements
  - Fast Scintillators for timing measurements
  - etc…